Progress in Polymer Science 39 (2014) 1934–1972

Contents lists available at ScienceDirect

Progress in Polymer Science

journal homepage: www.elsevier.com/locate/ppolysci

Graphene-polymer nanocomposites for structural and functional applications

Kesong Hu, Dhaval D. Kulkarni, Ikjun Choi, Vladimir V. Tsukruk*

School of Materials Science and Engineering, Georgia Institute of Technology, Atlanta, GA 30332-0245, USA

ARTICLE INFO

Article history:
Available online 29 March 2014

Keywords:
Graphene materials
Polymer interfaces
Flexible nanocomposites
Mechanical performance
Conductive polymer nanocomposites

ABSTRACT

The introduction of graphene-based nanomaterials has prompted the development of flexible nanocomposites for emerging applications in need of superior mechanical, thermal, electrical, optical, and chemical performance. These nanocomposites exhibit outstanding structural performance and multifunctional properties by synergistically combining the characteristics of both components if proper structural and interfacial organization is achieved. Here, we briefly introduce the material designs and basic interfacial interactions in the graphene-polymer nanocomposites and the corresponding theoretical models for predicting the mechanical performances of such nanocomposites. Then, we discuss various assembly techniques available for effectively incorporating the strong and flexible graphene-based components into polymer matrices by utilization of weak and strong interfacial interactions available in functionalized graphene sheets. We discuss mechanical performance and briefly summarize other physical (thermal, electrical, barrier, and optical) properties, which are controlled by processing conditions and interfacial interactions. Finally, we present a brief outlook of the developments in graphene-based polymer nanocomposites by discussing the major progress, opportunities, and challenges.

Contents

* Corresponding author. Tel.: +1 404 894 6081; fax: +1 404 385 3112.
E-mail address: vladimir@mse.gatech.edu (V.V. Tsukruk).

http://dx.doi.org/10.1016/j.progpolymsci.2014.03.001
0079-6700/

1. Introduction to polymeric nanocomposites

Synthetic polymer composite materials were introduced centuries ago and used as structural components due to their much improved mechanical properties, chemical inertness and stability, versatile processing techniques, and reduced cost [1,2]. For many traditional composite materials, polymers conventionally serve as elastomeric and flexible matrices by contributing high elasticity, strength, flexibility, controlled surface and bulk properties, and other unique physical properties.

1.1. Choice of polymeric matrices

Benefiting from almost infinite choices of monomers, oligomers, and chemistries available, polymer matrices can be precisely tuned and controlled to exhibit the whole spectrum of physiochemical properties for very different applications, including controlled hydrophobicity, ionizibility, crystallinity, transparency, toughness, strength, densities, conductivity, and degradability [3–8].

Among the structural polymeric matrices for the advanced nanocomposites, elastomers, thermoplastics, epoxy, block copolymers, and hydro/aerogels are used widely due to their unique physical and chemical properties, which can be tailored to various applications [2,9–13]. For example, elastomers are highly stretchable polymers consisting of lightly crosslinked (chemically or physically) long chains [14,15]. In contrast, epoxy resins contain rigid segments and are very heavily crosslinked so that their mechanical strength, stiffness, as well as their brittleness, are extremely high [16,17]. Thermoplastic polymers are reinforced by physically ordered (e.g., crystalline) domains, which are not chemically crosslinked so they can be processed, shaped, melted, and recycled.

Block copolymers are essentially composed of two or more chemically divergent polymer chains that are covalently linked end to end (or differently) in order to create complex nanoscale morphologies [2,9,11]. One of the biggest benefits of the block copolymers is that the physiochemical properties of the resulting nanomaterials can be tuned by adjusting the content of species that make up the chain and the lengths of each component [18,19]. Block copolymers have the inherent advantage of possessing heterogeneous properties, e.g., amphiphilicity, which are controlled by microphase states with sharp interfaces and tailored 3D morphologies [20]. Hydrogels or aerogels with their porous morphology and permeable properties can be swollen in water or contain gas. These materials can be used for scaffolds, catalyst support, controlled release/adsorption, shock absorbance, and low-density thermal or electromagnetic shielding [21–25].

Despite significant efforts in synthesis new polymers, the mechanical properties of polymer matrices can be considered to be modest in many cases. Indeed, the elastic modulus of linear amorphous polymers is usually several GPas in their bulk glassy state, except for some famous examples of rigid conjugated polymers and polymer fibers with highly oriented polymer chains [2]. Moreover, the mechanical strength of polymer materials will further decrease by several orders of magnitude when heated above the glass transition temperature, which can be relatively low and close to (or even below) ambient temperature. Therefore, a variety of high performance inorganic (glass, metal, semiconducting) fillers are frequently introduced as important reinforcing components in order to significantly improve the structural strength of polymer composites as well as to induce some additional functional properties (e.g., thermal or electrical conductivity).

1.2. Reinforcing components

Conventional polymer composites are usually fabricated from a relatively compliant matrix and stiff inorganic

fillers in the form of fibers, laminates, or particles. The philosophy of the fabrication of high performance composite materials is to synergistically combine the strengths of multiple constituents and optimize the primary mechanical properties. Glass fibers, carbon fibers, wood sheets, metal particles, and inorganic mineral particles are all common discrete fillers in conventional composites composed of continuous matrices of thermoplastic polymers, rubbers, hydrogels, or thermosets. However, conventional polymer composites suffer from some common issues caused by the very dissimilar properties of the compliant matrices and hard components, which include modest improvement of mechanical strength, reduced compliance, catastrophic failure caused by interfacial defects and weak interfacial bonding, accelerated degradation caused by mismatching of the coefficient of thermal expansion, and significant manufacturing cost in some cases [26].

On the other hand, nanocomposite materials with nanoscale fillers have emerged in the past decades as a promising novel class of materials, which take advantage of greatly increased specific interfacial area, higher achievable loads, controlled interfacial interactions, and higher overall compliance. The mismatch of the physical properties of the components becomes much less critical and the interfacial area between the filler and the matrix is maximized so that the interfacial strength can be much improved [27]. Currently, multifunctional nanocomposites with much improved mechanical performances are primarily fabricated by addition of pre-treated carbon nanotubes and nanofibers [28,29], inorganic nanoparticles [28,30], and metal nanostructures [30–32].

Among various reinforcing nanoscale components, clay, carbon nanotubes, and metal/ceramic nanoparticles are the most common nanofillers employed in the past two decades to fabricate a variety of high performance nanocomposite materials [25,33–42]. Clay nanoparticles (e.g., montmorillonite, MMT) possess excellent mechanical strengths and optical transparency, they are relatively cheap, and can be pre-treated and dispersed in common solvents and even in an aqueous environment [25,33]. The 2D geometry of the MMT nanoplatelets is also beneficial for their self-assembly in organized layered (laminated) morphologies, which are important to structural applications with directional mechanical loads. The mechanical performance of these nanomaterials can show much improvement compared to traditional composites. For example, the ultimate strength of MMT/poly(vinyl alcohol) (PVA) nanocomposites can reach 220 MPa with the elastic modulus can be as high as 19 GPa [43]. However, because MMT is a stiff inorganic platelet filler the flexibility and biodegradability of these nanocomposite can be compromised.

Metal and carbon nanoparticles show exceptional reinforcing properties and can also add electrical conductivity, catalytic activity, and plasmonic properties [4,40–42]. However, metal nanoparticles are not readily dispersible in polymeric matrices due to the hydrophobicity of the nanoparticles and limitations of the organic ligands utilized. Therefore, grafting of nanoparticles with various compatible polymeric ligands or growing metal nanoparticles in situ have been implemented [44–47]. Alternatively, metal oxide nanoparticles show good aqueous processibility, multifunctional properties, and high mechanical strength as compared to corresponding metal nanoparticles, but their integration in polymer matrices can be a challenging task [48–50].

Carbon black is the most commonly used nanomaterial in industry for the mechanical reinforcement and mechanical damping in synthetic rubbers, thermal properties of polymeric materials, and electrical modification of polymer matrices [51–53]. Carbon blacks are mainly amorphous particulate materials, with moderate physiochemical properties in all major aspects. However, these fillers are abundant, can be readily functionalized, and are inexpensive. The surface-to-volume ratio of carbon black is lower than that of activated carbon and its mechanical and electrical properties are not comparable to its crystalline carbon cousins, thus novel carbon-based fillers have been intensively elaborated in the past two decades.

Recently, organized carbon materials such as carbon nanotubes and buckyballs have become much more sophisticated and popular nanostructures. These materials are seen as one of the most promising nanofilling materials because of their low density, extremely high aspect ratio (nanotubes), minute dimensions, outstanding mechanical and thermal properties, good chemical inertness, and tunable electrical properties [34–37,54]. However, the progress in nanocomposite development made using carbon nanotubes is still continuing and great challenges still remain to be addressed. Among most critical unresolved issues are poor aqueous dispersibility, stubborn contaminations, excessive aggregation, high cost, poor control of surface chemistries, and low interfacial interactions with the polymeric matrix. Significant efforts in the development of these nanocomposites are summarized in a number of books and reviews and will not be further considered here [55–59].

Finally, various graphene materials have very recently emerged as a new class of prospective components for advanced nanocomposites with intriguing new opportunities for the integration into polymer matrices as will be discussed in this review.

1.3. Graphene-based nanocomposites

Indeed, the number of publications on graphene-based nanocomposites has grown exponentially in recent years from almost non-existing records before 2006 to more than a thousand annually in the past two years (Fig. 1). Prior to 2010 less than two hundred publications can be counted in total, with no significant records found before 2006 (probably caused in part by a terminology gap).

However, since 2010, the number of peer-reviewed publications on graphene-based nanocomposites has surged greatly and continues rapid growth. Apparently, the Nobel Prize in Physics for graphene has drawn vast attention from the materials research community and brought a number of new research groups to this field. Indeed, the number of the graphene nanocomposite publications appearing in the past two years exceeds several times those *ever published* in this field during all previous years (Fig. 1). Therefore, even if some comprehensive reviews

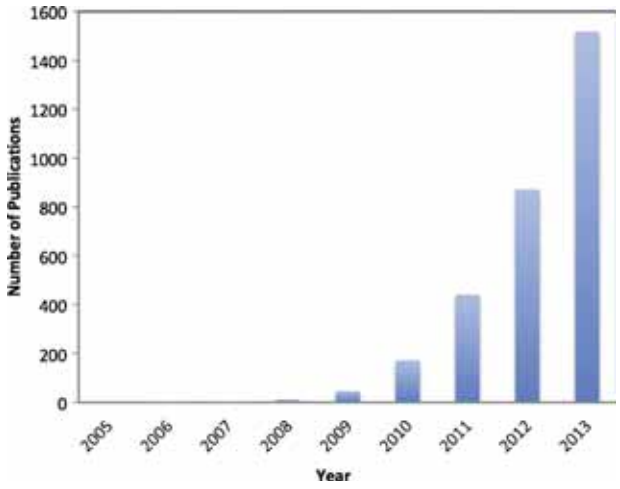

Fig. 1. Number of the peer-reviewed publications (articles and reviews) containing the keywords "graphene" and "(nano)composite(s)" since 2005.
Data source: Web of Knowledge, Thomson Reuters.

which have been recently published on this topic (mostly in 2010–2012, see summary of some recent reviews below) the overall landscape changed dramatically in the past two years alone and, therefore, it is necessary to summarize again very recent results and discuss the newest trends in this fast evolving field.

Overall, polymer-graphene (here under a general term of "graphene" we usually imply not just traditional graphenes but also various chemical derivatives such as graphene oxides if not specified otherwise) nanocomposites show not only record mechanical properties but also impressive functional properties, such as electrical (semi-) conductivity, unique photonic/optical transportation, anisotropic transport, low permeability, and fluorescence quenching. It has already been demonstrated that the introduction of even a small fraction of a graphene component can dramatically improve the mechanical performance of the variety of the polymeric matrices and some extraordinary reinforcing and functional properties have been reported very recently. Graphene materials and their various derivatives show tremendous potential in revolutionary enhancement of mechanical, electrical, thermal, and chemical properties of polymeric materials relevant for a wide range of emerging demanding applications (Fig. 2) [60–67].

Although the current research activities tend to focus on the understanding of fundamental phenomena and the utilization of the excellent properties of graphene materials as efficient nanofillers, the next exploding area on the graphene material research relevant to polymer nanocomposite materials might be the development of atomic multi-stacking of heterogeneous 2D structures (also known as "van der Waals crystals") with promising extraordinary functional properties [68].

The initial results on graphene-polymer nanocomposites are summarized in a number of excellent recent reviews as briefly introduced here. In an important "early" publication, Kim et al. provided a general review on graphene-polymer nanocomposites [69]. Kuilla et al. introduced examples of different combinations of polymers with graphene materials in addition to presented general background on graphene and its derivatives [70]. Compton et al. focused on graphene and graphene oxide, and discussed the properties of these nanofillers in detail [71].

In their review, Huang et al. paid major attention to devices made of polymer-graphene nanocomposites and the other constituents including metal, semiconductor, and organic small molecules [72]. Young et al. reviewed graphene-polymer nanocomposites and discussed the modeling, fabrication, and characterization of these materials [73]. Among the most recent reviews, Wu et al. discussed the structures and general functional applications of the nanocomposites made from chemically modified graphenes [74]. Yang et al. critically evaluated the fabrication of graphene multilayers, including graphene-polymer nanocomposite thin films fabricated by layer-by-layer assembly [75]. Finally, very recently Sun et al. provided an insight on the integration of both graphene and carbon nanotube materials in polymer nanocomposites [34].

In this review, we focus on recent (mostly published in 2010–2013) and the most significant results of the outstanding mechanical and other physical properties of polymer-graphene nanocomposite materials, and discuss some fundamental properties and the processing approaches of such nanocomposites. We highlight the fundamental properties and critical characteristics of graphene materials as prospective reinforcing nanofillers, their chemical and physical functionalities, the interfacial interactions important for the effective reinforcement, and the methods of the fabrication of these materials. Finally, we briefly summarize the theoretical work and experimental efforts on the optimization of the elasticity, strength, deformation, and toughness, and discuss the results of the ultimate mechanical performance of such nanocomposites with variable composition, chemistry, and morphology.

1.4. Graphene and graphene derivatives as prospective filler nanomaterials

In this section, we summarize some of the fundamental properties and microstructure of graphene materials of different types. Similar to carbon nanotubes, basic graphene is composed of only carbon atoms, but it is a 2D flat sheet rather than rolled up monolayer of carbon. Benefiting from its pure sp^2 hybridization network, graphene materials frequently possess record characteristics of mechanical, thermal and electrical properties. The most important materials characteristics for our discussion are: the highest, 1 TPa, elastic modulus [76], very high, 5.1×10^3 W m^{-1} K^{-1} thermal conductivity [77], and the highest known intrinsic electrical conductivity of 6×10^5 S m^{-1} [78]. Among the most interesting and fundamental properties we should mention the theoretical van der Waals thickness of individual graphene sheets of 0.34 nm, which is the thinnest 2D nanofiller known to date (Fig. 3a) [79]. Other critical parameters of these materials are extremely high aspect ratio of flakes (ratio of lateral dimensions to the thickness of 10^4 and higher) and high intrinsic flexibility.

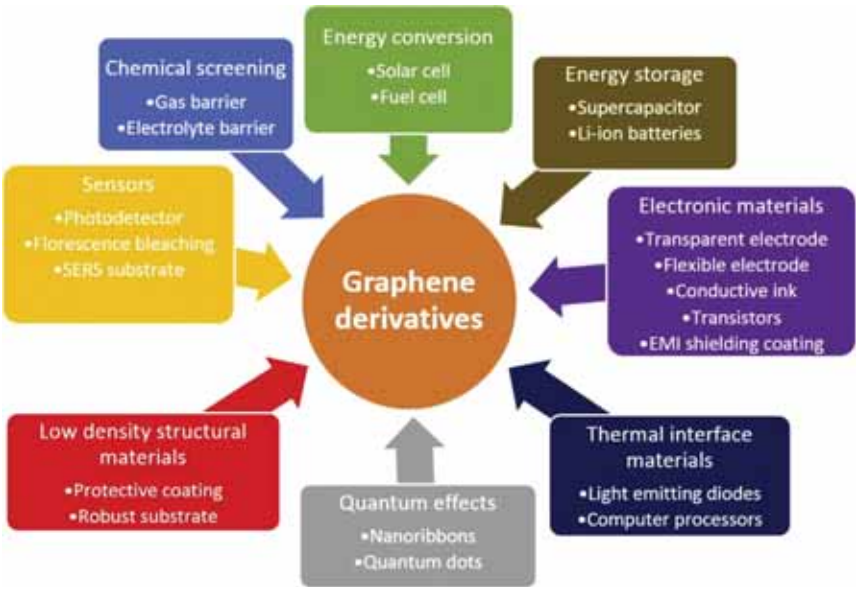

Fig. 2. Graphene derivatives show promising results for various fields, including energy conversion [60], energy storage [61], electronic materials [62], quantum effects [63], low density structural materials [64], sensors [65], chemical screening applications [66], and thermal interface materials [67].

Pristine graphene is usually obtained by mechanical exfoliation of graphite or synthesized by chemical vapor deposition (CVD) [79]. Mechanical cleavage or exfoliation of highly ordered pyrolytic graphite (HOPG) is a common top-down method that can easily produce large quantity of graphene sheets with different microscopic dimensions, individual or multilayered flakes, and modestly defective microstructure.

CVD synthesis of graphene uses carbon-rich precursors (e.g., methane) and recombines the carbon atoms on the surface of metal foil (copper or nickel) in inert atmosphere at over 1000 °C [69]. By controlling the reaction parameters, such as the ratio of the different precursors, temperature, and substrates, single, double or multiple layer graphene with various sizes can be produced. The synthesis of graphene does not require catalysts in gas phase that are hard to be removed, and the size of graphene can be controlled from nanoscale to millimeter scale, giving it huge potentials for nanocomposite applications. However, both mechanical exfoliation and the CVD synthesis result in defective and heterogeneous structures. Moreover, time and energy consumption for their fabrication are high for the mass-production of consistent graphene materials in large quantities.

Therefore, different graphene derivatives that partially preserve the extraordinary properties of graphene materials and overcome some of their deficiencies have attracted more attention. One of the most popular graphene derivatives, which can be utilized for the fabrication of polymer-graphene nanocomposites is graphene oxide, and derivatives with excellent mechanical and controlled chemical properties. Even though preliminary studies show that the biocompatibility of graphene oxide materials is good in many cases [80,81], extensive investigation is required to discriminate cytotoxicity and metabolic accumulation for prospective biomedical applications [82].

Graphene oxide (GO) is an oxidized graphene derivative, which can be widely used as an alternative or precursor for graphene materials due to its high dispersibility and processibility in aqueous environment [8,83,84]. It is produced from mineral graphite flakes by thermal oxidation method invented by Hummers and modified by successors [85]. The resulting single atomic layers graphene-like

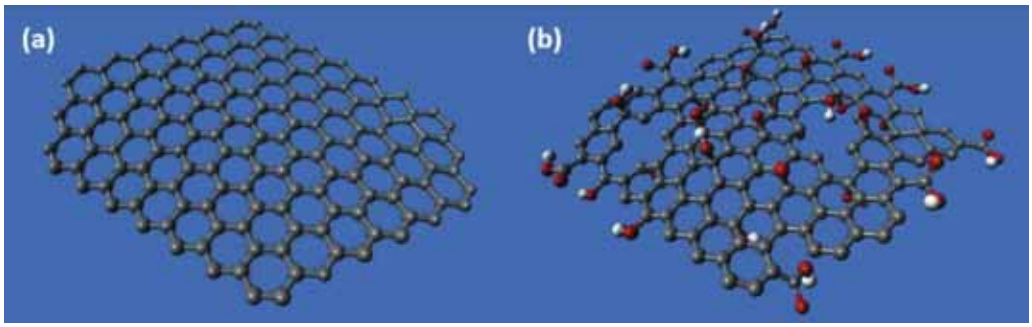

Fig. 3. Atomistic structures of individual sheets of basic graphene (a) and graphene oxide (b). The atoms are color-coded: gray – carbon, red – oxygen, and white – hydrogen. (For interpretation of the references to color in this figure legend, the reader is referred to the web version of the article.)

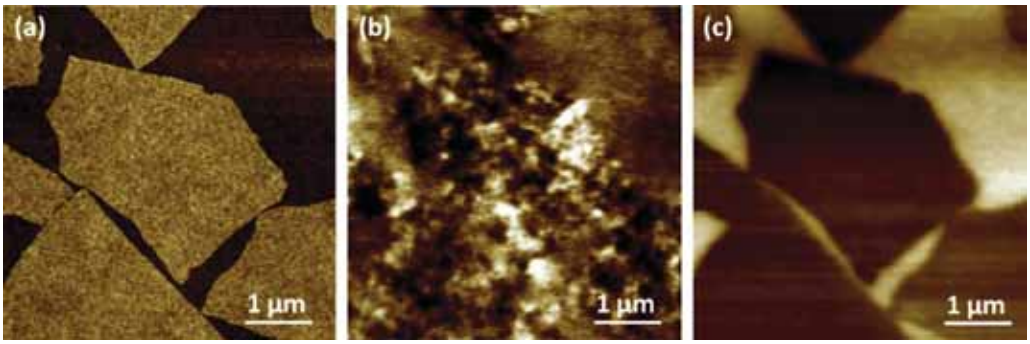

Fig. 4. (a) Topography, (b) EFM-phase image before reduction, and (c) after chemical reduction from the same graphene oxide flakes.

material possess high density of epoxy and hydroxyl groups on both sides of the basal carbon plane and carboxyl groups around their edges (Fig. 3b) [86]. Recent studies of surface defect distribution using electrostatic force microscopy (EMF) [87–89] demonstrated the heterogeneous distribution of nanoscale (~100 nm across) oxidized domains that completely dissipate after chemical reduction to graphene (Fig. 4) [90].

Molecular simulations have shown the bonding energy and shear strength have been significantly improved by inducing the surface and edge functionalities on graphene sheets, which is critically important for their integration into polymer matrix [91]. The usual ratio of carbon and oxygen in graphene oxide materials is close to 2:1, the overall surface coverage with oxidized regions can reach 60–70%, and point defects are present among the honeycomb primary structure, all reflecting an intense and highly localized oxidization processes (Fig. 3b) [3,70,71,92].

The theoretical thickness of graphene oxide is within 0.7–0.8 nm, doubling that of the pristine graphene due to the presence of additional prominent bulky surface functionalities resulting from the oxidation process [3]. The actual thickness of graphene oxide flakes might be slightly larger due to surface contaminants, organic adsorbates, underlying substrate roughening, or occasional presence of bulkier functionalities [3,64].

Although lacking electrical merits of graphene and being somewhat inferior in ultimate mechanical performance, graphene oxide and corresponding derivative materials still exhibit huge potential in nanocomposite fabrications due to its outstanding mechanical properties, high flexibility, high bonding potential, and extremely high aspect ratios. The elastic modulus of a single graphene oxide sheet is as high as 250 GPa despite the high concentration of local defects, which is much higher than modulust developed with most known fillers [93,94]. This high tensile strength is combined with high lateral flexibility, which facilitates nanocomposite flexibility but can be problematic during processing. Graphene oxide flakes are negatively charged in slightly acidic and basic conditions due to the surrounding surface carboxyl groups. The zeta potential of graphene oxide decreases progressively with higher pH values and can be as low as −50 mV at pH = 10.5 [84]. Graphene oxide does not precipitate in most polar solvents and can be incorporated into correspondingly charged polyelectrolyte matrices [3,83].

Even pure graphene oxide materials without any polymer matrices show outstanding performance. Graphene oxide "paper" made by vacuum-assisted self-assembly (VA-SA) and evaporation methods possess an elastic modulus of 18–36 GPa, with only water molecules serving as binders [95–97]. Localized water molecules link the neighboring graphene oxide flakes by hydrogen bonding while free water molecules that are intercalated in the interlayer spacing of graphene oxide layers lubricate the inter-layer spacing facilitating slippage behavior, which in turn decreases the efficiency of stress transfer between layers. That is why the mechanical performance of different graphene oxide papers have a marked dependence on the local humidity conditions and might disagree in some cases. To this end, it has been demonstrated that covalently bonded graphene oxide paper with the use of organic, ionic, or polymeric crosslinkers possesses enhanced mechanical strength compared to pure graphene oxide paper. An elastic modulus as high as 120 GPa can be reached with dense inter-layer crosslinking [95].

Graphene oxide can be reduced to graphene-like structures with similar mechanical and conductive properties by chemical, electrochemical, thermal, hydrothermal, and photothermal reducing techniques [98,99]. Hydrazine, hydriodic acid (HI), electron complexes in liquid ammonia, metal particles, sodium hydroxide, and infrared laser illumination can all remove the oxygen-containing groups from the graphene oxide surfaces and restore massive hybridization of sp^2 electronic orbitals [100–104]. Metal foil and laser beam can directly pattern graphene oxide films with controlled localization of the reduced regions. Aluminum foils have been employed to reduce graphene oxide paper with intercalated natural binders with controlled surface patterning and depth distribution [105]. Light-induced and plasmon-assisted graphitization of amorphous carbon may also be applied to pattern the reduction of graphene oxide [106]. These patterned reduced graphene oxide (rGO) materials can be made ready for integration of into flexible electronic devices as will be discussed below.

1.5. *Interfacial interactions and polymer matrices*

Interfacial interactions between polymers and graphene-based materials play a key role in the mechanical integrity of the corresponding nanocomposite and their mechanical performance. Due to the homogeneous carbon

Table 1
Intermolecular interactions relevant to graphene components.

Interaction	Strength (kJ mol^{-1})	Bond length (nm)	Restorability	Example
Covalent	355–730 [115]	0.15–0.26 [115]	N	C—C backbone
Hydrophobic	40r[a] [116]	<0.5	Y	Protein-graphene
π-Stacking	8–12 [117]	0.5 [117]	Y	Polystyrene-graphene
Coulombic	5.8–232[b] [115]	0.3–1.0 [115]	Y	Polyelectrolyte-graphene oxide
Hydrogen	4–20 [115]	0.24–0.35 [115]	Y	Poly(vinylalcohol)-graphene oxide
Van der Waals	2–4 [115]	0.3–0.5 [118]	Y	Any two molecules

[a] r is the radius (nm) of solute molecules in water.
[b] Varies largely by different dielectric constants of media.

composition of graphene without other heteroatom functionalities, the molecular interactions with polymers are limited to weak van der Waals forces, π–π-stacking, and hydrophobic–hydrophobic interactions [107,108]. Van der Waals forces are universal attractive interactions between molecules generated by the transient or permanent dipoles of the molecules. Although very weak, these forces contribute the major part of interfacial strength between graphene and common polymers, such as polyethylene, due to intimate contact and very large specific surface area [109]. Hydrophobic–hydrophobic interactions are a common means for binding graphene in hydrophobic polymer matrices. A special case of π–π interactions is especially important for the graphene materials with the electron-rich aromatic rings interacting with a variety of chemical species and matrices with phenyl rings, which can act as strong bonding sites [110,111]. Then, π–π-stacking can adapt to different space organizations and significantly enhance bonding in graphene nanocomposites.

By contrast, graphene oxide possesses abundant oxygen-containing polar functionalities, such as epoxide, carbonyl, hydroxyl, and carboxyl groups [98]. The choices of functionalization and resulting interactions with various polymers are much more versatile for graphene oxide materials. Furthermore, covalent grafting of polymer chains on graphene oxide surfaces can achieve improved blending of graphene oxide component and the polymer matrix [112]. The mechanical strength of the covalent bonds is the highest among the intermolecular interactions and the compatibility of grafted graphene oxide is much better due to the replacement of exposed functionalities. Polymers terminated with hydroxyl groups are directly used to crosslink the graphene oxide sheets with their carboxyl groups through esterification. The interfacial crosslinking dramatically increases the modulus of the nanocomposite, but the compliance can be compromised due to the permanent and interlocking structure caused by the covalent crosslinking [112]. The electrostatic interactions are also strong and restorable alternatives to covalent bonding for graphene oxides with polar functionalities. Due to the strong electrostatic interactions and restorability of these interactions during variable strain loading, the nanocomposites can be much stronger and tougher than their counterparts without graphene oxide fillers [3].

Hydrogen bonding between highly polarized donor and acceptor groups is abundant for graphene oxides. The epoxide, hydroxyl, carbonyl, and carboxyl groups on graphene oxide are all highly polarized with oxygen atom being the negative center [71]. As a result, graphene oxide can bond with various polar polymers, especially polyelectrolytes and proteins, through hydrogen bonding networks and polar interactions [113]. Due to the high density of the highly polar functionalities, the interfacial strength of the polymer-graphene nanocomposites with hydrogen bonding network can be as high as, if not higher, than that of the covalently crosslinked nanocomposites. The toughness of such hydrogen bonded nanocomposites is greatly improved due to the in situ restoration ability of the hydrogen bonds, which is another advantage over the permanent nature of the covalent crosslinking [64].

Graphene oxide has recently been suggested as amphiphilic material, meaning that their heterogeneous surface contains both hydrophobic and hydrophilic domains, which can interact concurrently with very different functionalities of hydrophobic and hydrophilic nature [114]. The amphiphilicity of graphene oxide suggests two important facts: (1) graphene oxide is readily bonded with either polar or non-polar polymers to improve the mechanical properties of the nanocomposites; and (2) the strength of the interface can be further improved if a matching heterogeneous polymer interfaces are chosen. For every domain on the graphene oxide surface, either hydrophobic graphitic areas or hydrophilic oxidized areas, the amphiphilic macromolecules can spontaneously assemble to maximize the interfacial interactions [115–118].

The common bondings for graphene-based materials, spatial range of interactions, and their relative strengths are compared in Table 1. Apparently, it is ideal to utilize all possible interactions in the nanocomposite, not only covalent bonding, to ultimately fabricate a strong, tough system. As indicated in Table 1, all the weaker interactions are restorable on site after being broken, which is favorable to facilitate the mechanisms of self-healing of nanocomposites.

2. Theoretical grounds for the selection of nanofillers

Due to the extreme contrasts in composition, interactions, and properties between the dissimilar components in nanocomposites, conventional models of composite reinforcement have limitations in describing the mechanical performances of the new materials with non-traditional reinforcing nanofillers. Therefore, in this section we will briefly present common models that are used to evaluate the mechanical properties of the nanocomposites based on the geometry, dispersion, and interfacial properties, and

their applicability to the graphene-polymer materials considered here.

Young's modulus is an intrinsic property under small elastic deformations. Unlike ultimate strength and ultimate strain, Young's modulus values only reflect the stress–strain behavior in the initial state of the loading process, and can be readily predicted by models. For example, the popular Takayanagi model for the fiber/laminate composite systems predicts simple rules of mixing under different types of stress transfers [2]:

$$E_{||} = E_m v_m + E_f v_f \tag{1}$$

$$\frac{1}{E_\perp} = \frac{v_m}{E_m} + \frac{v_f}{E_f} \tag{2}$$

where $E_{||}$ and $E_\perp$ represent the Young's modulus parallel and perpendicular to the direction of fiber axis or laminate plane, respectively; E_m and E_f are the Young's modulus of the matrix and the filler, respectively; v_m and v_f are the volume fractions of the matrix and the filler, respectively.

The Takayanaqi model assumes sharp interfaces, perfect bonding, and complete stress transfer across the interface. It is a reliable model for evaluating the upper ($E_{||}$) and lower ($E_\perp$) limits of the aligned fiber nanocomposites and laminated composites. However, due to the discontinuous nature of nanofillers, the Takayanagi model fails to include the end effect of the nanofillers, which plays a significant role in a well dispersed nanocomposite systems. Nevertheless, the model is still widely used for rough evaluation of the upper ($E_{||}$) and lower ($E_\perp$).

2.1. Models for particulate nanocomposites

Kerner has proposed another model to describe the lower limit of the shear modulus of the particulate-reinforced polymer composites with spherical particles and perfect particle/particle and particle/matrix bonding [2,119]:

$$\frac{G_c}{G_m} = \frac{(G_f v_f/a)+b}{(G_m v_f/a)+b}; \quad a = (7-5\sigma_m)G_m + (8-10\sigma_m)G_f; b = \frac{v_m}{15(1-\sigma_m)}. \tag{3}$$

where G is the shear modulus; σ is Poisson's ratio; v is the volume fraction; and subscripts c, m, and f represent composite, the polymeric matrix, and the particulate fillers, respectively. The number of components in the nanocomposite system is not limited, so it is suitable to analyze the complex multicomponent systems.

For particulate reinforced elastomers with carbon black and silica, Guth and Smallwood proposed a simple model to predict the lower bound shear modulus of the nanocomposite [2,120]. The increase in the shear modulus of the composite in this model is depends on the volume fraction of the particulate fillers. This model assumes perfectly spherical fillers, complete adhesive bonding, and uniform dispersion, which are challenging to realize in nanocomposites.

2.2. Models for nanocomposites with anisotropic fillers

The Halpin–Tsai model was developed for composites with nanoparticle fillers of various geometries, including rods, disks, and spheres [3,121]. It includes a shape factor to account for filler shape and is widely adapted for composite behavior analysis [40,64,122]. Also, the Halpin–Tsai model considers the distribution of 2D aligned anisotropic fillers as well as 3D randomly oriented fillers with different shapes. For composite materials with parallel aligned short platelets, the Halpin–Tsai equation is presented as [123]:

$$E_{||} = \left[\frac{1+2\alpha\eta_{||}v_f}{1-\eta_{||}v_f}\right]E_m \tag{4}$$

$$\eta_{||} = \frac{E_f/E_m - 1}{E_f/E_m + 2\alpha};$$

where $E_{||}$ and E_m are the Young's modulus of the parallel aligned nanocomposite and the matrix, respectively; α is the aspect ratio of the nanofiller. The Halpin–Tsai equation regresses to the rule of mixture for a high aspect ratio. When the aspect ratio is low (approaching spherical particles), the equation regresses to the common inverse rule of mixture for composite materials.

For randomly orientated nanoparticles, the Halpin–Tsai considers the contribution of the transverse mode, modifying its format to the following:

$$E_{random} = mE_{||} + nE_\perp \tag{5}$$

$$E_\perp = \left[\frac{1+2\eta_\perp v_f}{1-\eta_\perp v_f}\right]E_m; \eta_{||} = \frac{(E_f/E_m)-1}{(E_f/E_m)+2};$$

where m and n are the coefficients that evaluating the contributions from the longitudinal and the transverse modes [2,124].

Another development, the average-stress theory (Mori–Tanaka model) calculates the elastic stress field around an ellipsoidal particle in order to derive the longitudinal and transverse Young's moduli [125]:

$$E_{||} = \left[\frac{A}{A + v_f(A_1 + 2\sigma_m A_2)}\right]E_m \tag{6}$$

$$E_\perp = \left\{\frac{2A}{2A + v_f[-2\sigma_m A_3 + (1-\sigma_m)A_4 + (1+\sigma_m)A_5 A]}\right\}E_m \tag{7}$$

where A, A_1 through A_5 are model-specific coefficients that are primarily functions of the physical properties and geometries of the filler and the matrix [2,125]. By adjusting the geometry parameters of this model, the filler could be represented as high-aspect ratio fibers or platelets and even spheres. However, it should be pointed out that the Mori–Tanaka model treats the geometries of fillers based on ellipsoidal parameters, while the Halpin–Tsai model treats the fibers as cylinders and considers rectangular platelets.

Finally, Jäger–Fratzl model predicts the elastic modulus of the layered, nacre-like biocomposites, where the

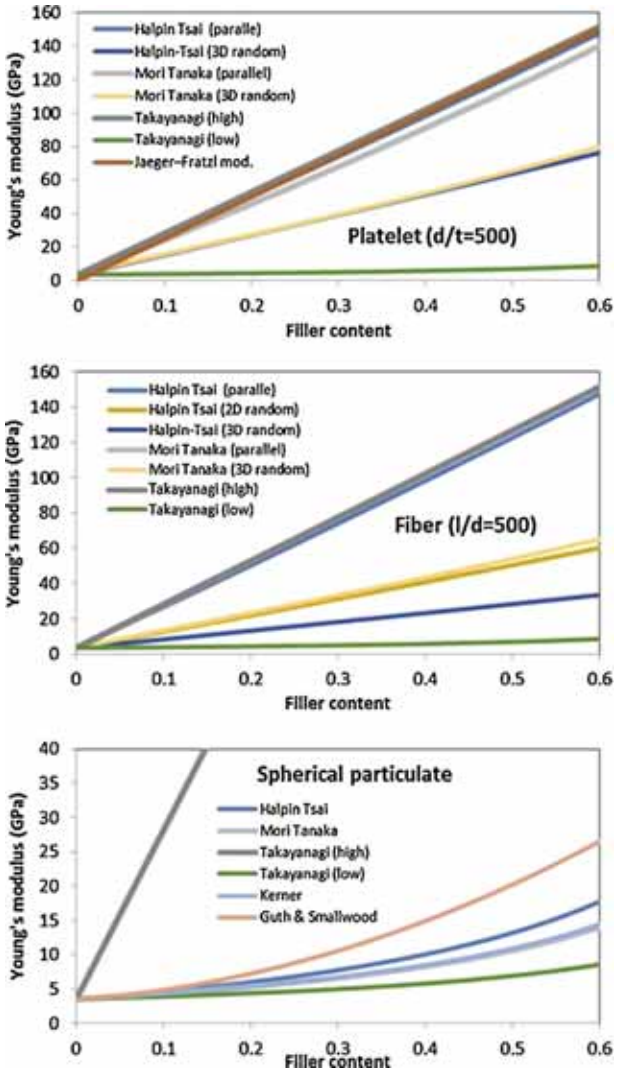

Fig. 5. Calculations of the theoretical values of elastic modulus predicted by different models described above with the elastic modulus of 150 GPa and 3.5 GPa, and Poisson's ratio of 0.25 and 0.4 for the filler and the matrix, respectively.

flexible polymeric matrix regressed to a minute binder of the dominating stiff inorganic phases in the form [126]:

$$E_c = \left[\frac{8\nu_m(1+\sigma_m)}{E_m\nu_f^2\alpha^2} + \frac{1}{\nu_f E_f}\right]^{-1} \quad (8)$$

In summary, to compare different models, we calculated the expected increase of the elastic modulus with increasing filler content for different filler shapes (Fig. 5). This comparative analysis shows that the careful selection of an appropriate model with consideration of composite properties and morphologies is critical for the prediction of the properties of nanocomposites.

It is striking to see that differences in the predicted values among various models can easily reach 200%. In general, spherical particulates have much weaker reinforcing effect on the nanocomposite properties. Randomly distributed platelets should result in the strongest isotropic nanocomposites, while aligned fibers or platelets exhibit a similar, but direction-dependent reinforcement effect in the anisotropic nanocomposites.

Overall, the existing mechanical models, which have been developed for conventional composite materials are generally suitable for coarse evaluation of the nanocomposite behavior. However, these models ignore some critical differences and unique characteristics of nanocomposites, such as developed interfaces and complex morphologies. For example, the models discussed above assume an ideal non-slipping boundary condition between the filler and the matrix, and sharp interface between them, which is not the case for graphene-polymer nanocomposites. More adequate mechanistic models should be developed especially those, which consider the role of interphases, end-to-end interactions, and extremely high specific interfacial area.

2.3. Interphases in nanocomposites

In the special case of nanocomposites, the large surface-to-volume ratio might result in high binding efficiency. On the other hand, the strong interfacial binding might alter the macromolecular conformation in the vicinity of the filler surface. Such a transitional zone might alter the properties of polymer matrix with gradual change across the interface. This region is called the "interphase" in contrast to the conventional sharp interface with an abrupt change in property and composition [127]. The additional reinforcing effect comes from the interphase layer of the polymer matrix.

The stronger, but ultrathin interphases are usually ignored in regular composites due to their minute contribution to the overall mechanical properties. In nanocomposite materials, however, the mechanical properties of the interphase region might play significant role. For example, an interphase model has been developed to account for the exceedingly high elastic modulus of polymer-graphene oxide nanocomposites [122,128]. The model assumes that the adsorption of polymers on graphene oxide surfaces alters the modulus of the adsorbed polymer layer. By estimating the modulus change, adsorption ratio, and the specific surface area of graphene oxide, the model adjusted the volume fraction of the nanofiller to an effective value after the polymer adsorption. In another recent study, Hu et al. suggested a different interphase model for layered graphene oxide nanocomposites [64], based on the deformational analysis of the layered elastic solids [129]. The model suggested correlated deformation of continuous interphases and described the experimental data for graphene oxide nanocomposites as will be discussed in detail below.

3. Processing of the graphene-polymer nanocomposites

The ultimate properties of graphene-based polymer nanocomposites are critically dependent upon the processing conditions in the course of nanocomposite fabrication [130–132]. The functionality of graphene components is critical to lower filler loading rate, make them highly dispersed and organized sheets within polymer

matrix to enhance overall performance of nanocomposites. In particular, the mechanical properties such as Young's modulus, ultimate tensile strength and strain, and flexural strength depend on the specific surface area, aspect ratio, organization, and loading content of graphene materials. The dispersion, interfacial strength, affinity of components, and spatial organization are all of great importance in determining the final stiffness, strength, toughness, and elongation of polymer nanocomposites under various loading conditions [133–137].

The pretreatment procedures and the fabrication methods control the fine morphology and physical/chemical properties of graphene-based polymer nanocomposites. For various graphene-polymer nanocomposites known to date, the extent of dispersion and exfoliation of graphitic layers is controlled by the applied shear force, temperature, and solvent polarity. Effective control of restacking, wrinkling, and aggregation of graphene sheets is required for the development of functional nanocomposites with high performance. In fact, extremely flexible and high-aspect ratio graphene components are prone to random wrinkling, buckling, or folding during processing, which dramatically affects the ultimate performance. In the case of the post-treatment, the degree of dispersion can be further influenced by the hydrophobic nature of reduced graphene oxide sheets and dewetting processes at the interfaces.

The choice of fabrication methods is determined by the surface functionalization of integrated graphitic sheets. Generally, traditional fabrication routines include solution-based processing [136,138–141] and melt-based processing [142–144]. Among most popular approaches for chemical modification and assembly are in situ polymerization, chemical grafting, latex emulsion blending, layer-by-layer (LbL) assembly, and directed assembly [3,145–149]. For the in situ polymerization method, intercalated monomers within expanded graphite clusters can promote their efficient exfoliation into single sheets throughout the polymer matrix caused by catalysis reactions [150].

Solution processing maximizes filler dispersion in polymer matrix by using pre-suspended single layered graphene sheets. Different solvents (aqueous to organic) can be used to dissolve graphene materials, including graphene oxide and reduced graphene oxide materials. This approach has been widely exploited due to its high dispersion efficiency, facile and fast fabrication step, and a high level of control on component behavior. Disadvantages of this approach are challenges in finding common solvents, toxic solvent utilization, thin-film limitation, difficulties in solvent removal, and common aggregation issues during mixing and solvent evaporation stages [151,152].

On the other hand, melt-based mixing is a solvent-free process in which applied mechanical shear force distributes the fillers in the polymer matrix using a screw extruder or a blending mixer [142,153]. This method allows stacked graphite or reduced graphene oxide sheets to be exfoliated into a viscous polymer melt by suppressing unfavorable interactions and inducing component dispersion. Melt mixing is recognized as a practical approach that can be adapted to the graphene-based polymer nanocomposites. However, thermal heating and high local mechanical stresses can affect the stability of components, flake shapes, and the reduction state of graphene oxide sheets. Several examples of various processing approaches are discussed below.

3.1. Examples of solution-based processing

Solution mixing methods have been employed as a powerful strategy widely utilized in a combination with high shearing (e.g., due to ultrasonication) for a range of common polymer matrices including poly(vinly alcohol) (PVA) [140,154], poly(methyl methacrylate) (PMMA) [138], polyurethane (PU) [136], and polyaniline (PANI) [155]. Water-soluble PVA, which is nontoxic and hydrophilic polymer, has been used for the fabrication of graphene oxide nanocomposite films by simple solution mixing, which enables the graphene oxide components to be dispersed on a molecular scale and aligned in the polymer matrix [156]. The authors suggested that the resulting homogeneous dispersion and preferential alignment of graphene oxide sheets in PVA matrix combined with the strong interfacial interactions are responsible for the much improved mechanical properties in the nanocomposite films.

In another case of solution-based process, intense ultrasonication was employed to exfoliate graphite oxide materials into single-layer graphene oxide sheets that results in better graphene oxide dispersion in the polymer matrix [157]. The effect of ultrasonication of the solution with graphene oxide on the final mechanical properties of GO-PVA nanocomposites was explored in another study [158]. Here, graphene oxide solution treated under different ultrasonication conditions was then mixed with the PVA solution, and stirred at room temperature. The ultrasonication time was considered as a critical factor to determine the ultimate reinforcement in a nanocomposite system via the controlled exfoliation of graphene oxide component. The fabrication of nanocomposites with fully exfoliated graphene oxide sheets and maximum sheet size was demonstrated for optimal ultrasonication power.

Recently, Wajid et al. reported a comparative study of a freeze drying and solution mixing strategies for high-strength conductive pristine graphene/epoxy nanocomposites [159]. Aggregation-resistant polyvinlypyrrolidon (PVP)-stabilized graphene dispersions have been obtained with the choice of the matrix in consideration. The authors demonstrated that PVP modification can effectively stabilize the graphene component and enhances the interfacial interactions between graphene filler and matrix due to the polarity and affinity of the ring structure on PVP component. Additionally, polymer-stabilized graphene dispersions in water can be freeze-dried and then re-dispersed with stirring and sonication prior to the final curing process. The authors reported that the ability to increase dispersion of graphene component led to enhanced mechanical properties by about 40% at 0.46 vol% of graphene loading. Moreover, the nanocomposites also showed a very low electrical percolation threshold at 0.088 vol% of graphene content.

Poly(ε-caprolactone) (PCL) is a biodegradable and biocompatible aliphatic polyester with good resistance to

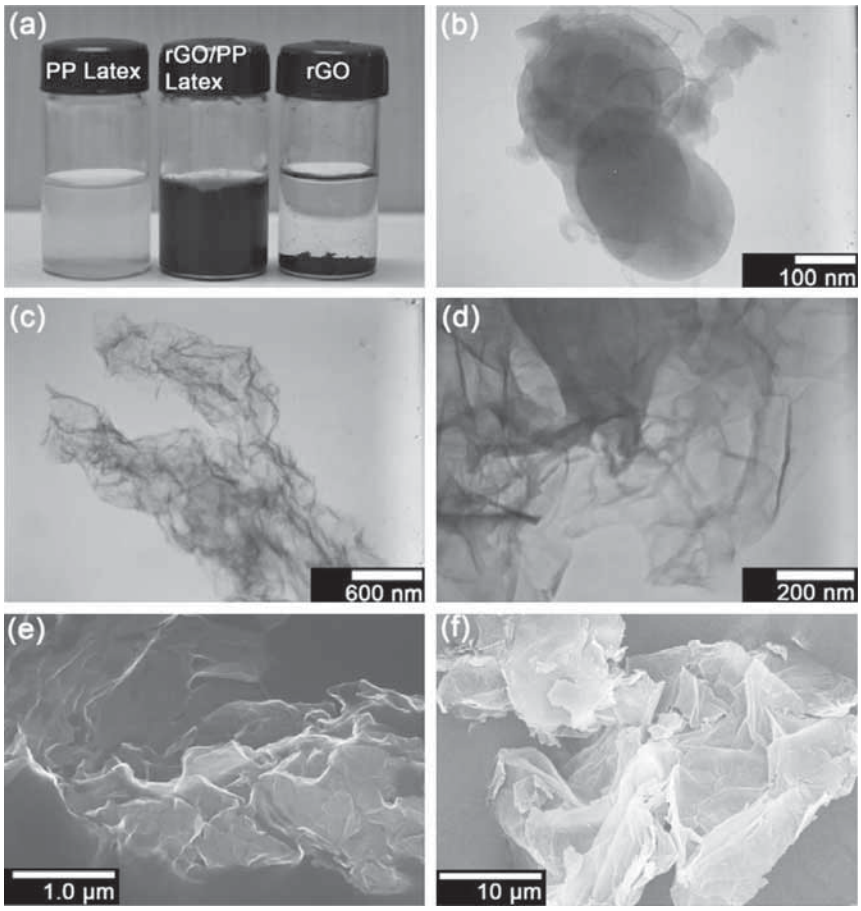

Fig. 6. (a) Aqueous suspensions of PP latex and graphene oxide. (b) TEM image of PP latex. (c) and (d) TEM images of the rGO/PP latex composite dispersed in water before filtration. (e) SEM image of fracture surface of the rGO/PP composite (after hot-press molding). (f) SEM of agglomerated rGO nanosheets [161]. Copyright 2013.
Reproduced with permission from Elsevier Ltd.

water, solvents and oil, which is synthesized for biomedical and biomaterials applications [160]. Sayyar et al. reported a fabrication route for obtaining graphene-polymer nanocomposites by covalent bonding of PCL and well dispersed, chemically reduced graphene oxide for biodegradable tissue engineering [160]. The covalently linked and chemically reduced graphene-based nanocomposite showed improved mechanical properties and electrical conductivity for nanocomposites with homogeneously dispersed graphene filler. The subsequent chemical bonding of the components after rigorous solution mixing was critical for the stabilization of the finely dispersed morphology and the strong interfacial bonding between components.

A popular semi-crystalline thermoplastic polymer, polypropylene (PP) is employed in capacitors due to its outstanding dielectric properties. It has been demonstrated that the dielectric constant of PP can be substantially modified if conductive graphene is incorporated. Wang et al. developed a graphene-filled nanocomposites by mixing PP latex with graphene oxide (Fig. 6) [161]. The reduced graphene oxide (rGO) mixed with PP matrix was prepared through an emulsion polymerization followed by a in situ chemical reduction of graphene oxide and a subsequent filtration.

The introduction of latex-type morphology has been recognized as a versatile and environmental friendly approach to fabricate polymer nanocomposites with a fine dispersion and spatial stability as compared to traditional melt mixing of bulk polymer components [161]. The rGO/PP nanocomposites prepared by the emulsion method revealed the homogeneous dispersion of reduced graphene oxide sheets in the PP matrix, which facilitates strong interactions at the interface (Fig. 6). Moreover, an ultralow percolation threshold of 0.033 vol% was observed with the dielectric permittivity of the nanocomposites increasing by three orders of magnitude above this limit.

In another study, Lalwani et al. reported a thermal crosslinking method for laminated polymeric nanocomposites and investigated the efficacy of graphene nanostructures as reinforcing agents for highly cross-linked nanocomposites [162]. Biodegradable and biocompatible nanocomposites have been prepared from polypropylene fumarate (PPF) with very low concentration of reinforcing graphene component of 0.01–0.2 wt%. The graphene oxide sheets have been dispersed under sonication as individual nanoparticles in the PPF polymer matrix with high cross-linking density. The resulting nanocomposites showed significantly improved mechanical properties, which were considered appropriate for bone tissue engineering.

3.2. Examples of melt-based processing

In a recent study, melt mixing under a high shear force has been employed for the fabrication of graphene-based nanocomposites with polylactide (PLA) and polyethylene terephthalate (PET) as matrices [163–165]. As another example, elastomer/graphene platelets nanocomposites have been developed by a melt compounding method [166]. Thick graphene platelets (partially exfoliated materials) from graphite intercalated compounds obtained using thermal shock followed by ultrasonication were exploited in this study. This material was mixed with an elastomer – ethylene–propylene–diene monomer rubber (EPDM) using a two-roll mill and then crosslinked through vulcanization. Increased graphitic contents led to the enhanced tensile strength and reduced strain at fracture due to confinement effects. Electrically and thermally conductive elastomeric nanocomposites have been obtained with a modest percolation threshold.

It has been demonstrated that the melt extrusion process promotes the exfoliation of reduced graphene oxide in various polymer matrices of different polarity, such as isotactic poly(propylene) (iPP), poly(styrene-co-acrylonitrile) (SAN), polyamide 6 (PA6) and polycarbonate (PC), yielding thermoplastic nanocomposites with uniformly dispersed graphene materials [167]. Similar to the conventional expanded graphite, graphene oxide can be converted into thermally reduced graphite oxide with very low bulk density by a rapid thermal heating process. In that study, the reduced graphite oxide materials were obtained by oxidation of graphite followed by thermal expansion at 600 °C. As a result, the functionalized graphene with large specific surface areas of 600–950 $m^2 g^{-1}$ exhibited exfoliation during processing.

Enhancement of the flame retardancy with addition of graphite oxide has been attributed to the oxidation barrier of natural graphite and the graphite oxide [168]. To exploit this phenomenon, graphite oxide with different oxidation degrees or graphene materials were blended with PS matrix to serve as a flame retarding additive. Melt mixing the graphite oxide and graphene with the PS was conducted under different melt-mixing conditions. The incorporation of low concentration of graphene (5 wt%) showed the enhanced flame retardant properties (increased by 50%) compared to the pristine PS material.

Melt mixing can be employed for post treatment after solution processing as described in a recent study [169]. Song et al. presented PP nanocomposites with homogeneous dispersion of CNTs and reduced graphene oxides obtained via a facile polymer-latex-coating. A combination of this routine with subsequent melt-mixing has been considered for developing an advanced hybrid nanocomposites. PP-based nanocomposites were obtained by mixing graphite oxide and CNTs with PP latex (a water-based emulation of maleic anhydride grafted isotactic polypropylene), followed by a reduction of graphite component to the partially reduced state. The ternary system of PP/rGO/CNTs showed a continuous interconnected network of reduced graphite oxide and CNTs (Fig. 7) [169]. This processing strategy enabled the uniform dispersion of two

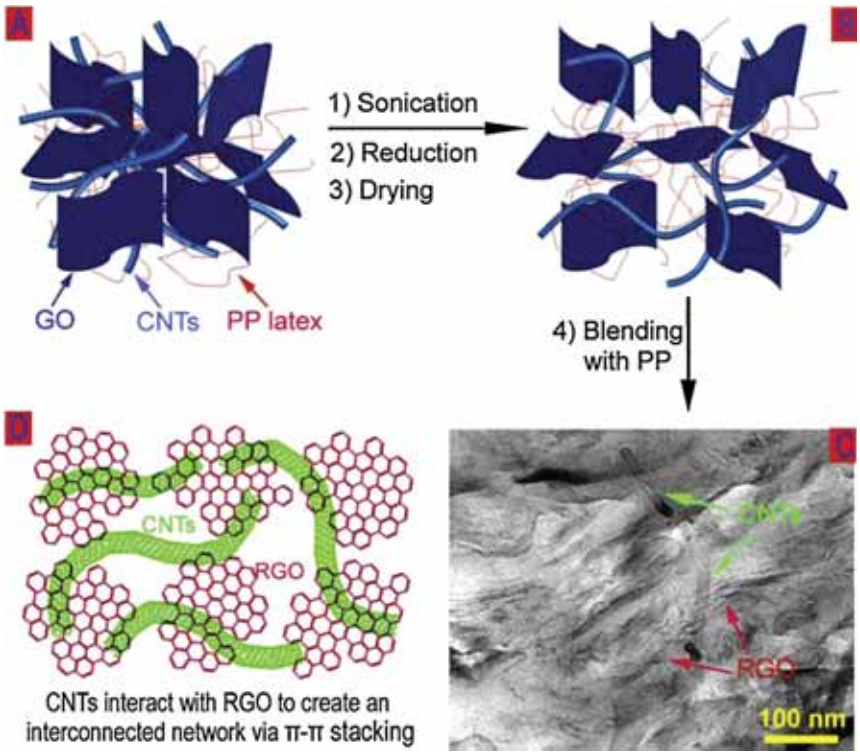

Fig. 7. (A) and (B) The formation from interconnected network of rGO and CNTs using PP latex as a dispersing agent. (C) TEM image of PP/RGO/CNTs ternary system. (D) Schematic of strong interactions between RGO and CNTs via stacking [169]. Copyright 2013.
Reproduced with permission from the Institute of Physics.

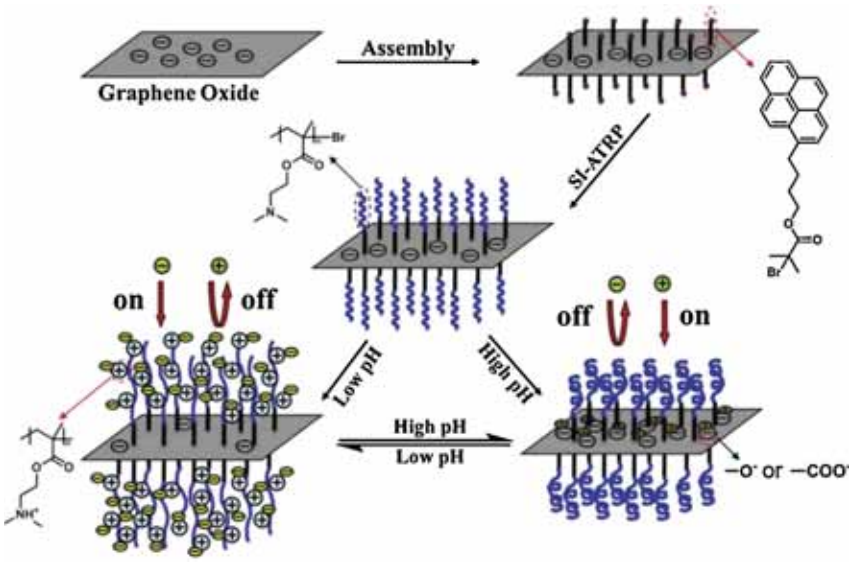

Fig. 8. The preparation from PDMAEMA-modified graphene oxide and charging state of the GO-g-PDMAEMA composite at different pH values [170]. Copyright 2013.
Reproduced with permission from John Wiley & Sons Inc.

different carbon components that resulted in remarkable multiple synergy in their mechanical properties, electrical and thermal conductivity.

The formation of the strong chemical bonding between graphene sheets and polymer matrices via covalent interactions has been considered an attractive route for the modification of functionalized graphene oxide components with mostly preserved intrinsic structure and properties. In recent study, Gao et al. demonstrated the efficient grafting of poly[(dimethylamino)ethyl methacrylate] (PDMAEMA) brushes onto graphene oxide sheets via "grafting – from" process [170,171]. A two-step grafting methods included a non-covalent modification of graphene oxide surfaces by pyrene terminated initiator via π–π interaction followed by in situ surface-initiated atom transfer radical polymerization (SI-ATRP) (Fig. 8).

The resulting positively charged PDMAEMA brush layer has been used for the modification of the negatively charged graphite oxide sheets to produce GO-g-PDMAEMA hybrid fillers. These nanostructures exhibit zwitterionic behavior because of the presence of different functional groups including phenol hydroxyl, carboxyl, and amine groups and further demonstrated the ability of these composite systems to serve as a template for metal nanoparticle synthesis [170].

Based on a similar brush-modification approach, Shen et al. proposed an efficient strategy for the chemical modification of graphene oxide sheets and demonstrated the preparation of polycarbonate (PC)/(GO-epoxy) nanocomposites with strong interfacial interactions [172]. In this study, an epoxy-containing layer was coupled to graphene oxide sheets via the "grafting to" method and then mixed with PC matrix by solution casting. In addition, terminal epoxide groups were exploited to covalently connect two graphene oxide sheets together, which resulted in the efficient crosslinking of graphite oxide layers via a coupling reaction. The residual functionalized sites in the grafted epoxy chains also formed chemical bonds with the PC matrix, leading to the enhanced mechanical properties of these nanocomposites.

The high pseudocapacitance of PANI arising from the versatile redox reactions and corresponding color changes allow for use in electrochemical capacitors and for electrochromic colorimetric applications [173,174]. Wei et al. described a facile electropolymerization method for the preparation of PANI-graphite oxide nanocomposite films by electrodeposition of aniline monomers in sulfuric acid solution onto indium tin oxide (ITO) coated with graphite oxide. In another study, Zhu et al. reported the interfacial polymerization method for the fabrication of PANI nanofibers with graphite oxide materials with excellent interfacial strength and the enhanced specific surface area [175]. The elongated fibrous structures were synthesized via a facile surface initiated interfacial polymerization method. A random growth of PANI fibers derived from the PANI coated graphite oxide sheets were instrumental in enhanced interfacial strength.

In an alternative approach, Ning et al. reported the one-step template-free polymerization of 3D hybrid materials composed of 2D fish scale-like PANI morphologies on graphene oxide sheets and carbon nanotubes [176]. These multicomponent nanomaterials were synthesized by a one-step process using a simplified template-free oxidative polymerization method. As a result, complex 3D microstructures were assembled from hybrid PANI nanosheets combined with graphite oxide sheets. In this approach, the graphite oxide sheets were readily dispersed in an aqueous solution and further acted as nucleation sites for PANI deposition to fabricate hybrid reinforcing elements.

In situ polymerization has also been demonstrated to provide another efficient means to help intercalate the graphene fillers in diverse polymer matrices including PS, PMMA, polystyrene sulfonates (PSS), polyimides (PI), and PET [177–179]. One study demonstrated graphene oxide/PI nanocomposites based on 4,4-bisphenol A dianhydride,

4,4-oxydiphthalic anhydride, and diaminodiphenyl methane (MDA) as comonomers [180]. In one example, the addition of a small amount of graphite oxide component (0.03–0.12 wt%) was found to significantly improve the mechanical properties of PI nanocomposites without a substantial decrease of film transparency (sustained above 80% in 500–800 nm range).

Overall, although solution and melt mixing methods offer many benefits in the processing of graphene-based polymer nanocomposite in terms of scalability and processing time, they are limited in the level of control of the microstructure due to predominantly random distribution of the flexible fillers during mixing process and their easily crumpling and folding. To obtain higher ordering, uniform alignment, unfolded states, and control over the orientation of loaded graphene sheets a step-wise LbL assembly considered in several recent studies is discussed in the next section.

3.3. Layer-by-layer (LbL) assembly of graphene components

As is well known, LbL assembly is an efficient fabrication approach for the development of ultrastrong and robust thin and ultrathin films, membranes, and coatings with high strength, controlled adhesion, flexibility, and environmental stability [181–186]. These organized layered assemblies can provide a route to precisely engineer the graphene-polymer interface and control the distribution and content of graphene component on a molecular level by alternating deposition of complementary components from graphene filler suspension and polymer solution [75]. Furthermore, the morphology of the nanocomposite films can be finely tuned by the deposition mode, solvent removal procedure, or applied shear force through either direct dipping or spin and spray assisted LbL methods. On the other hand, vacuum-assisted assembly employs micro-flow at the filter/solution interface thus making the deposition process continuous [64]. However, the vacuum-assisted method might not control precisely the arrangement of different components in the resulting nanocomposite paper.

To date, few studies have employed LbL assembly for the fabrication of graphene-based nanocomposites. However, the use of graphite oxide layered assemblies was demonstrated in 1996 for the intercalated graphene oxide and poly (diallyldimethylammonium chloride) (PDDA) components [187]. The chemical and electrochemical post-reduction led to conductive nanocomposite films with high structural uniformity and chemical stability. In a later study, Kovtyukhova et al. investigated multilayer assemblies by alternate adsorption of anionic colloidal graphene oxide sheets and cationic poly (allylamine hydrochloride) (PAH) [188]. Multilayer films have been formed by dip-assisted LbL assembly, which facilitated controlled coverage on the substrate and low surface roughness. Cassagneau et al. reported multilayer assembly of graphene oxide and polyelectrolytes (PDDA/GO/PEO) by a dip-assisted LbL method based on electrostatic and epitaxial adsorption of polymers for lithium ion battery electrode applications [149].

Zhao et al. fabricated multilayer films of PVA and exfoliated graphene oxide by a hydrogen bonding LbL method and measured their mechanical properties [189]. The dip-assisted LbL fabrication enabled the formation of the uniform ultrathin multilayer nanofilms with high homogeneity in morphology and flake orientation and led to a significant improvement of mechanical strength and a manifold increase of nanocomposite strength with respect to the original polymer matrix.

In recent development, Zhu et al. compared the mechanical and electrical properties of the PVA/rGO nanocomposites with the same composition fabricated by either dip-assisted LbL assembly or vacuum-assisted method [190]. Their results revealed that the mechanical properties are largely determined by the micro-morphology of the well-layered nanocomposites, which is concluded from the almost identical mechanical properties of both series of samples. On the other hand, the electrical conductivities are predominantly affected by the dispersed nanostructures because the transportation of electrons is predominantly dependent on the tunneling barrier among the finely distributed conductive components.

Recently, Li and coworkers fabricated hybrid multilayered films based on negatively charged graphene oxide nanosheets and polyoxometalate clusters with cationic polyelectrolytes using traditional dip-assisted electrostatic LbL assembly [113]. Film formation was followed by UV photoreduction of graphene oxide sheets by taking advantage of the photocatalytic activity of embedded clusters without the use of toxic chemicals. This approach enabled the formation of uniform and large-area nanocomposite films with precisely controlled thickness on various substrates by varying the number of deposited graphene oxide layers.

In a study from our group, ultrathin free-standing graphene oxide/polyelectrolyte multilayers were fabricated based synthetic polyelectrolytes (PSS/PAH) by a spin-assisted LbL assembly in a combination with Langmuir Blodgett (LB) deposition (Fig. 9) [3]. This combined LbL-LB fabrication strategy facilitated the fabrication of a highly integrated nanocomposite membrane with large lateral dimensions (centimeters) and a thickness of around 50 nm by suppressing wrinkling and folding of graphene oxide sheets during deposition procedure. Micromechanical measurements on these freely suspended nanocomposite membranes revealed dramatic enhancement of the mechanical properties with the elastic modulus increased by an order of magnitude to about 20 GPa at only 8.0 vol% graphene oxide loading content (see more discussion below) [3].

In subsequent study, Hu et al. demonstrated ultrathin, robust nanocomposite papers obtained with spin-assisted LbL assembly by incorporating graphene oxide sheets into silk fibroin matrix through heterogeneous surface interactions [64]. Remarkable mechanical properties of these LbL membranes were attributed to the effective coupling of the graphene oxide filler with the silk fibroin matrix. Both polar random silk domains and the hydrophobic β-sheet nanocrystals interact with oxidized and graphitic regions of graphene oxide sheets via all hydrogen bonding, polar-polar, and hydrophobic–hydrophobic interactions.

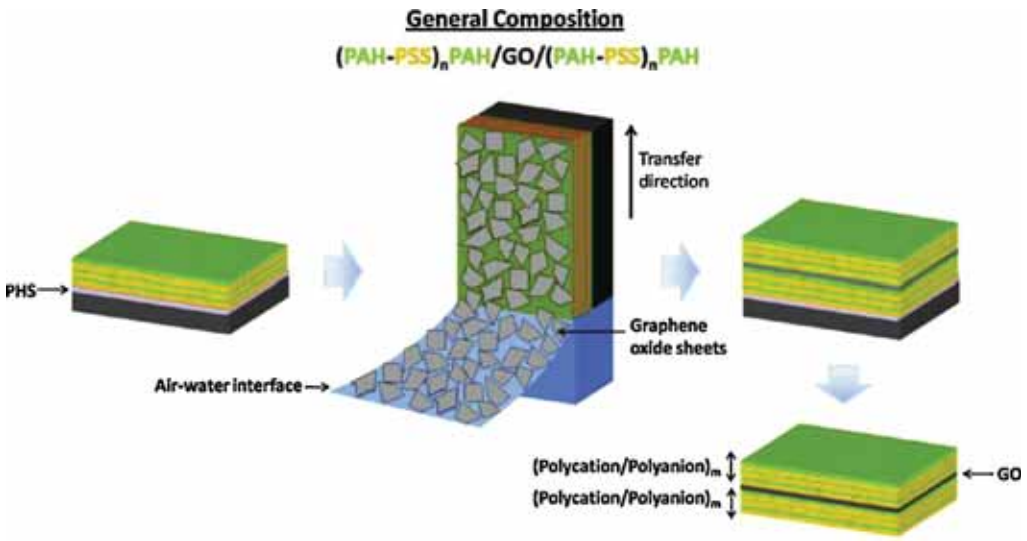

Fig. 9. Fabrication from ordered and hierarchical multilayered graphene oxide-polyelectrolyte nanomembranes via combination from LbL and LB techniques [3]. Copyright 2010.
Reproduced with permission from the American Chemical Society.

In another example, conductive nanocomposite films from PS microspheres wrapped by graphene oxide sheets were prepared via LbL assembly followed by graphite oxide reduction [191]. The nanocomposite films with a graphene conductive network were fabricated by hot pressing graphene-wrapped PS microspheres into thin films with network-like morphology. The use of PS polymer latex facilitated the uniformity of the graphene filler distribution in the polymer matrix. The combination of latex technology and LbL assembly offers a facile, efficient, and environmentally friendly method for the fabrication of electrically conductive graphene/PS nanocomposites with well-developed network morphology.

Supramolecular self-assembly has also been recognized as a method to enhance the interfacial adhesion based on diverse chemical functionality [192]. An interface-mediated assembly method has been exploited for the fabrication of micelle-decorated graphene oxide sheets with ordered polymer morphology. Amphiphilic heteroarm star copolymers (PS_nP2VP_n and $PS_n(P2VP\text{-}b\text{-}PtBA)_n$ ($n=28$ arms)) were adsorbed on the pre-suspended graphene oxide sheets at the air-water interface due to the peculiar surface activity of graphene oxide sheets. The resulting nanocomposites were composed of flat graphene oxide sheets uniformly covered with a highly ordered and discrete assemblies of unimolecular micelles of amphiphilic star macromolecules in pancake conformation. This organized morphology of polymer material at graphene oxide sheets has been attributed to the strong affinity among positively charged pyridine groups of star polymers onto the negatively charged basal plane and the edges of graphene oxide (Fig. 10).

Nanocomposites of PVA matrix with functionalized (sulfonated) graphene oxide components show fibrillar, dendritic and rod like structures under different processing conditions [193]. Since reduced graphene oxide has a limited dispersion in aqueous medium, the anchoring of $-SO_3H$ group on the graphene oxide surface prior to chemical reduction with hydrazine offers a promising method for producing a highly conducting and dispersible graphene-based materials in an aqueous medium. The fibrillar morphology, highly branched dendritic morphology, and rod-like structures were all observed due to hydrogen-bonded controlled supramolecular organization with different balances of interfacial interactions.

To follow the preceding discussion of various processing routines, in the next section, we consider the mechanical properties of resulting nanocomposites in conjunction with their composition, morphology, and processing conditions.

4. Mechanical properties of graphene-polymer nanocomposites

It is well known that strong mechanical interfaces are critical for the fabrication of tough nanocomposites as has been briefly been discussed above [194,195]. Carbon nanomaterials also offer an advantage of fabricating multi-functional nanocomposites with high electrical and thermal conductivities along with strong mechanical properties. The most important factor along with the increased specific interfacial area is the control of the stress transfer across the interface, which can be achieved by means of covalent bonding, electrostatic interactions, hydrogen bonding, or van der Waals interactions [196–198]. It is expected that the strength of the filler material would dominate the properties of the nanocomposite material but, in fact, it is the interfacial strength that usually controls the ultimate mechanical properties. Fine dispersion of a reinforcing component determines the high specific interfacial area. Poor dispersion and excessive aggregation of the carbon nanomaterials in the polymer matrix results in a decreased interfacial area along with weaken interfaces thereby leading to poor mechanical properties.

Fig. 11 shows the different scenarios encountered during polymer nanocomposite fabrication with laminated reinforcing materials [199]. It is widely accepted

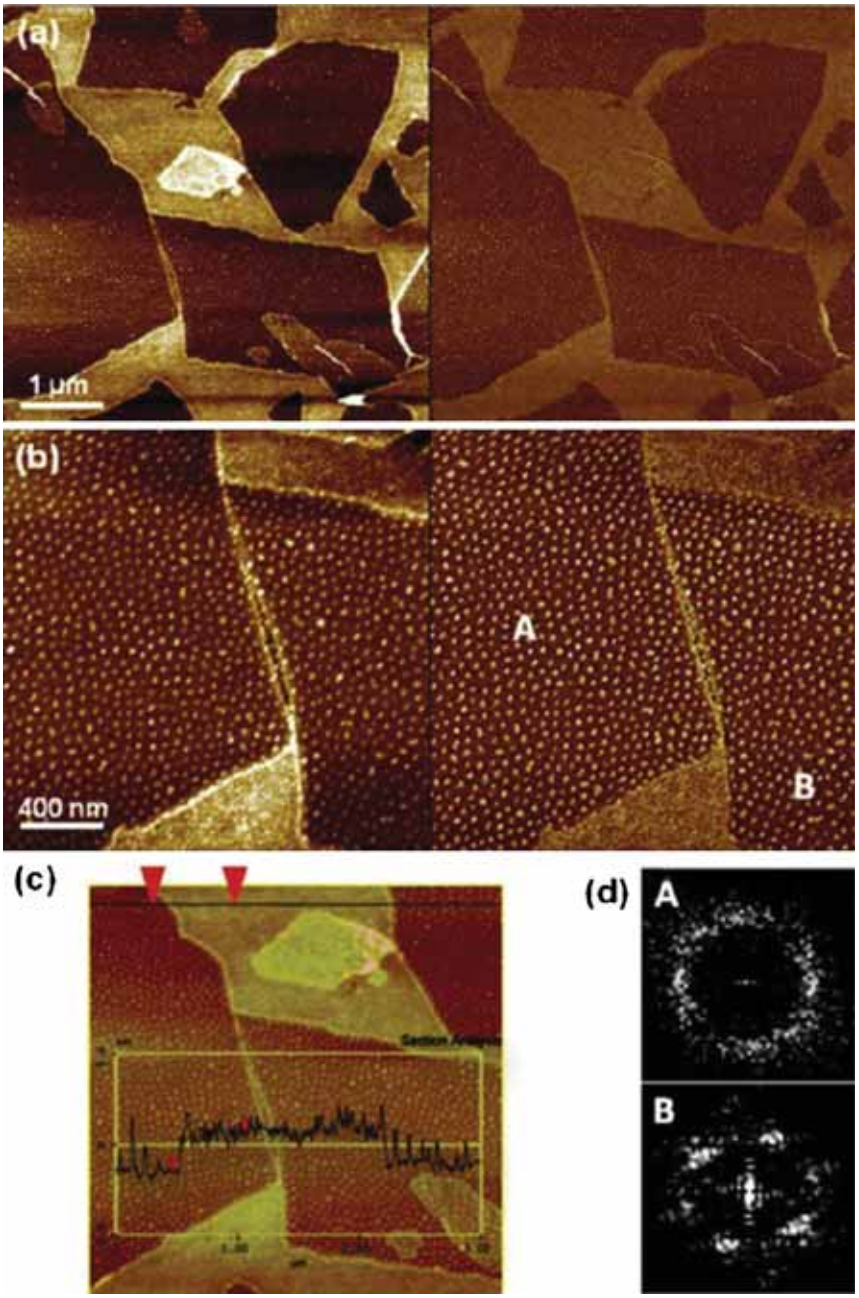

Fig. 10. AFM topography (left) and phase (right) of (a and b) GO/$PS_{28}P2VP_{28}$ star copolymer at pH 2 for surface pressures of 15 mN/m; (c) the height profile of corresponding topography image; (d) FFT of domain morphologies for A and B regions from Fig. 10b. *z*-scale: 5 nm (topography) and 30° (phase) [192]. Copyright 2013.
Reproduced with permission from the American Chemical Society.

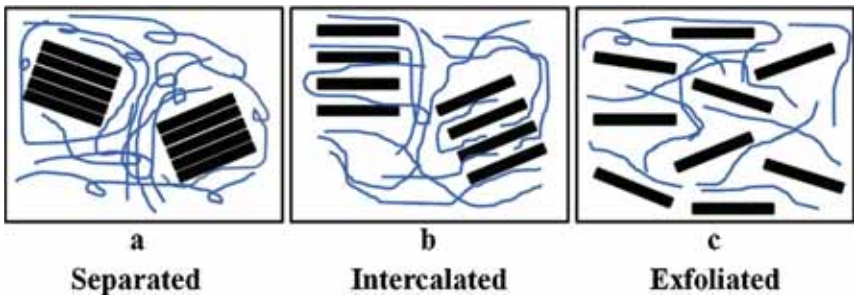

Fig. 11. Representative dispersing scenarios of laminated nanofillers in polymer matrix [199]. Copyright 2012.
Reproduced with permission from InTech.

that the efficient exfoliation of stacked laminates followed by intercalation can improve the interfacial strength and dramatically rise the interfacial area thus leading to stronger nanocomposite materials. Efficient intercalation can lead to stronger interfacial interactions and a localized improvement in the properties. Thus, a uniform dispersion and exfoliation of graphitic components inside the polymer matrix are important for improved performance.

Carbon nanomaterials are usually difficult to disperse in the polymer matrix and their simple mixing results in the formation of a weak interface and significant aggregation, leading to poor mechanical properties if special efforts are not applied [200,201]. Most frequently, carbon nanomaterials are functionalized to ease the dispersion and improve the chemical interactions with the polymer matrix. Numerous studies on functionalization of the carbon materials have been reported [132,202,203]. Nevertheless, the properties of these nanocomposites still falls short of the expected characteristics, considering the superior properties of many nanofillers. Theoretically, it is not possible to achieve a complete stress transfer across the interface, but a strong interface with the efficient stress transfer is essential to maximize the mechanical strength [204]. However, further development might be hindered due to a poor dispersion of these reinforcing nanostructures within the polymer matrix.

The mechanical properties of a nanocomposite material are judged based on the enhancement of the performance as characterized by the elastic modulus, tensile strength, elongation, and toughness [205]. It is difficult to obtain a multicomponent material exhibiting record values for all these factors due to conflicting reinforcing mechanisms. Usually, efforts to improve one of these characteristics show an adverse effect on the other factors. Thus, selective improvement of one or more of these mechanical characteristics is usually considered as a priority depending on a specific end-application.

Many applications require high toughness thus requiring a balance between increasing mechanical strength, elastic modulus, and the preservation of materials compliance. Considering that toughness relates to overall energy dissipation and is formally evaluated by the area under the stress–stain curve, a material that can withstand high stress under maximum elongation will possess the highest toughness. Adding stiff nanofillers and tailoring strong polymer-filler interactions, a usual routine for reinforcement, frequently results in higher elastic modulus and mechanical strength but lower ultimate elongation. However, more compliant interfacial interactions might result in a slippage mechanism to be activated at the polymer-filler interface well before the ultimate fracture. The materials would eventually fail under higher load and thus demonstrates higher toughness. Consequently, finding the optimum combination of reinforcing and deformational mechanisms should be carefully considered for the design of graphene-polymer nanocomposites with ultimate mechanical performance.

Graphene-based derivatives are mechanically strong but flexible that makes them an ideal nanofiller component for the fabrication of high-performance multi-functional polymer nanocomposites with high toughness [70,130]. Graphene oxide components incorporated into different polymer matrices might result in a dramatic improvement in the mechanical properties such as elastic modulus, tensile strength, elongation, and toughness. A high level of dispersion and a rich balance of interfacial interactions play key roles, as will be illustrated in the following with selected examples from recent studies.

4.1. Graphene papers

Graphene oxide sheets can be assembled into highly layered "paper" as fabricated by a vacuum-assisted assembly technique [97,112,130,131]. These popular strong "paper" materials show very good mechanical properties including elastic modulus of 30–40 GPa, strength of 120 MPa, and toughness of 0.26 MJ m^{-3} [130]. Chen et al. reported similar paper materials using reduced graphene oxide and achieved 300 MPa ultimate strength, around 40 GPa elastic modulus, and higher toughness of 1.22 MJ m^{-3} [206]. However, despite these examples, the ultimate values reported are still well below those of the pristine graphene oxide materials or predicted by mechanical models. Furthermore, the reported mechanical properties of the graphene oxide papers are frequently divergent, inconsistent, poorly reproducible, and difficult to control [131,207].

In the original graphene paper materials, water molecules were considered to be intercalated between the graphene oxide flakes [131]. Submolecular water layers are suggested to act as a binder, which enables the hydrogen bonding network between water molecules and the oxygen-containing functionalities on the surface of the graphene oxide, thereby, linking the neighboring flakes together. However, hydrogen bonding represents weak forces compared to ionic or covalent interactions and even a high density of the bonding network might be compromised by a high mobility of small molecules. Moreover, an excessive amount of water can act as a plasticizer or lubricant in the layered graphene oxide paper that can compromise its mechanical strength. As an alternative option, borate-assisted crosslinking of graphene oxide paper has been suggested to fabricate extremely strong, yet, brittle materials [95].

Additional crosslinking of graphene oxide sheets in the multi-layered papers has been suggested to improve mechanical performance [97,112,208]. It is plausible to employ flexible polymers with proper functionalities as the binder in graphene oxide materials with various oxidized surface functionalities. For example, the carboxyl functional groups primarily located around the edge of the graphene oxide flakes are available for chemical crosslinking with amine groups to reinforce the inter-flake binding.

Cheng et al. reported successful crosslinking of graphene oxide flakes with 10, 12-pentacosadiyn-1-ol (PCDO) monomers via esterification (Fig. 12a) [112]. The monomers can be polymerized after intercalation to form a conjugated polymer with an integrated network of covalently bonded graphene oxide sheets.

The resulting material in this study is significantly tougher than the regular graphene/graphene oxide based polymeric nanocomposites without crosslinking. The

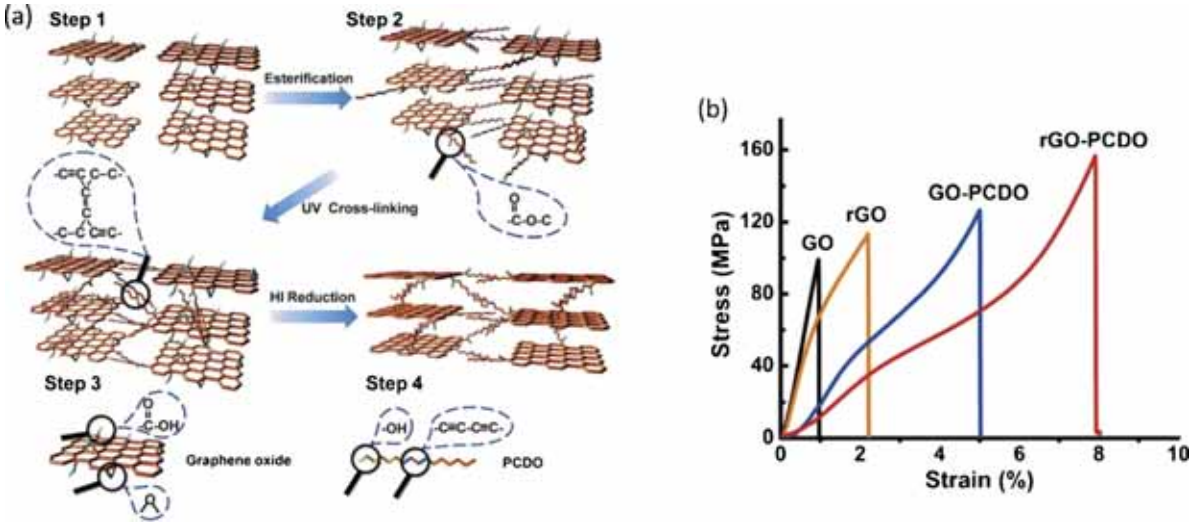

Fig. 12. Schemes of the esterification, crosslinking, and reduction from the graphene oxide nanocomposites and corresponding changes of mechanical properties [112]. Copyright 2013.
Reproduced with permission from John Wiley & Sons Inc.

toughness reached a record value of about 3.0 MJ m^{-3}, with a 120 MPa tensile strength, and significant, 5%, elongation to break. The authors attributed such outstanding mechanical properties to multiple strengthening mechanisms, including hydrogen bonding, entropic elasticity of the polymeric binders, covalent bonding between the graphene oxide and the polymer, as well as between polymer chains. The chemical reduction of graphene oxide further improved the mechanical properties of the nanocomposite, resulting in a tensile strength of about 160 MPa, 8% elongation to break, and around 4.0 MJ m^{-3} toughness (Fig. 12). The crosslinking through the edge functionalities is inspiring because such reinforcement maintains the hydrogen bonds. This network acts at the initial stress thus facilitating large flexibility and compliance with covalent bonding adding strength at small strain. The synergistic strategy employed in this research is important for developing robust graphene-based polymer nanocomposites.

A recent study employed silk fibroin as a biopolymeric binder to crosslink the graphene oxide flakes with a highly ordered layered morphology (Fig. 13) [105]. Heterogeneous functionalities of silk fibroin multidomain backbones act as a natural "universal" binder with hydrophobic–hydrophilic interactions, which matches random oxidized domains and graphitic functionalities on the surfaces of graphene oxide flakes. Such a balance facilitates the outstanding mechanical properties of the layered nanocomposites, greatly improving the ultimate strength, strain-to-failure, elastic modulus, and toughness of the graphene-silk nanocomposite films to the value of 150 MPa, 2.8%, 14 GPa, and 2.7 MJ m^{-3} respectively by intercalating only 5 wt% of silk fibroin.

Further reinforcement of nanocomposite films can be realized by controlled conditions to reduce the graphene oxide sheets using a green and facile aluminum reduction strategy, with a defined depth and pattern of microscopic regions [105]. The toughness of the chemically reduced graphene nanocomposite films was not compromised as a result of this treatment, but the strength increased by 100%, to above 300 MPa, and the elastic modulus increased to 26 GPa (Fig. 13). Patterning of the reduced graphene oxide surface has also been demonstrated with high resolution and uniformity for a large area (Fig. 13e and f). The mild and environmental friendly strategy to restore the electrical properties and dramatically improve the mechanical properties introduced in this study can be widely applied to almost all graphene oxide based nanocomposite materials without the concern of excessive damage of the polymeric binders that is always a critical issue if the traditional harsh and toxic reducing techniques are employed.

Park et al. reported robust paper materials from graphene oxide sheets crosslinked by polyallylamine (PAA) [97]. PAA contains periodic reactive amine groups along the polymer backbones which are ready to react with the oxygen-containing functionalities on graphene oxide surfaces (Fig. 14a). By adding 21% of PAA in the graphene oxide suspension and by employing extensive sonication, the homogeneous mixture can be initially formed. After filtration of this suspension, uniform paper-like morphologies can be achieved. The mechanical properties of the PAA-cross-linked graphene oxide paper are somewhat improved as compared to the non-modified graphene oxide paper (Fig. 14).

The ultimate stress increased from 82 MPa to 91 MPa, whereas the ultimate strain slightly decreased from 0.4% to 0.32%. A significant improvement was observed in the elastic modulus values of the nanocomposites as well. The elastic modulus measured at three different stages of loading (i.e., initial, straightening, and maximum) was significantly higher for the graphene oxide paper with PAA-modified components, reaching the highest value of 33 GPa (Fig. 14b). The authors suggested that the modification of graphene oxide with a PAA component is critical for efficient mechanical reinforcement by chemical crosslinking, but the overall reinforcing effect is modest when compared to the other results reported in literature.

The subdued effect on the mechanical properties of the PAA-crosslinked graphene-polymer nanocomposites may

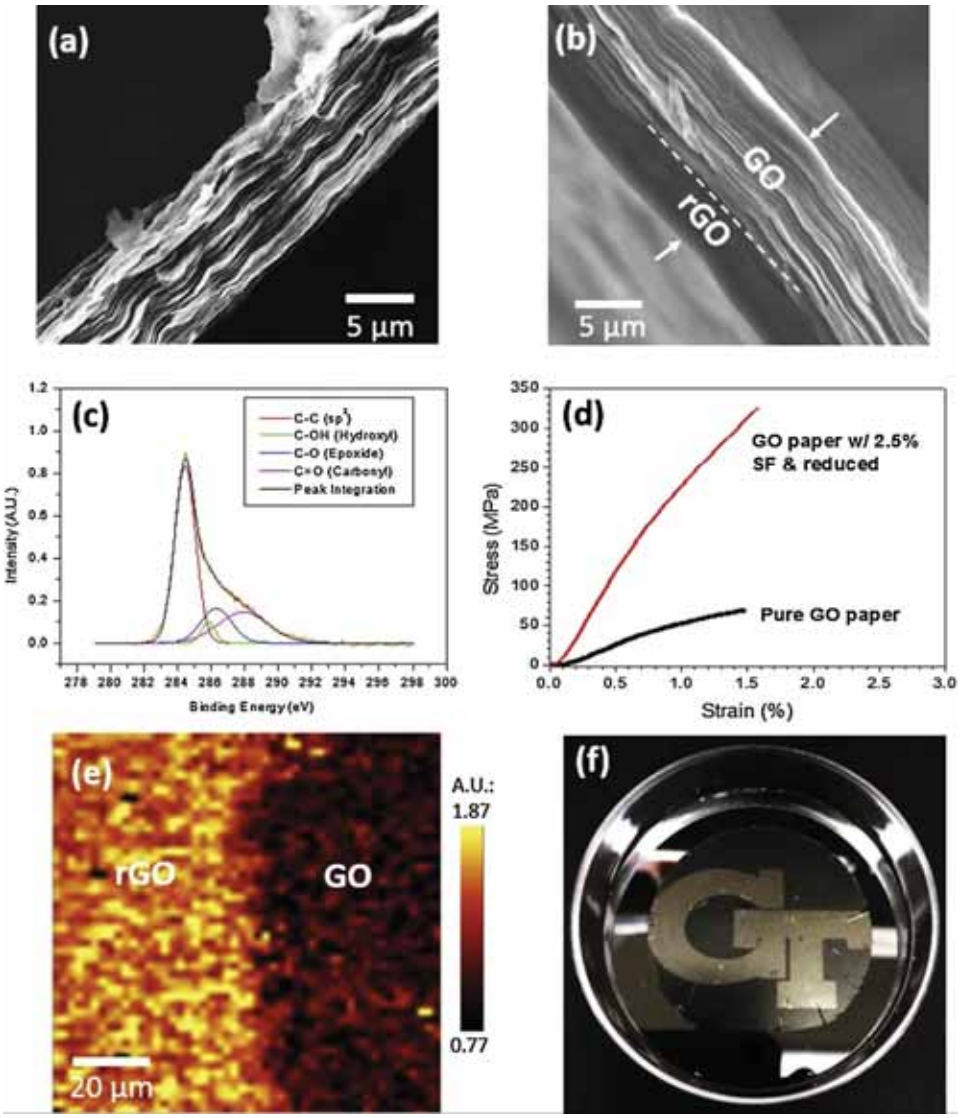

Fig. 13. The morphology of the non-reduced (a) and partially reduced (b) graphene oxide-silk fibroin nanocomposite films. (c) XPS C1s spectrum and (d) stress–strain curves of the reduced graphene oxide nanocomposite films. (e) Raman mapping of the I_d/I_g ratio shows distinct boarder between the reduced and intact area of GO. (f) Digital photograph shows the uniformity and high resolution from the reduced pattern (shiny silver, approximate diameter: 40 mm) [105]. Copyright 2013.
Reproduced with permission from John Wiley & Sons Inc.

be due to macroscopic aggregation caused by the strong chemical interactions between PAA and graphene oxide materials. In order to obtain a homogeneous dispersion to assure uniform morphology, the initial mixture underwent extensive sonication. It is suggested that during the sonication the graphene oxide flakes are broken into smaller pieces, which undermines the strength characteristics of the resulting nanocomposites. Nevertheless, although the dispersion is more homogeneous after sonication, the presence of small aggregated nanoparticles compromises the final mechanical performance.

Similar results have been reported by Tian et al., who used polyethyleneimine (PEI) polymer to crosslink dopamine-functionalized graphene oxide materials [208]. The paper-like materials fabricated by vacuum-assisted assembly were additionally crosslinked with relatively high, 30%, PEI content. These crosslinked papers showed very high elastic modulus of about 100 GPa and excellent ultimate mechanical strength of 210 MPa. However, the ultimate strain of these crosslinked nanocomposites significantly decreased to around 0.2% due to the inevitable dense and poorly deformable covalent chemical crosslinking network with low molar weight component (Fig. 15).

4.2. Graphene-polymer nanocomposites with weak interfacial interactions

Another strategy for toughening the graphene oxide-polymer nanocomposites is employing restorable network rather than permanent covalent bonding. Hydrogen bonding, hydrophobic interactions, electrostatic attractions, and polar-polar interactions with the potential of self-restoration and large deformation are considered for this purpose (Table 1). The network of such multiple weak interactions can facilitate significant reinforcement and compensate the weaker individual bindings. Elastomeric

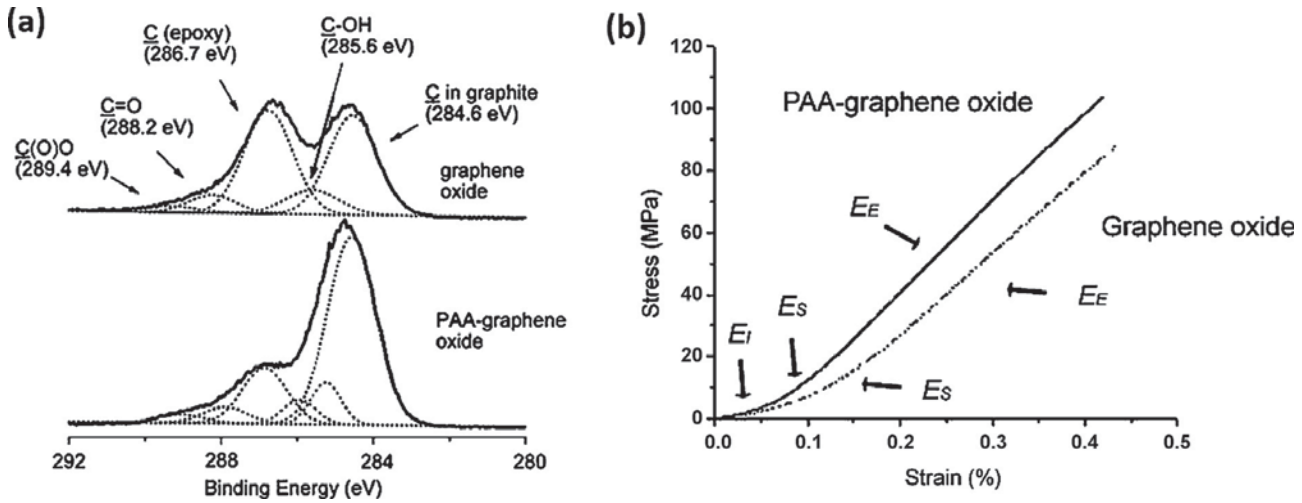

Fig. 14. (a) XPS spectra of the graphene oxide paper and the PAA modified graphene oxide paper, showing effective chemical crosslinking; (b) stress–strain curves of the PAA modified and pristine graphene oxide papers, respectively [97]. Copyright 2009.
Reproduced with permission from the American Chemical Society.

synthetic and biological materials might be efficient binders due to their wide spectrum of chemical compositions and functions. In addition, their easy processability, high mobility, and conformational flexibility are important advantageous features.

In recent study, Kulkarni et al. exploited electrostatic interactions to bind the negatively charged graphene oxide sheets and oppositely charged polyelectrolyte multilayers [3,132]. Negatively charged monolayer graphene oxide flakes in high concentration (60% of surface coverage) were incorporated into the polyelectrolyte matrix without folding and wrinkling (Fig. 9). The multiple electrostatic interactions at the graphene oxide-polyelectrolyte interface resulted in a significant toughening the ultrathin membrane by 500%, from 0.4 MJ m^{-3} to a high value of 1.9 MJ m^{-3} (Fig. 16) [3]. The application of LbL assembly significantly increased the interaction area of the two components, thus optimizing the stress transfer during large strain. The content of graphene oxide required to achieve the optimum toughness was only 3.3 vol%, owing to the high density of electrostatic interactions and the ability to restore the interactions under large strains.

Meanwhile, the elastic modulus value increased by 8-fold to 18 GPa; the ultimate stress increased by 120% to 130 MPa, and the ultimate strain increased by 50–2.3% (Fig. 16). The increase in strain is unusual for graphene oxide reinforced polymeric materials because the ultrastrong graphene oxide tends to make the nanocomposite brittle. However in this case, the interactions are either too strong (e.g., covalent bonding) or too weak (e.g., van der Waals force), facilitating the stress distribution and the constituent reorganization. Utilizing moderate, but high density interactions to bind graphene oxide and the polymeric component is a plausible philosophy to develop nanocomposites with balanced mechanical properties.

The formation of hydrogen bonding networking is the most utilized reinforcement mechanism for the integration of graphene oxide component in various polymeric matrices. Putz et al. compared the effect of the incorporation of graphene oxide nanofillers in the matrices of such different

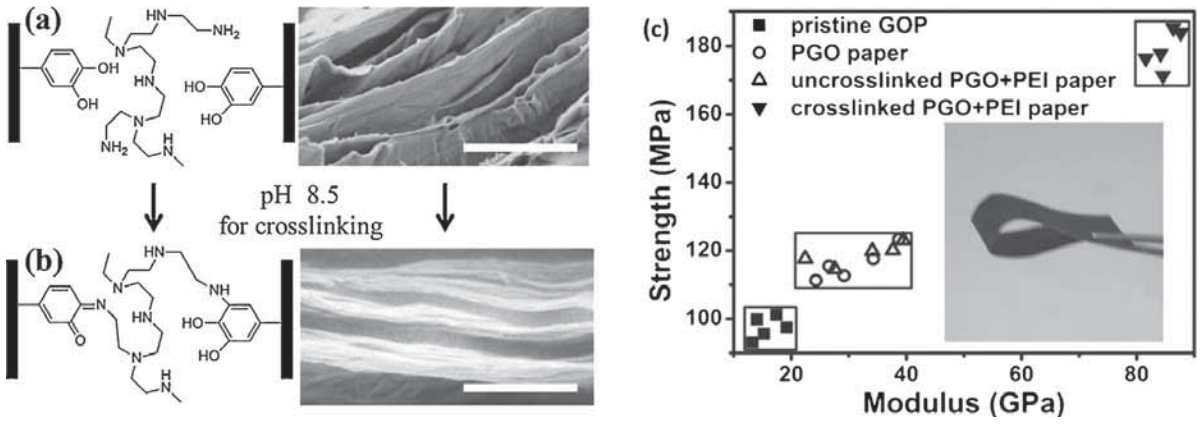

Fig. 15. The chemical structure and SEM morphologies of the graphene oxide paper before (a) and after (b) PEI crosslinking. (c) Summary of the mechanical performance of the PEI crosslinked graphene oxide paper [208]. Copyright 2013.
Reproduced with permission from John Wiley & Sons Inc.

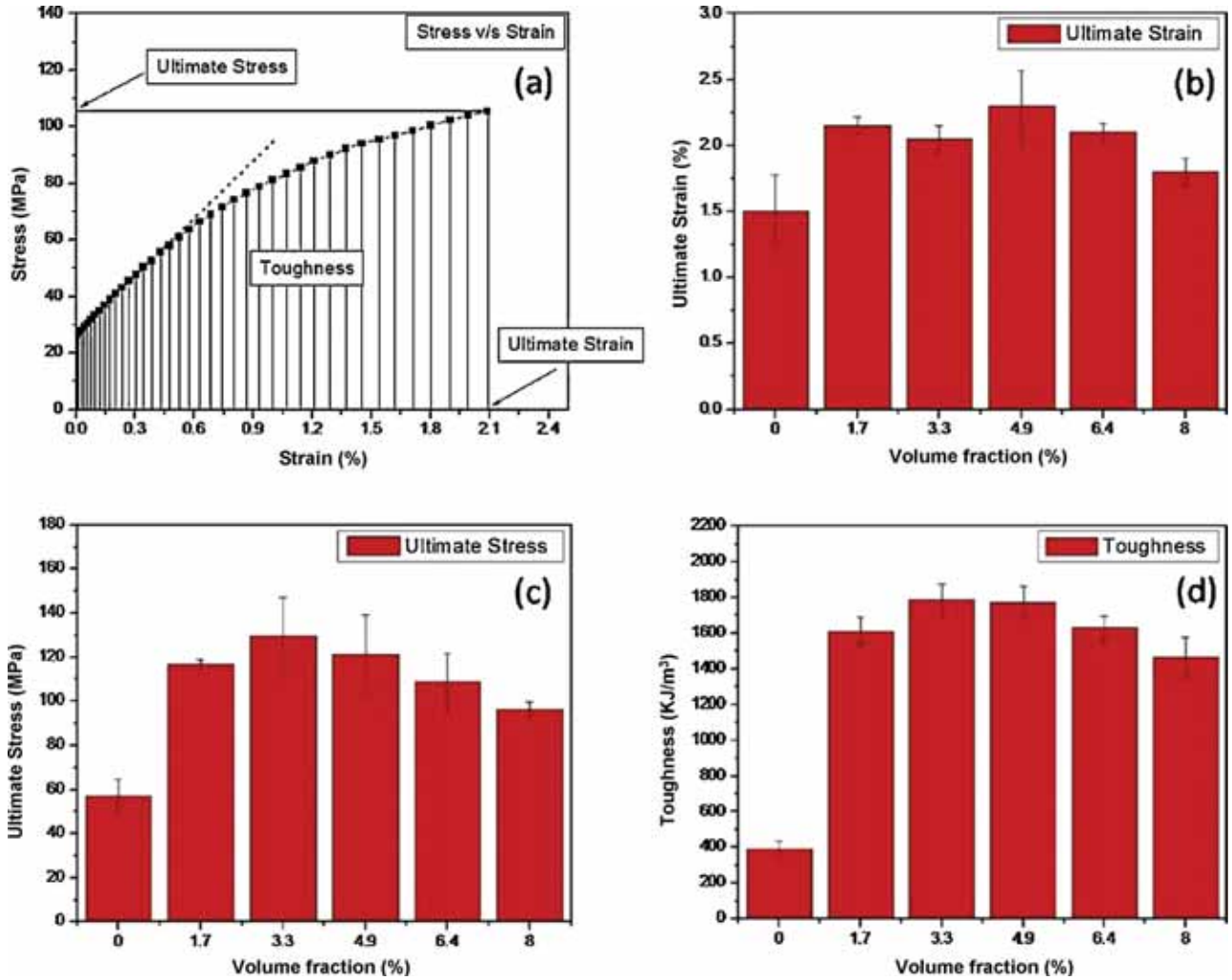

Fig. 16. Representative stress–strain curve (a) of the graphene oxide-polyelectrolyte nanomembranes and the effect of graphene oxide content on the mechanical properties: (b) ultimate strain, (c) ultimate stress, and (d) toughness [3]. Copyright 2010.
Reproduced with permission from the American Chemical Society.

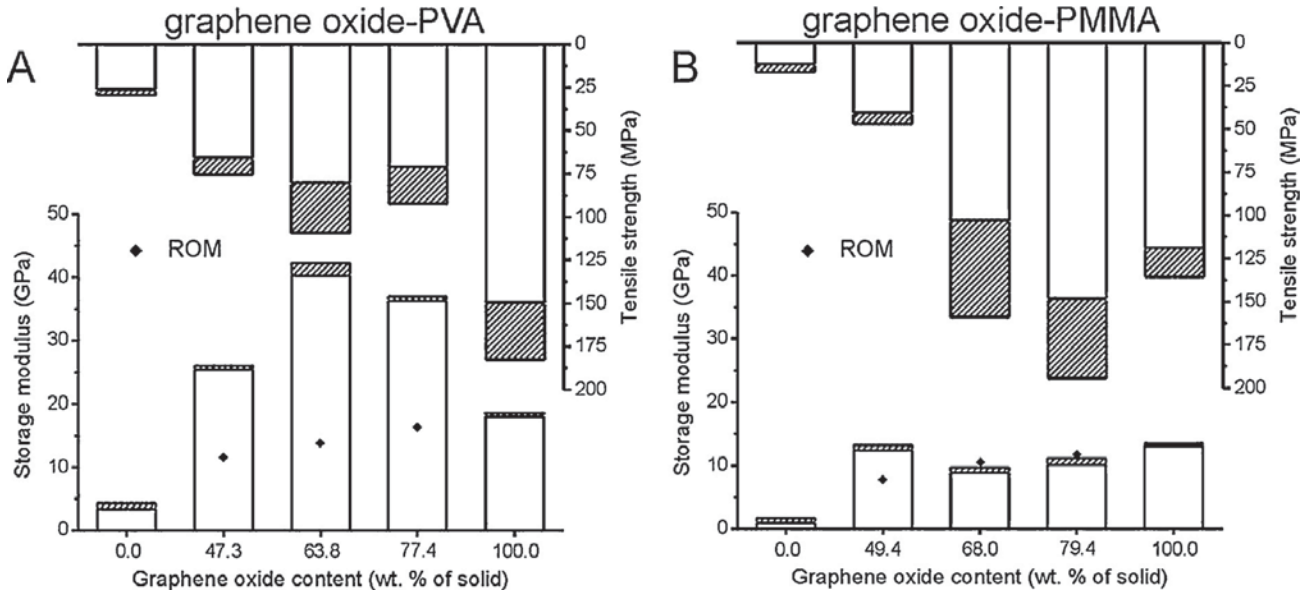

Fig. 17. Storage moduli and tensile strengths of: (A) PVA-based and (B) PMMA-based nanocomposites. The average and maximum values are shown by the white and shaded bars, respectively [209]. Copyright 2010.
Reproduced with permission from John Wiley & Sons Inc.

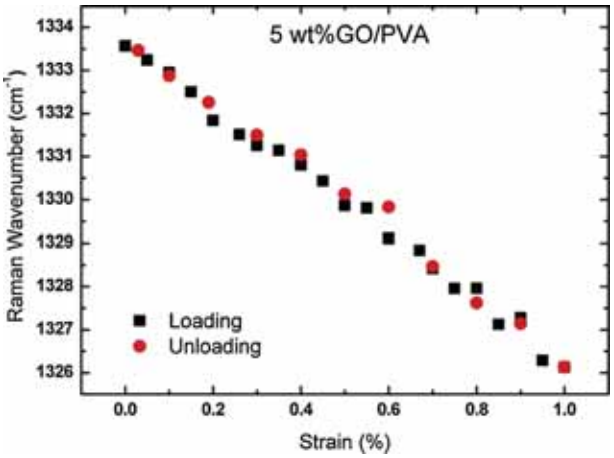

Fig. 18. Shift of the D band position with strain to the PVA-graphene oxide nanocomposite for loading and unloading [210]. Copyright 2013. Reproduced with permission from the American Chemical Society.

matrices as PVA (hydrophilic) and PMMA (hydrophobic) [209]. Due to the contrasting hydrophobicity of these matrices, the reinforcing effects caused by the addition of graphene oxide are very different. As 64% of graphene oxide is added to the hydrophilic PVA matrix, the strong hydrogen bonding networking results in dramatically increased elastic modulus of 36 GPa and significantly improved tensile strength of 80 MPa (Fig. 17a). However, the strain to failure of these nanocomposites plunged from 14.2% to 0.25%, indicating stiffening of the reinforced material.

The change in mechanical properties is attributed to the strong hydrogen bonding between PVA matrix and graphene oxide. In contrast, for the hydrophobic PMMA matrix, the hydrogen bonding is much weaker because the PMMA molecules can only serve as hydrogen bond acceptors through the ester oxygen. As a result, the Young's modulus of the 68% graphene oxide filled PMMA matrix is very modest, around 6 GPa (Fig. 17). On the other hand, the ultimate strain is higher, around 2.6% (Fig. 17).

In different study, Li et al. reported the effect of addition of a small content of graphene oxide in PVA and the load transfer using polarized Raman spectroscopy [210]. Addition of 3% of graphene oxide to the PVA matrix caused a modest increase in the storage modulus value by 50% to around 6 GPa. On the other hand, the ultimate strength increased by 100% to 60 MPa with minimal compromise of the ultimate strain (decreased from 180% to 155%).

Furthermore, the authors have employed Raman spectroscopy to understand the stress development in these nanocomposites and observed the shift of the D band of graphene oxide material as a function of engineering strain (Fig. 18). The D band of the graphene oxide embedded in the nanocomposite shifted linearly and reversibly from 1334 cm^{-1} to 1326 cm^{-1} when 1.0% strain was applied, indicating good interfacial transfer between the nanofiller and the matrix (Fig. 18) [210]. The calculated modulus value for graphene oxide is much smaller than the nominal value of 250 GPa. The use of Raman spectroscopy to monitor the strain in the nanocomposite is important for the understanding of the load transfer between graphene oxide sheets and polymer matrices.

Xu et al. also reported the mechanical strengthening of reduced graphene oxide to the PDMS matrix using Raman spectroscopy [211]. The authors demonstrated that the elastic modulus, toughness, damping capability, and strain energy density were all increased by 42%, 39%, 673%, and 43%, respectively, with the addition of only 1% graphene component. Also, a G band shift rate in Raman measurements of 11.2 cm^{-1} per 1% strain for compression and 4.2 cm^{-1} per 1% strain for tensile stress was observed for these nanocomposites. These values are much higher than the common values reported for the graphene sheets embedded in PDMS matrix [212]. The higher shift rate of the Raman bands in this study was primarily attributed to the efficient bonding of monolayers of reduced graphene oxide sheets to the hydrophobic PDMS matrix in contrast to the stacked graphitic platelets.

Hu et al. reported on the ultra-strong graphene oxide nanocomposites fabricated by LbL assembly by using silk fibroin as a novel binder as was introduced above [64]. The ultimate stress was estimated to be above 300 MPa, which was a 2-fold increase compared to the silk fibroin films. The toughness was also boosted to 2.8 MJ m^{-3}, and the elastic modulus reached an extremely high value of about 150 GPa (Fig. 19).

The mechanical properties of these nanocomposites were much higher than those measured for the individual components, and moreover, the elastic modulus of the nanocomposite films was higher than the predicted values of the well-established models (Fig. 19). Such a significant reinforcement was attributed to the complementary heterogeneous nature of the interactions between graphene oxide and silk fibroin that resulted in the formation of finely distribute silk molecules on graphene oxide flakes (Fig. 19). Adequate prediction of the mechanical performance of such nanocomposite materials was suggested by introducing a continuous interphase layer between the two components. The interphase region with gradual variation of silk matrix properties in the graphene oxide-silk fibroin nanocomposite was calculated to be a little less than 1 nm in thickness (Fig. 19b). Thus, the contribution of the interphase layer (reinforcing about 1/3 of total silk matrix) was significantly improved to the overall mechanical properties, which are well beyond those predicted by traditional mechanical models with sharp interfaces.

Interaction of graphene oxide with the polymer matrices can be enhanced by chemical functionalization of graphene oxide surfaces. In order to crosslink epoxy resin with graphene oxide, Bao et al. functionalized graphene oxide surface with hexachlorocyclotriphosphazene and glycidol treatment to graft chains with epoxide groups [17]. The functionalized graphene oxide was mixed with epoxy oligomer and polymerized in situ to fabricate dispersed and crosslinked morphologies. The resulting highly crosslinked nanocomposites with only 2% graphene oxide content showed an improvement in elastic modulus from 1.5 GPa to 3.2 GPa. The ultimate strength also improved to 217 MPa when 4% graphene oxide was added.

In another recent study, a solution of graphene oxide was mixed with ultra-high molecular weight polyethylene (PE) and hot pressed to prepare a composite film [213]. Addition of small quantities of graphene oxide increased

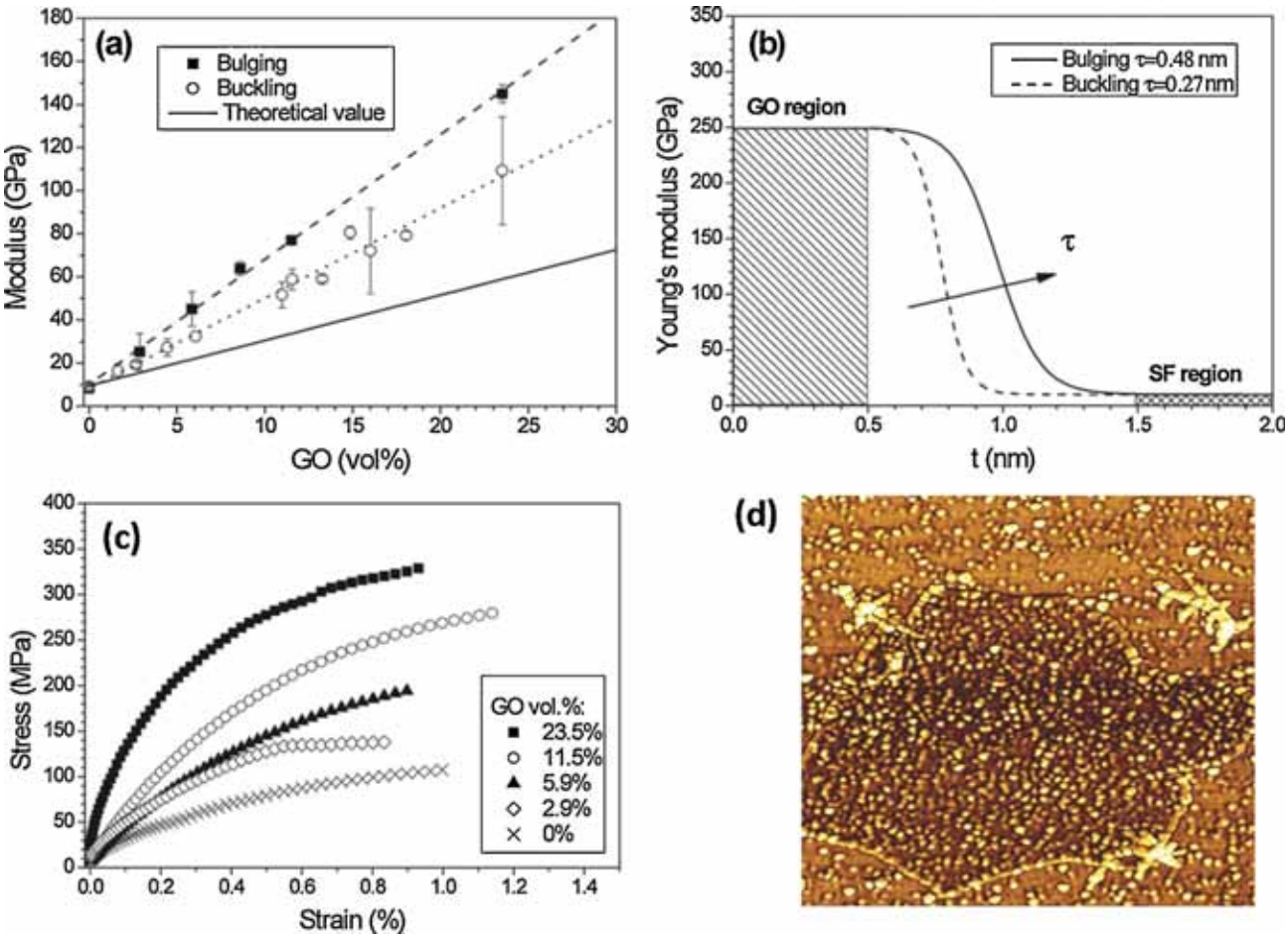

Fig. 19. (a) Elastic moduli of the graphene oxide-silk fibroin nanocomposite versus GO content and (b) the interphase modulus transition model (distribution from modulus across GO-silk region). (c) Representative stress–strain curves. (d) AFM phase image of the silk fibroin adsorbed on graphene oxide flake [64]. Copyright 2013.
Reproduced with permission from John Wiley & Sons Inc.

the mechanical properties of the neat PE films with the composite having 0.5 wt% graphene oxide showing the best tensile strength. Moreover, the biocompatibility of these nanocomposites was tested and no negative effect on the cell growth was observed.

4.3. Incorporation of graphene into nanocomposites

To date, very few results have been reported on the fabrication of polymer nanocomposites with a pristine graphene component. This is primarily due to the chemical inertness of graphitic surfaces and difficulties in the exfoliation. Graphene is highly hydrophobic and non-dispersable in most conventional organic solvents, which is another challenge for materials processing. The range of interactions between graphene and various polymer matrices is very limited as well. Hydrophobic–hydrophobic interactions and π–π stacking are usually employed to enhance interfacial interactions with proper polymer matrices like PS but they are not extremely strong [110].

Laaksonen et al. reported graphene-nanofibrillated cellulose (NFC) nanocomposites as mechanically robust materials [214]. The approach employed genetically engineered materials to match the properties of the two components, which opens wide opportunities for the field of bio-nanocomposites. The authors exploited a diblock protein, which can bind graphene layers through hydrophobic interactions and cellulose fibrils with biological terminal group, to crosslink the different components (Fig. 20).

The elastic modulus, ultimate strength and toughness increased to 20 GPa, 280 MPa, and about 5 MJ m^{-3}, respectively, with only 1.25 wt% graphene added (Fig. 20d–f). Virtually all polymeric materials can be engineered to fit in this strategy and bond strongly with graphene. However, the genetic modification requires significant synthetic efforts and long term screening and purification procedures.

Another approach for the incorporation of graphene components into polymeric matrices is the in situ reduction of graphene oxide. Li et al. reported graphene-PVA nanocomposites through mixing of graphene oxide suspension and PVA solution [215]. The mechanical properties of the nanocomposite were already excellent even before chemical reduction of graphene oxide component with the ultimate stress and ultimate strain reaching 120 MPa and 1.2%, respectively. After HI reduction, the ultimate stress, ultimate strain and stiffness increased significantly

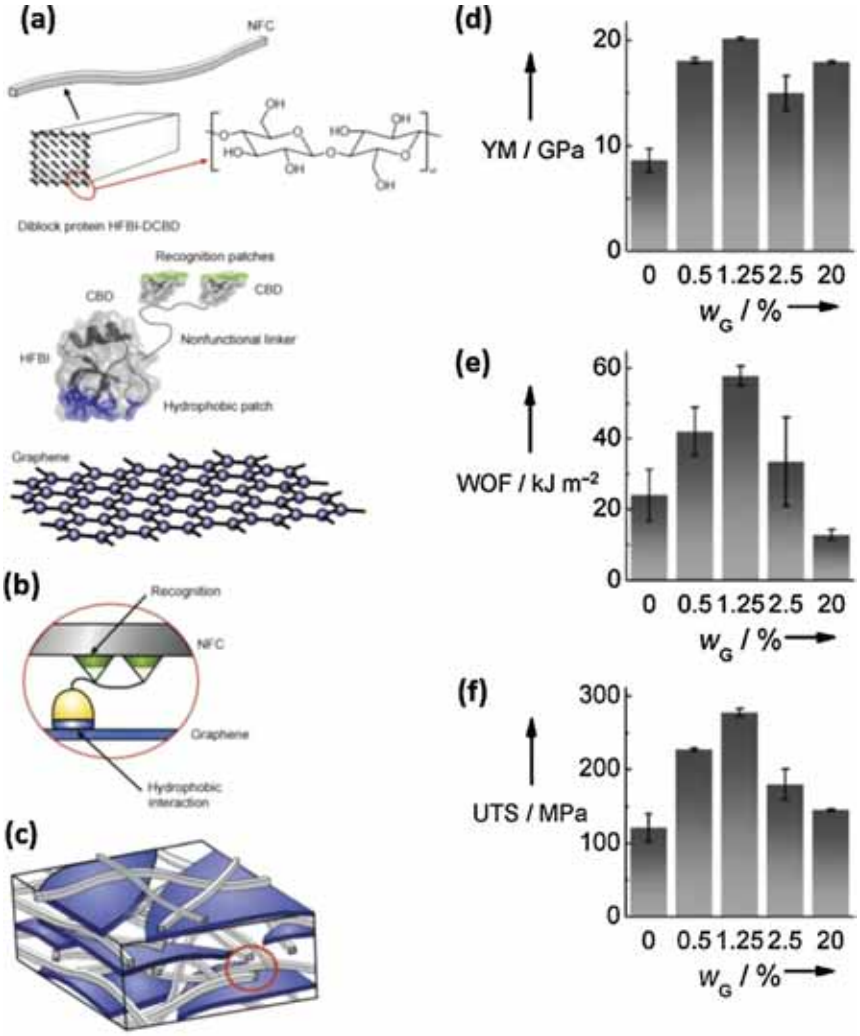

Fig. 20. (a)–(c) The assembly of the graphene-NFC nanocomposites; (d)–(f) mechanical properties of the graphene nanocomposites: Young's modulus (YM), work of fracture (WOF), and ultimate tensile stress (UTS) versus the weight fraction from graphene in the nanocomposite, respectively [214]. Copyright 2011.
Reproduced with permission from John Wiley & Sons Inc.

to 190 MPa, 2.6%, 11 GPa, respectively. The reinforcement is claimed to be strong because of the restoration of the defected carbon network and the reduction of the interlayer spacing after the chemical reduction of graphene oxide. However, the real reinforcing mechanism is still unclear because the strength of the affinity between PVA matrix and the reduced graphene oxide which is hydrophobic is not clarified.

4.4. Hydrogels reinforced by graphene derivatives

Hydrogels are known for their wide applications, including tissue engineering, drug delivery, and energy storage owing to their large specific surface area, high compliance, responsive behavior, and biocompatibility [216–222]. In particular, polymer hydrogels are promising for biomedical applications including controlled drug release, enzyme immobilization, sensors and actuators, and as tissue culture substrates. However, conventional hydrogels show modest mechanical properties such as low mechanical strength and low elastic modulus. Thus, significant effort is devoted to improving mechanical properties (mostly mechanical strength and toughness) of the hydrogels by employing organic and inorganic cross-linkers, hydrophilic silica particles, and functionalized clay nanoplatelets as reinforcing agents.

Recent studies have reported the incorporation of graphene and graphene oxide into hydrogels. In particular, Shen et al. reported the fabrication of graphene oxide-PAA hydrogels and investigated the mechanical, thermal, and swelling behavior of these reinforced hydrogels (Fig. 21) [223]. The functional groups on the graphene oxide surface were used as anchoring sites for the in situ polymerization of PAA matrix by N,N-methylenebisacrylamide (BIS). Moreover, the oxygenated functionalities also enabled the formation of the network of hydrogen bonds of graphene oxide with the compliant PAA matrix.

The analysis of the stress–strain behavior of the hydrogels fabricated with and without the graphene oxide component showed that the incorporation of graphene

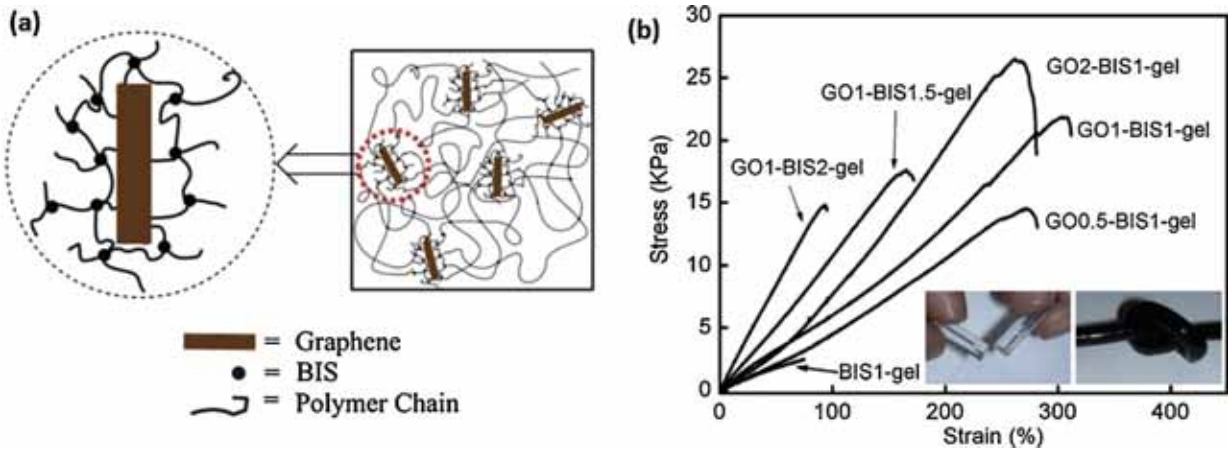

Fig. 21. (a) Scheme of the crosslinked gel network consists of graphene, BIS, and PAA; (b) stress–strain curves of PAA gels with different combinations of GO and BIS contents. The inset shows the photographs of BIS-gel and GO-BIS gel from left to right, respectively [223]. Copyright 2012. Reproduced with permission from the Royal Society of Chemistry.

oxide sheets resulted in a significant increase in the elongation to break up to 300% (Fig. 21). Also, the nanocomposite PAA hydrogels with graphene oxide were found to be more ductile and capable of sustaining large deformation and complex shear force fields. The simultaneous increase in the mechanical strength and ductility was attributed to the strength and flexibility of graphene oxide components.

Poly (N-isopropylacrylamide) (PNIPAAm) is a material of choice for thermoresponsive applications owing to the ability of polymer chains to undergo a reversible coil-to-globule transition at the Lower Critical Solution Temperature (LCST) [224–227]. PNIPAAm is considered for biomedical applications such as drug delivery on-demand. However, the poor mechanical properties with low compressive modulus and poor elastic recovery limit its use. Thus, graphene-based PNIPAAm nanocomposites have gained attention as a prospective material exhibiting enhanced mechanical properties along with high temperature sensitivity.

Thermoresponsive graphene-nanocomposite PNIPAAm hydrogels were fabricated by Mariani et al. [228]. Graphene was dispersed in N-methyl pyrrolidone by subjecting graphite to ultrasound treatment. The resulting solution was mixed with NiPAAm monomer and polymerized using a frontal polymerization technique. Mechanical analysis of the resulting nanocomposites revealed that the addition of graphene into the hydrogel matrix resulted in a material with thermoplastic behavior. The storage modulus and viscosity of hydrogels increased with increasing graphene content; however, at higher concentrations, a significant decrease in the mechanical strength of these nanocomposites was observed, possibly due to slippage of the sheets at higher loading rates.

In another study, pH-responsive and thermal-responsive graphene oxide hydrogels have been fabricated by covalently attaching graphene oxide sheets to PNIPAM-co-AA microgels in water [229]. However, the mechanical properties of these reinforced hydrogels were not mentioned. Hydrogels made from conducting polymers such as polypyrrole (PPy) can be promising for electrochemical and energy storage applications. Shi et al. demonstrated the fabrication of graphene oxide-PPy hydrogels using in situ polymerization of monomer in graphene oxide solution and tested their electrical properties (Fig. 22) [230].

Graphene oxide components, known for their effective gelation properties, are expected to have a strong interaction with the conducting polymer, resulting in a cross-linked network. Indeed, the hydrogels showed a frequency independent storage modulus and the values were much higher than the loss modulus suggesting the fabrication of strong hydrogels (Fig. 22). These hydrogels were much stronger than the other graphene oxide based-hydrogels reported in literature due to the strong π–π interactions between the graphene oxide and PPY matrix. The enhanced crosslinking and the high moduli of conjugated polymer with a stiff backbone both contributed to improved mechanical performance.

5. Other functional properties and applications

Beside the strong mechanical performance which has been discussed in the preceding, graphene materials play a critical role in the fabrication of polymer nanocomposites with novel functionalities. Most important functionalities addressed in current studies are enhanced optical, electrical, thermal, or barrier properties. To date, graphene components have been included in a variety of polymer matrices such as epoxy polymers, PS, PANI, Nafion, and poly (3,4-ethyldioxythiophene) to fabricate nanocomposites with new functionalities [231–233]. The percolation threshold, conductivity, and mechanical properties of the nanocomposites were tested for prospective applications, including supercapacitors, transparent conducting electrodes, gas barrier membranes, and biosensors [147,234–236].

To improve the functional performance of the nanocomposite, efficient uniform dispersion of the graphene components inside the polymer matrix without aggregation should be implemented. This is a challenging task for potentially functional matrices similarly to those discussed above for mechanical performance. For example, as was mentioned in the preceding, inert graphene is

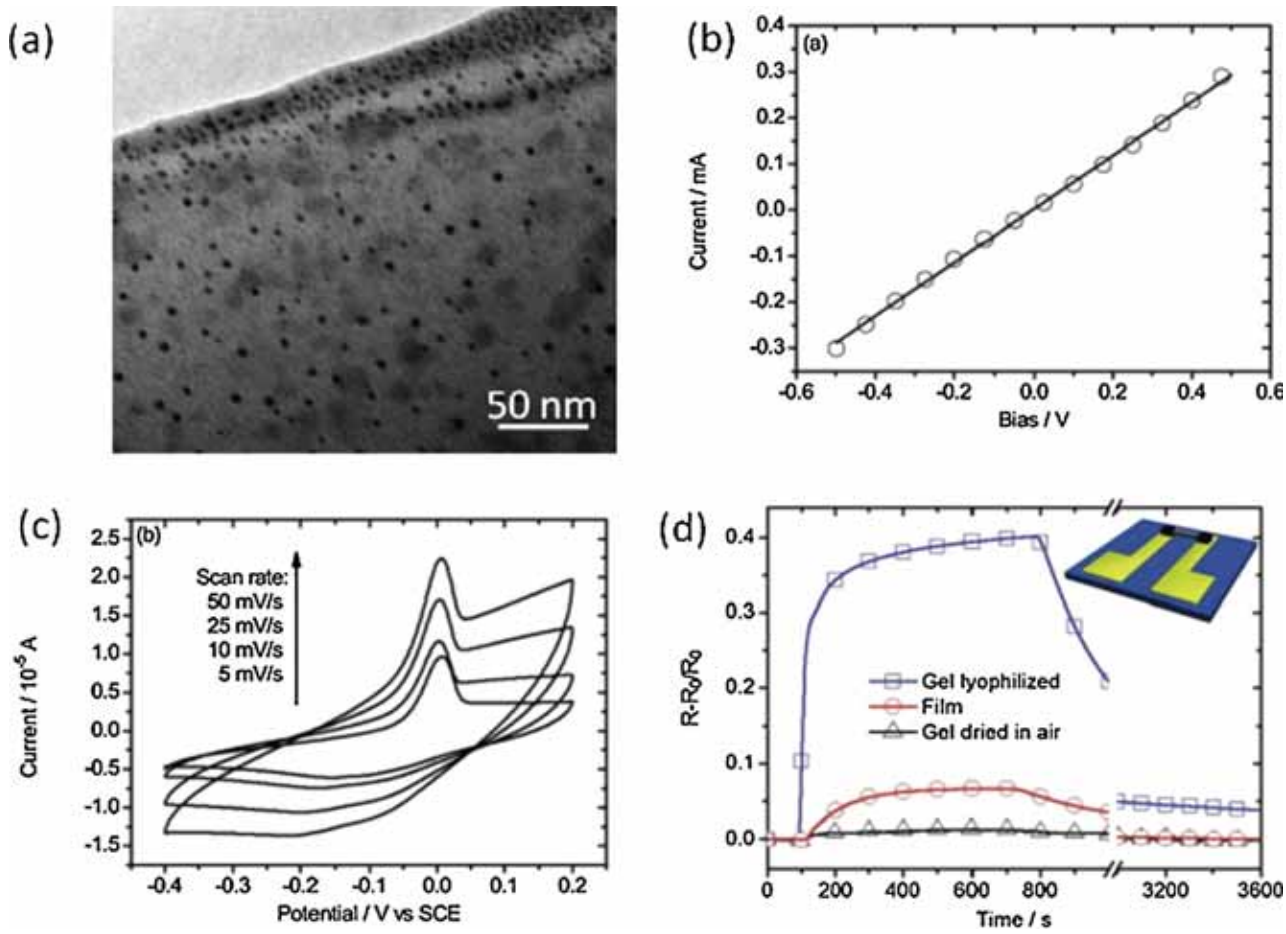

Fig. 22. (a) TEM of a GO/PPy nanocomposite sheet with platinium nanoparticles embedded, (b) *I–V* curve of a lyophilized GO/PPy hydrogel, (c) cyclic voltammograms of GO/PPyl hydrogel in 0.1 M $LiClO_4$ at different scan rates, and (d) Ammonia gas sensing performance of three devices with different sensing elements [230]. Copyright 2011.
Reproduced with permission from the Royal Society of Chemistry.

difficult to disperse in commonly used organic solvents and also in the functionalized polymer matrices. Thus, efforts to employ reduced graphene oxide or decorate the surface of graphene or graphene oxides with different functionalities are needed for improving the dispersibility and functionality [70,235,237].

5.1. Graphene-polymer nanocomposites for sensing applications

In one of the earlier studies, reduced graphene oxide was mixed with Nafion, a well-known material [238]. The resulting mixed solution was to fabricate an electrochemically active polymer nanocomposite. These materials were used as a sensing platform to detect trace levels of toxic elements, such as lead and cadmium. It was observed that the resulting Nafion-reduced graphene oxide films possess a high sensitivity toward metal ions and exhibit an improved detection limit of 0.02 $\mu g\,L^{-1}$ for selected metal ions.

Graphene-PANI nanocomposites have also been fabricated for hydrogen sensing applications [239]. Hydrogen sensing of the nanocomposite material was compared with that of PANI nanofibers and graphene sheets. The nanocomposite films were found to have a much higher sensitivity for hydrogen gas detection than films fabricated solely from graphene sheets or PANI nanofibers. In another study, graphene oxide-PP nanocomposites have further been fabricated by polymerization of pyrrole in graphene oxide solution [230]. These hydrogels were used as a sensing element in a chemoresistor structures to detect ammonia gas. The lyophilized graphene oxide-PP composites showed a good sensitivity toward ammonia with a 40% increase in sensitivity.

Several recent developments include the fabrication of multicomponent polymer nanocomposites from silica and other oxide particles coated with graphene oxide for detection of dopamine [240] and monitoring of mammalian nervous cells, proteins and *Escherichia coli* cells [241–243]; conducting reduced graphene oxide-polymer with high barrier and gas sensing properties [244,245] and electrochemical sensing of isomers [246]. Methanol-sensitive nanocomposites with enhanced characteristics from PANI-graphene oxides [247], amplified colorimetric sensors for target DNA detection [248,249], sensing skins for detection of volatile organic vapors [250], advanced electrochemical electrodes for peroxide and glucose detection [251], and electrically conductive aerogels for catalysis and sending applications [252] have also been reported.

5.2. Graphene-polymer nanocomposites as gas barriers

Solid, non-porous fillers with a high surface area to volume ratio are one of the prime necessities in fabricating polymer nanocomposite thin films to prevent the permeation of gas and water molecules through the film. Sensors, electronics, Li-ion batteries, and fuel cells are sensitive to the presence of gases such as oxygen and moisture and require protective/active elements [147,253]. Strong and modestly flexible metal thin films such as aluminum foils form excellent barriers, but the presence of pin holes and defects during stretching, bending, and handling limits their broad use. On the other hand, flexible polymer nanocomposites offer an alternative due to their high mechanical strength combined with high transparency and a tendency to reduce the permeation of gases and moisture through the films. Traditionally, clay-based polymer nanocomposites known for their low permeability to gases and moisture are exploited for these applications [254].

Recent studies have also considered the use of graphene for gas barrier and gas sensing applications owing to its non-permeable sheets-like structure. For example, Yang et al. deposited graphene oxide sheets alternatively with PEI polymer to form a stacked polymer nanocomposite to investigate the oxygen barrier properties (Fig. 23) [253]. A 91 nm thick film comprising of 10 bilayers of 0.1 wt% graphene oxide and 0.2 wt% PEI on top of PET supporting film showed an improved oxygen permeability of 2.5×10^{-20} cm^2 s^{-1} Pa^{-2}. This low permeability is comparable to the oxygen permeability observed in case of 100 nm thick SiO_x nanocoatings. Also, these films were found to be useful for gas separation with a H_2/CO_2 selectivity (i.e., the ratio of permeabilities of different gasses, H_2 and CO_2) higher than 383.

A significant reduction of oxygen and carbon dioxide permeation and the potential for high selectivity of hydrogen permeation has been reported for in situ polymerized, paper-like, and LbL graphene oxide-conjugated polymer nanocomposite films [253,255,256]. In another study, high moisture barrier properties combined with high transparency has been reported for robust graphene-based polyimide nanocomposite materials [257]. Graphene oxide-polymer films have been suggested for use as flammable-resistant coatings based on their high gas barrier properties and reduced oxidation [258], as well as highly elastomeric nanocomposites, which combine low permeability with good electrical conductivity [147].

5.3. Graphene-polymer nanocomposites for photovoltaic applications

Graphene components are well known as hole transport materials, which can be effective in fabricating organic photovoltaic materials [259]. However, these nanocomposite materials are frequently deposited from highly acidic aqueous solutions, which adversely affects the commonly used ITO electrodes and degrades device performance.

Chhowalla et al. demonstrated the use of graphene oxide as alternative, solution processable hole-transport material in organic photovoltaic films (Fig. 24) [260]. Graphene oxide thin films were obtained from neutral solutions between the photoactive poly(3-hexylthiophene) (P3HT): phenyl-C61-butyric acid methyl ester (PCBM) layer

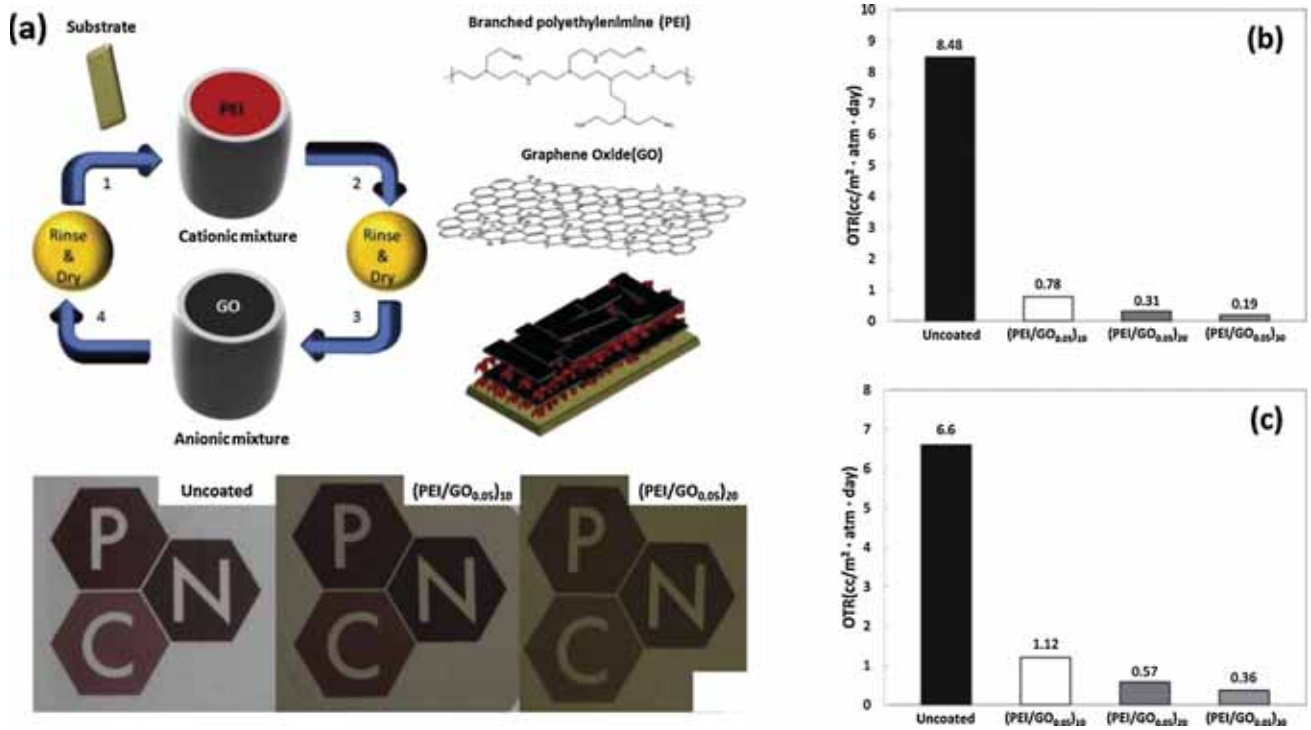

Fig. 23. (a) LbL assembly of PEI-GO nanocomposites as gas barrier films. Oxygen transmission rate of PEI-GO composites assembled on PET, measured at 23 °C under (b) 0% RH and (c) 100% RH [253]. Copyright 2013.
Reproduced with permission from John Wiley & Sons Inc.

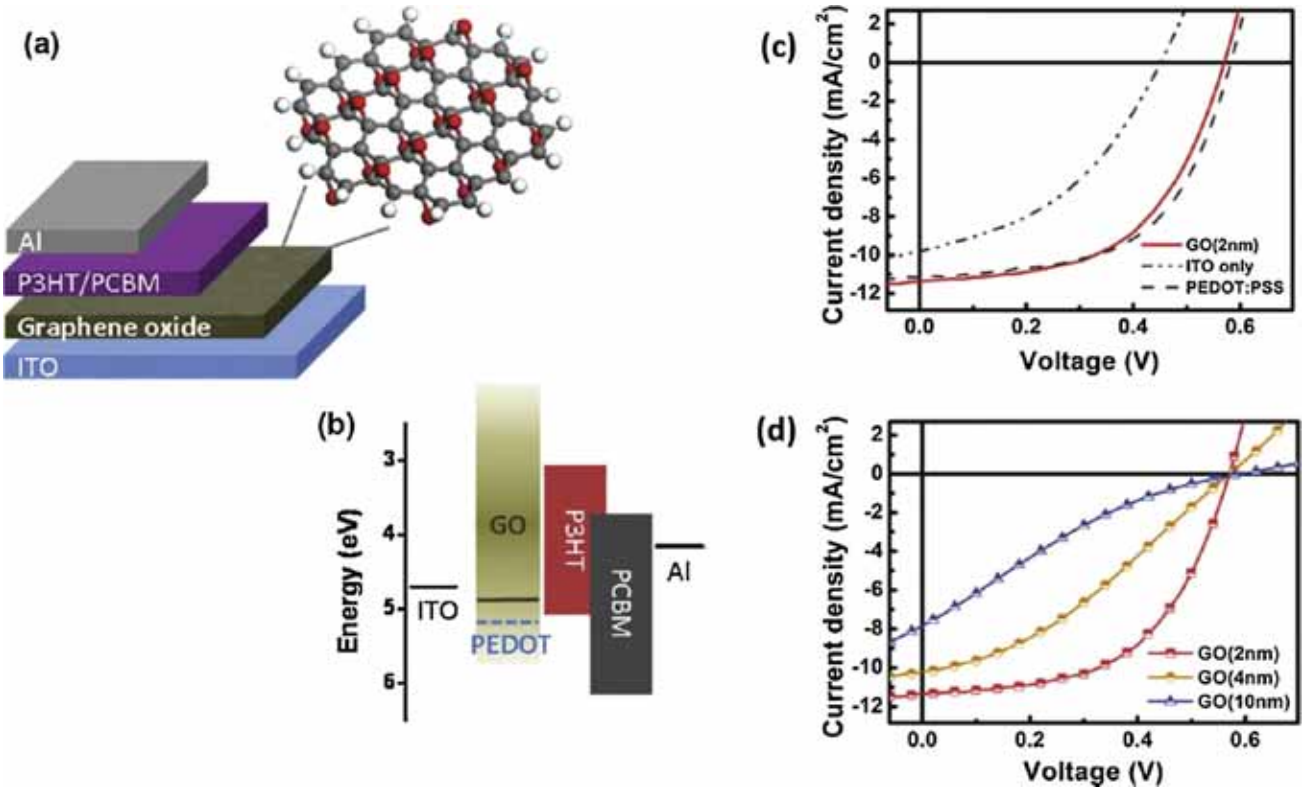

Fig. 24. Device schematic (a) and energy level diagram (b) of the photovoltaic device structure consisting of ITO/GO/P3HT:PCBM/Al components. Current–voltage characteristics of (c) photovoltaic devices with no hole transport layer (curve labeled as ITO) and (d) ITO/GO/P3HT:PCBM/Al with different GO thicknesses [260]. Copyright 2010.
Reproduced with permission from the American Chemical Society.

and transparent conducting ITO electrode. This design resulted in a dramatic improvement of the photovoltaic efficiency, comparable to devices fabricated using traditional poly(3,4-ethylenedioxythiophene) (PEDOT):PSS pair. Also, the use of non-aqueous solvents for the deposition of graphene oxide was suggested for further improvement of the device performance and to ensure the reliability of these films.

Thin layers with graphene oxide and carbon nanotubes were also used as a replacement for PEDOT:PSS in P3HT:PCBM layers in a tandem devices [261]. Regular and inverted tandem photovoltaic cells fabricated in this study showed significant increase in open-circuit voltage (V_{oc}) by 84% and 80% of the sub-cell V_{oc}. Power conversion efficiency (PCE) as high as 4.1% was achieved for these modified tandem cells. The tandem cells showed high transparency in the near-infrared region and were expected to work well with tandem cells with a low band gap polymer component. Also, doping of the carbon nanotubes was expected to further improve the charge recombination at the interface. This study indicates that graphene oxide can effectively serve as the hole transport component and electron-blocking layer for photovoltaic and light-emitting applications.

Recent publications in this field discussed all-polymer-graphene nanocomposites with various graphene components and conjugated polymer matrices for a variety of related applications including those for optoelectronic phenomena [262,263] and other energy-related and broader prospective applications [264–266]. Additional results include a combination of graphene with solid polymer electrolytes and dye-sensitized solar cells [267,268], fabrication of nanocomposites with photoluminescent quenching [269], non-covalent integration of variously reduced graphene oxide and stamping transfer into bulk heterojunction polymer solar cells [270–274].

5.4. Graphene-polymer nanocomposites with high thermal conductivity

Decreases in the size of electronic devices necessitate the fabrication of high density electronics leading to an increase in the heat generation. Fillers with high thermal conductivities efficiently transfer the phonons, but the transport is slowed at the polymer-filler interfaces in polymer nanocomposites due to the amorphous characteristics of the polymer with low thermal conductivity and imperfect interfacial binding [275].

Graphitic nanoplatelets composed of a few graphitic layers were incorporated in the epoxy matrix at different loading concentrations to prepare nanocomposites that were tested for their thermal conductivities [276]. A linear increase in the thermal conductivity of the nanocomposite was observed for higher graphene content. The incorporation of 5 wt% graphene oxide in the epoxy matrix resulted in a fourfold higher thermal conductivity than the neat polymer, and can be further increased by incorporating 20 wt% graphene oxide, or up to 20 times

for a graphene loading of 40 wt%. Expanded graphite was acid-functionalized and used as a filler material for fabrication of polymer nanocomposites with high electrical conductivity [277]. At similar loadings, functionalized graphite was found to be more effective filler in improving the thermal conductivity of the polymer nanocomposites.

A number of recent publications addressed improving of thermal conductivity graphene-polymer nanocomposites such as in silane-crosslinked graphene oxide nanocomposites [278] and in nanocomposites with strong interfacial interactions [278,279]. Several studies reported nanocomposites with enhanced thermal conductivity and dimensional stability [278], fabrication of dielectric epoxy thermosets with increased thermal conductivity [280], design of stable nanocomposites which exhibit a high dielectric constant and low dielectric loss along with high thermal conductivity [281], improving thermal properties of polyimide and polyamic acid matrices [282], and controlling thermoelectrical properties of PANI films [283].

5.5. Graphene-polymer nanocomposites with electrical conductivity

Large-scale graphene electrodes have been demonstrated for industrial applications with reasonable cost and productivity [284,285]. Graphene oxide is known to become highly conductive on chemical reduction or thermal reduction, or a combination of both techniques [98–104]. The extent of the restoration of the electrical conductivity during the reducing procedure is largely dependent on the effectiveness of the removal of the oxygen-containing functionalities, especially the epoxide groups, from the surface and the restoration of carbon-carbon sp^2 bonds [98]. Therefore, graphene oxide-polymer nanocomposites are potentially useful for the integration into electronic devices if an effective reducing treatment is applied.

Graphene oxide incorporated into a PDMS matrix was found to show unique electric properties [286]. On application of an electric field of low strength, the composite showed a lower conductivity compared to the neat power due to the blockage of ion transport by the graphene oxide network. Further increase in the electric field resulted in nonlinear conductivity that is progressively more sensitive to the applied electric field. At a high electric field, the electrical conductivity is dominated by the electron transport across the graphene oxide network, which can be tuned by varying the oxidation state, the volume fraction of graphene oxide, and morphology. The authors suggested that the unique electrical properties, combined with high mechanical strength, has potential applications, such as field electromagnetic field protective materials or insulation materials in high voltage power system and electronic devices.

Koratkar et al. compared the electrical conductivity of multi-walled carbon nanotube-PS materials and graphene-PS nanocomposites fabricated by mixing the filler materials followed filtration and drying [287]. The conductivity of the nanocomposites was found to increase significantly, but still was several orders of magnitude lower than the PS films with carbon nanotubes. Further, selective localization of graphene was achieved by adding PLA into the matrix. PLA interacts poorly with graphene and the higher viscosity of PLA compared to PS results in the isolation of PLA in the matrix. As a result of this phase separation, graphene migrates into the hydrophobic PS regions, which resulted in a decrease in the percolation threshold for electrical conductivity to 0.075 vol%.

Electrical conductive PP-graphene oxide nanocomposites were fabricated by in situ polymerization [288]. The use of a supported catalyst system helped overcome the incompatibility between polar graphene oxide and non-polar PP matrix. Although, the nanocomposites showed a poor electrical conductivity of 0.3 S m^{-1} at a 4.9 wt% loading, it enabled a means of incorporating graphene oxide into a variety of incompatible polymer matrices.

Nanocomposite films of polypyrrole, a well-known conducting polymer and graphene functionalized with sulfonic acid groups were electrochemically deposited from aqueous solutions containing pyrrole monomer, sulfonated graphene, and dodecyl benzene sulfonic acid [289]. The negatively charged sulfonated graphene resulted in the doping of the polypyrrole during the polymerization process. The resulting composite films with 40 wt% sulfonated graphene sheets showed a specific capacitance of 285 F g^{-1} at a discharge rate of 0.5 A g^{-1} with improved electrochemical stability. In another study, isocyanate functionalization of graphene oxide and its subsequent reduction after solvent blending within the PS matrix resulted in a highly dispersed uniform nanocomposite film at a graphene oxide loading of 2.4 vol% [130]. These nanocomposites revealed a percolation threshold for electrical conduction of 0.1 vol% graphene oxide, which is three times lower than the values obtained for other filler materials.

Stable nanocomposite films of graphene oxide and PANI nanofibers were prepared by vacuum filtration to form a layered material with the PANI nanofibers sandwiched between the graphene oxide layers (Fig. 25) [155]. These mechanically robust and flexible nanocomposite films with 44% graphene oxide showed a 10 times higher electrical conductivity than the pristine PANI nanofiber films. These films were further employed in the fabrication of supercapacitor micro-devices and resulted in a 210 F g^{-1} electrochemical capacitance at a discharge rate of 0.3 A g^{-1}.

Flexible PANI electrodes doped with graphene oxide were fabricated by in situ polymerization of aniline in the presence of graphene oxide [290]. Incorporation of graphene oxide resulted in a remarkable enhancement in the electrical conductivity and specific capacitance of the nanocomposite materials as compared to individual PANI materials. The nanocomposite showed an electrical conductivity of 1000 S m^{-1} at a PANI:GO ratio of 100:1 and specific capacitance of 531 F g^{-1} (compared to 216 F g^{-1} for pure PANI). This process was further improved by incorporation of carbon nanotubes into the GO-PANI composite [176]. For this material, graphene oxide was mixed with carbon nanotubes to form a 3D network and further mixed with PANI by a one-step template-free process. The PANI formed a scale-like structure on the graphene oxide sheets aided by electrostatic interaction, hydrogen bonding, and π–π interaction. These multicomponent nanocomposite materials exhibited a specific capacitance of 589 F g^{-1} and

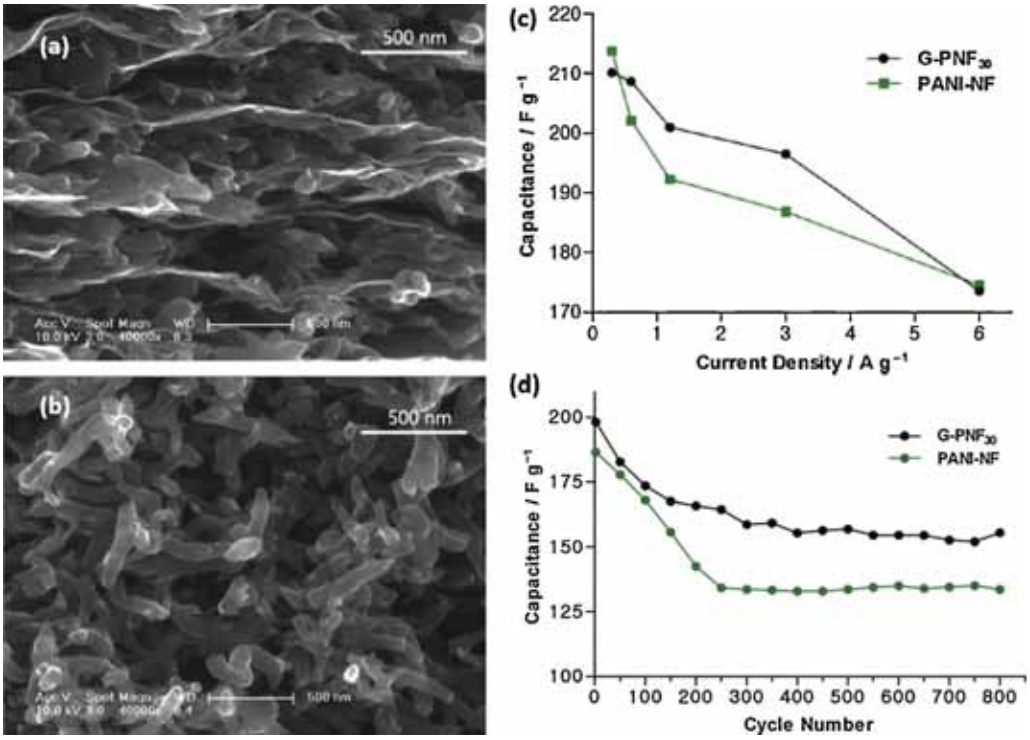

Fig. 25. Cross-section SEM images of (a) pure chemically converted graphene and (b) graphene-PANI nanofiber composite film. (c) Plot of specific capacitance versus current density of graphene-PANI composite and PANI, and (d) cycling stability of graphene-PANI composite and PANI films [155]. Copyright 2010.
Reproduced with permission from the American Chemical Society.

retained 81% of its initial capacitance even after 1000 cycles.

Different graphene-PANI nanocomposites were prepared by the use of a polymerized ionic liquid [291]. Graphene sheets were dispersed in N,N-dimethylformamide (DMF) and polymerized ionic liquid poly(1-vinyl-3-butylimidazolium chloride) (PIL) in order to stabilize the dispersion. PIL was found to adsorb on the graphene surface due to non-covalent π–π interaction and helped in stabilizing the graphene dispersion in DMF. Aniline was polymerized on the surface of the PIL stabilized graphene sheets and resulted in a fivefolder higher electrical conductivity at a 21 wt% loading due to excellent electronic transport of graphene and the π–π interactions with the PANI. Graphene-PANI nanocomposites were fabricated by in situ polymerization of graphene oxide and aniline followed by the reduction of graphene oxide [232]. The relative concentration of polymer and the graphene filler was tuned by varying the mass ratio of graphene in mixed suspension. The nanocomposites with 80 wt% graphene showed a remarkable specific capacitance of 480 F g^{-1} at a current density of 0.1 A g^{-1} along with good reliability.

Chemically reduced graphene oxide was stabilized with cationic PEI to fabricate supercapacitors [292]. The charged polymer component ensured good dispersibility of reduced graphene oxide and acted as binding sites for negatively charged carbon materials. These hybrid films showed an interconnected network of carbon structures with well-defined pores to enable the diffusion of ions through the interconnected morphology. Finally, these conducting nanocomposites showed a good specific capacitance of 120 F g^{-1} even at a high scan rate of 1 V s^{-1}.

3D porous structures of reduced graphene oxide and cellulose composites were fabricated by ball milling, template shaping, coagulating, and lyophilization [293]. Ball milling ensured the formation of homogeneous hydrogel composed of reduced graphene oxide embedded in cellulose matrix, improved thermal stability, and enhanced crystallinity of the cellulose matrix inside the nanocomposite. Reduced graphene oxide along with the coagulation effect of cellulose material facilitated the preservation of 3D porous morphology during freeze-drying and the conducting material. This nanocomposite material with a GO/cellulose ratio of 70:100 showed a modest electrical conductivity of 15 S m^{-1}. Also, these composites showed an ideal capacitive behavior and showed a specific capacitance of 71 F g^{-1} at a current density of 0.5 A g^{-1}.

A facile technique to selectively write conductive layers in graphene oxide nanocomposite films with a predefined pattern and controlled depth of the conductive layer has been introduced recently by the Tsukruk group [105]. The reduced graphene oxide-silk fibroin nanocomposite films exhibit high electrical conductivity reaching 1500 S m^{-1} along with outstanding mechanical performance. The eco-friendly reduction strategy using aluminum metal at ambient conditions and the versatility of 3D conductivity patterning of graphene oxide containing nanocomposite films are attractive for further development of flexible electronics.

Numerous recent publications on this topic include studies on inkjet printing of nanocomposite films with highly conductive patterns [294], high performance and flexible electromagnetic shielding nanocomposites [294], elastic and conducting hydrogels with double network morphology [295], and conducting melt-spun nanocomposite fibers [296]. Among other interesting developments are free-standing flexible graphene-PANI papers with good cycling stability [297], polycarbonate nanocomposites with much improved electrical conductivity [298], a variety of natural electroconductive cellulose nanocomposites [299,300], electrical memory devices from conjugated polymers and reduced graphene oxides [301], and melt processed polyamide conductive films [302]. However, large-scale production of graphene-polymer nanocomposites are rarely mentioned despite the numerous prospective applications suggested in sensing, gas permeation, energy conversion/storage, thermal management, and the other electronic applications discussed in this chapter.

6. Outlooks

6.1. Dispersion and distribution of the graphene nanofillers

A fine control of dispersion and distribution of the graphene nanofillers remains the major problem for the effective reinforcement of the mechanical properties and adding functional properties to the graphene-based nanocomposites. Distributed network morphology and suppressed flexible component aggregation enable the optimal exposure of the graphene surface to the polymer matrix. For these optimal dispersion levels, the interfacial binding can be maximized and interconnected morphology can be realized. The achievement of such optimal morphology represents a great challenge and indeed is an acute issue for the integration of graphene components that, considering their flexibility and high aspect ratio, can be easily folded, crumpled, and wrinkled by even modest shearing forces and complex force field distribution during processing.

Although the conventional solution and melt stirring-mixing techniques can facilitate, to some extent, prevention of macroscopic aggregation, it is difficult to prepare a uniform morphology with a fine dispersion of the interconnected graphene derivatives due to inherent affinity of the same species of material components. Several mixing techniques such as high-speed stirring, forced convection flow, and sonication, might improve the uniformity of mixing, but it usually ignores the negative impact of the violent preparation processes on flexible graphene components. In fact, vigorous mixing with external stirring and intense sonication may tear or crumple the large flakes of the graphene derivatives, which can be exceptionally unfavorable to achieving the ultimate mechanical, electrical, optoelectronic, and thermal properties of the resulting nanocomposites [83].

Various assembling techniques and in situ polymerization approached should be considered to suppress the problems associated with of the inhomogeneous distribution and coarse dispersion of graphene components by conventional mixing or the presence of small, broken or crumpled flakes by forcibly enhanced mixings. One of them is via an LbL assembly, facilitated by alternative nanoscale assembly of the polymer and graphene components. The highly ordered LbL layered nanocomposite films are built through natural or force-assisted adsorption of complementary components. Vacuum assisted formation of layered papers is another promising and practical approach. These techniques control the nanostructures of graphene-polymer nanocomposites from bottom up and result in optimized distribution and dispersion of components in a layered fashion thus enhancing interfacial interactions and mechanical performance.

However, these approaches are usually only capable of constructing layered and relatively thin (usually micrometer range) materials; bulk items cannot be formed easily. Moreover, the functional properties of the resulting films and coatings are highly anisotropic. Due to the 2D sheet geometry of the graphene derivative materials, the mechanical, electrical, and thermal properties are outstanding only in the in-plane directions, while the out-of-plane properties being modest. In addition, vacuum-assisted fabrication techniques are usually slow, compromise on precise control of graphene distribution, and are not very suitable for the robust fabrication of bulky macroscopic items with complex shapes.

In situ polymerization approaches utilize an initially homogeneous mixture of the graphene derivatives and reactive monomers. Because the entropy penalty for the mixing of the small molecules with graphene derivatives in solution is much smaller than that of the macromolecules, phase separation of different components is less severe problem and might be avoided by proper selection of components. The uniformly distributed monomer can be polymerized without significant distortions of dispersed phase and the graphene derivatives can be encapsulated in the resulting polymer matrix. However, due to the potential chemical instability of the graphene derivatives, the in situ polymerization approach faces some limitations. For example, large graphene oxide flakes might precipitate in acidic reactive conditions and in the course of polymerization or be reduced in high temperature or strong basic conditions.

6.2. Improving interactions between graphene and the polymer matrix

Although graphene has by far the best mechanical properties of all potential reinforcing components, the binding options are limited to weak van der Waals forces, hydrophobic interactions, and π–π interactions due to the homogeneous sp^2 carbon composition. These forces are generally too weak as the primary binding means and only π–π-interactions might be a promising candidate to assemble graphene and polymers with a strong interface [130,303]. Therefore, enhanced functionalization of graphene components with proper surface and edge chemical groups must be considered in order to improve interfacial binding with various polymer matrices and implement reinforcing effects. To this end, graphene oxide sheets and other functionalized graphene-based components are considered as promising reinforcing agents.

Graphene oxide is a widely explored derivative of graphene with a lot of advantages over graphene itself from the prospective of nanocomposite design, including aqueous processibility, low cost, the ability to further functionalization, and large-scale production. The heterogeneous surfaces of these graphene derivatives caused by the heavy localized oxygen-containing groups might facilitate the diverse options for the strong interfacial binding. A whole class of polar interactions becomes available for designing new strong interfaces, including hydrogen bonding, Coulombic and polar interactions, in addition covalent bonding.

To fully unveil the binding potential of functionalized graphene derivatives, a careful choice of the matching polymer matrices is critical. Pre-treatment of these derivatives by grafting proper polymer chains compatible with a polymer matrix can be considered as a plausible routine for enhanced reinforcement, which, however, requires additional complex polymerization routines. For heterogeneous graphene oxide sheets it is paramount to have a heterogeneous binder that can bind with the different functionalities so that the integrated interfacial binding is maximized. Biomacromolecules or block-copolymers with multi-domain composition should be considered to explore such strategies. However, this approach is largely unexplored to date.

6.3. Controlled reduction of graphene oxide in nanocomposites

It is well established that the next important property to be considered, electrical conductivity, is greatly compromised for graphene oxide by the scission of sp^2 bonds, high concentration of hole defects and surface oxygen functionalities. Therefore, for emerging applications, which require the ultimate conductivity of graphene-polymer nanocomposites, graphene oxide has to be reduced through a variety of chemical and thermal methods before, during, and after nanocomposite fabrication [61,101–103,304–306]. Efficient reduction results in the partial restoration of pristine electrically conducting state of reduced graphene oxide sheets and graphene-polymer nanocomposites as a whole to a practically relevant high level.

The electrical conductivity may be restored to relatively high values, at least 1000 S m^{-1}, high enough for many "soft" electronic applications such as those considered in flexible organic/polymer electronics and bioelectronics. The corresponding graphene-polymer materials may be considered for the integration into flexible electronic devices. It is also critically important that the mechanical properties of the reduced graphene can be improved as well due to the restoration of the sp^2 hybridized carbon network and reduction of surface defects. Both electrical and mechanical properties may be improved significantly to a level suitable for various structural and functional applications by controlling the reduction level of the graphene oxide in the polymer nanocomposites.

However, it is important to remember that many of the of reducing agents and approaches, employed through harsh thermal, chemical, or light means, may damage the less stable polymeric matrix in the nanocomposite. More material components and environmentally friendly processing options should be developed to assure the feasibility of this approach. Both a careful choice of reducing techniques and a combination of reducing techniques with minimum damage for the polymer components are critical for the control of the mechanical, electrical, optical, thermal, and chemical properties of the graphene-polymer nanocomposites.

7. Conclusions

This review has summarized recent efforts on the materials selection, binding approaches, processing methods, theoretical models, design rules, and resulting mechanical, thermal, electrical and other functional properties of graphene-polymer nanocomposites. Graphene derivatives have outstanding mechanical properties and versatile functionalities to bind with various polymeric materials. Generally, the ultimate performance might be potentially outstanding as has been already demonstrated on a number of occasions.

Solution and melt-mixing, LbL assembly, vacuum-assisted routines, and in situ polymerization have unique characteristics and their own advantages for the fabrication of graphene-based nanocomposites with ultimate mechanical and functional properties. Critical issues are related to homogeneous dispersion in initial mixed states and fine dispersion with exfoliations of individual layers and the establishment of the interconnected morphology. Choosing the appropriate dispersion technique or the combination of processing techniques and finding proper functionalized components is critical for reaching the best mechanical performance as illustrated with major characteristics such as those collected for a number of representative nanocomposite materials reported to date in Table 2.

In conclusion, the best performing graphene-polymer nanocomposites presented in Table 2 in terms of the most important mechanical properties for the ultimate mechanical applications such as the elastic modulus value and toughness are visualized in Fig. 26. The data points, related directly to numbering from Table 2, are color-coded to reflect their ultimate mechanical strength in terms of stress-to-break values.

This summary plot shows that the majority of the best results reported to date for graphene-polymer nanocomposites are skewed to different axes and can be grouped in two very dissimilar groups. The first group represents tough graphene-polymer nanocomposites with record values of toughness, which, however, do not show very high mechanical performance in terms of elastic modulus (mostly below 20 GPa) and the ultimate mechanical strength. The second group of materials includes mechanically strong nanocomposites with the extremely high elastic modulus value of 100–150 GPa (higher than steel), which, however, possess lower toughness due to their brittle behavior (well below 2 MJ m^{-3}).

A wide area of the potentially best performing tough, strong, and compliant graphene-polymer nanocomposites (central region) remains largely empty currently. Only few recent examples (3, 12, 15) cross the critical lines

Table 2
The mechanical properties of the recent polymer-graphene nanocomposites.

No.	Materials [reference]	Form	Polymer content (%)	Fabrication method	Ultimate strength (MPa)	Young's modulus (GPa)	Ultimate strain (%)	Toughness ($MJ m^{-3}$)
Graphene derivative predominant								
1	GO [130]	Microfilm (paper)	0	VA-SA	120	36	0.42	0.26
2	rGO [206]		0	VA-SA + thermal annealing	293.3	41.8	0.83	1.22
3	rGO-silk fibroin [105]		2.5 wt	VA-SA	300	26	1.5	2.8
4	GO-PCDO [112]		6.5 wt	VA-SA + crosslinking	106.6	2.5–3.6	4.5	2.52
5			~6.5 wt	VA-SA + crosslinking + HI reduction	129.6	1.5–4	6.9	3.91
6	GO-PEI [208]		14.7 wt	VA-SA + immerse crosslinking	179	84.8	0.23	0.21
7				VA-SA + vacuum-assisted crosslinking	209.9	103.4	0.22	0.23
8	rGO-PVA [215]		20 wt	Drop cast + HI reduction	190	11.4	2.6	2.7
9	GO-PAA [97]		21 wt	VA-SA	91	11.3–33.3	0.32	0.2
10	GO-PMMA [209]		31 wt		102.9	6	2.58	~1.3
11	GO-PVA [209]		34 wt		80.2	36.4	0.25	0.1
Polymer predominant								
12	GO-silk fibroin [64]	Ultrathin membrane	76.5 vol	SA-LbL	300	145	0.9	2.2
13	GO-PAH/PSS [3]	Ultrathin membrane	96.7 vol	SA-LbL + Langmuir Blodgett	130	18.2	2.3	1.9
14	GO-PVA [210]	Film	97 wt	Drop cast	62	~6	155	77.5
15	Graphene-NFC [214]	Microfilm (paper)	98.75 wt	VA-SA	278	20.2	3.2	~5
16	Graphene-PDMS [211]	Film	99 wt	Shear mixing + spin	3.4	$\sim 2.3 \times 10^{-3}$	135	2.3

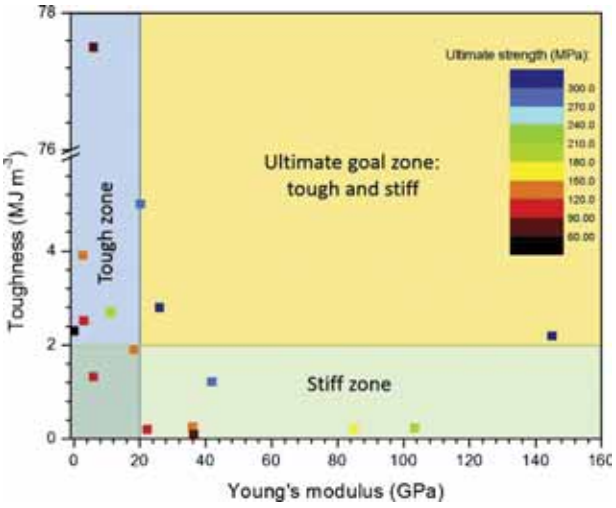

Fig. 26. Mechanical properties of the graphene-polymer nanocomposites in the toughness-modulus space with data points color-coded with ultimate strength and data points numbered according to Table 2.

separating these data into the two groups (Fig. 26). Currently, such a general pattern, common for many composite materials, leaves exciting opportunities for the synergistic reinforcement of the universal mechanical properties of graphene-polymer nanocomposites to be explored in the near future.

Finally, various theoretical models with different assumptions are used to predict the mechanical properties of the graphene-polymer nanocomposites with various successes. The validity of the predicted values by different models largely depends on the assumptions made by the models are not always valid for these nanocomposite materials with developed interphases, posing a subject for further development.

Acknowledgements

The authors thank the support for activities in the field of advanced nanocomposite materials by Grant FA9550-11-1-0233 from the Air Force Office for Scientific Research (Bioinspired nanomaterials), the U.S. Department of Energy, Office of Basic Energy Sciences, Division of Materials Sciences and Engineering Award # DE-FG02-09ER46604 (energy-related nanostructures), 2008OJ1864.1281 grant from Semiconductor Research Corporation (graphene conductivity), and Grant NSF-DMR 1002810 from the National Science Foundation (polymer-filler interfaces).

References

[1] Baekeland LH. The synthesis, constitution, and uses of Bakelite. J Ind Eng Chem 1909;1:149–61.
[2] Sperling LH. Introduction to physical polymer science. 4th ed. Hoboken: John Wiley & Sons Inc.; 2006, 845 p.
[3] Kulkarni DD, Choi I, Singamaneni SS, Tsukruk VV. Graphene oxide-polyelectrolyte nanomembranes. ACS Nano 2010;4:4667–76.
[4] Kharlampieva E, Kozlovskaya V, Gunawidjaja R, Shevchenko VV, Vaia R, Naik RR, Kaplan DL, Tsukruk VV. Flexible silk-inorganic nanocomposites: from transparent to highly reflective. Adv Funct Mater 2010;20:840–6.

[5] Jiang C, Wang X, Gunawidjaja R, Lin YH, Gupta MK, Kaplan DL, Naik RR, Tsukruk VV. Mechanical properties of robust ultrathin silk fibroin films. Adv Funct Mater 2007;17:2229–37.
[6] Podsiadlo P, Kaushik AK, Arruda EM, Waas AM, Shim BS, Xu J, Nandivada H, Pumplin BG, Lahann J, Ramamoorthy A, Kotov NA. Ultrastrong and stiff layered polymer nanocomposites. Science 2007;318:80–3.
[7] Xue L, Dai S, Li Z. Biodegradable shape-memory block co-polymers for fast self-expandable stents. Biomaterials 2010;31:8132–40.
[8] Li C, Adamcik J, Mezzenga R. Biodegradable nanocomposites of amyloid fibrils and graphene with shape-memory and enzyme-sensing properties. Nat Nanotechnol 2012;7:421–7.
[9] Bovey F, Winslow FH, editors. Macromolecules: an introduction to polymer science. New York: Academic Press; 1979, 549 p.
[10] Ram A. Fundamentals of polymer engineering. New York: Plenum Press; 1997, 237 p.
[11] Painter PC, Coleman MM. Fundamentals of polymer science: an introductory text. Chicago: Technomic Publishing Company; 1997, 478 p.
[12] Ebewele RO. Polymer science and technology. London: CRC Press; 2000, 483 p.
[13] Brazel CS, Rosen SL. Fundamental principles of polymeric materials. Hoboken: John Wiley & Sons Inc.; 2012, 407 p.
[14] Dongyu C, Kamal Y, Mo S. The mechanical properties and morphology of a graphite oxide nanoplatelet/polyurethane composite. Nanotechnology 2009;20:085712.
[15] Kai W, Hirota Y, Hua L, Inoue Y. Thermal and mechanical properties of a poly(ε-caprolactone)/graphite oxide composite. J Appl Polym Sci 2008;107:1395–400.
[16] Fang M, Zhang Z, Li J, Zhang H, Lu H, Yang Y. Constructing hierarchically structured interphases for strong and tough epoxy nanocomposites by amine-rich graphene surfaces. J Mater Chem 2010;20:9635–43.
[17] Bao C, Guo Y, Song L, Kan Y, Qian X, Hu Y. In situ preparation of functionalized graphene oxide/epoxy nanocomposites with effective reinforcements. J Mater Chem 2011;21:13290–8.
[18] Bates FS, Fredrickson GH. Block copolymer thermodynamics: theory and experiment. Annu Rev Phys Chem 1990;41:525–57.
[19] Lazzari M, López-Quintela MA. Block copolymers as a tool for nanomaterial fabrication. Adv Mater 2003;15:1583–94.
[20] Gröschel AH, Löbling TI, Petrov PD, Müllner M, Kuttner C, Wieberger F, Müller AHE. Janus micelles as effective supracolloidal dispersants for carbon nanotubes. Angew Chem Int Ed 2013;52:3602–6.
[21] Hu H, Zhao Z, Wan W, Gogotsi Y, Qiu J. Ultralight and highly compressible graphene aerogels. Adv Mater 2013;25:2219–23.
[22] Sun H, Xu Z, Gao C. Multifunctional, ultra-flyweight, synergistically assembled carbon aerogels. Adv Mater 2013;25:2554–60.
[23] Jay SM, Shepherd BR, Bertram JP, Pober JS, Saltzman WM. Engineering of multifunctional gels integrating highly efficient growth factor delivery with endothelial cell transplantation. FASEB J 2008;22:2949–56.
[24] Kim UJ, Park J, Li C, Jin HJ, Valluzzi R, Kaplan DL. Structure and properties of silk hydrogels. Biomacromolecules 2004;5:786–92.
[25] Das P, Schipmann S, Malho JM, Zhu B, Klemradt U, Walther A. Facile access to large-scale, self-assembled, nacre-inspired, high-performance materials with tunable nanoscale periodicities. ACS Appl Mater Interfaces 2013;5:3738–47.
[26] Mallick PK. Fiber-reinforced composites: materials, manufacturing, and design. New York: Marcel Dekker Inc.; 1993, 584 p.
[27] Ajayan PM, Schadler LS, Braun PV. Nanocomposite science and technology. Weinheim: Wiley; 2006, 239 p.
[28] Ko H, Jiang C, Shulha H, Tsukruk VV. Carbon nanotube arrays encapsulated into freely suspended flexible films. Chem Mater 2005;17:2490–3.
[29] Cheng Q, Wang B, Zhang C, Liang Z. Functionalized carbon-nanotube sheet/bismaleimide nanocomposites: mechanical and electrical performance beyond carbon-fiber composites. Small 2010;6:763–7.
[30] Mamedov AA, Kotov NA. Free-standing layer-by-layer assembled films of magnetite nanoparticles. Langmuir 2000;16:5530–3.
[31] Aroca RF, Goulet PJG, dos Santos DS, AlvarezPuebla RA, Oliveira ON. Silver nanowire layer-by-layer films as substrates for surface-enhanced Raman scattering. Anal Chem 2004;77:378–82.
[32] Kovtyukhova NI, Martin BR, Mbindyo JKN, Smith PA, Razavi B, Mayer TS, Mallouk TE. Layer-by-layer assembly of rectifying junctions in and on metal nanowires. J Phys Chem B 2001;105:8762–9.
[33] Podsiadlo P, Tang Z, Shim BS, Kotov NA. Counterintuitive effect of molecular strength and role of molecular rigidity on mechanical properties of layer-by-layer assembled nanocomposites. Nano Lett 2007;7:1224–31.
[34] Sun X, Sun H, Li H, Peng H. Developing polymer composite materials: carbon nanotubes or graphene? Adv Mater 2013;25:5153–76.
[35] Shi Z, Chen X, Wang X, Zhang T, Jin J. Fabrication of superstrong ultrathin free-standing single-walled carbon nanotube films via a wet process. Adv Funct Mater 2011;21:4358–63.
[36] Mamedov AA, Kotov NA, Prato M, Guldi DM, Wicksted JP, Hirsch A. Molecular design of strong single-wall carbon nanotube/polyelectrolyte multilayer composites. Nat Mater 2002;1:190–4.
[37] Shim BS, Zhu J, Jan E, Critchley K, Ho S, Podsiadlo P, Sun K, Kotov NA. Multiparameter structural optimization of single-walled carbon nanotube composites: toward record strength, stiffness, and toughness. ACS Nano 2009;3:1711–22.
[38] Jalili R, Aboutalebi SH, Esrafilzadeh D, Konstantinov K, Moulton SE, Razal JM, Wallace GG. Organic solvent-based graphene oxide liquid crystals: a facile route toward the next generation of self-assembled layer-by-layer multifunctional 3D architectures. ACS Nano 2013;7:3981–90.
[39] Eitan A, Fisher FT, Andrews R, Brinson LC, Schadler LS. Reinforcement mechanisms in MWCNT-filled polycarbonate. Compos Sci Technol 2006;66:1162–73.
[40] Gunawidjaja R, Jiang C, Peleshanko S, Ornatska M, Singamaneni S, Tsukruk VV. Flexible and robust 2D arrays of silver nanowires encapsulated within freestanding layer-by-layer films. Adv Funct Mater 2006;16:2024–34.
[41] Jiang C, Markutsya S, Tsukruk VV. Compliant, robust, and truly nanoscale free-standing multilayer films fabricated using spin-assisted layer-by-layer assembly. Adv Mater 2004;16:157–61.
[42] Markutsya S, Jiang C, Pikus Y, Tsukruk VV. Freely suspended layer-by-layer nanomembranes: testing micromechanical properties. Adv Funct Mater 2005;15:771–80.
[43] Wang J, Cheng Q, Lin L, Chen L, Jiang L. Understanding the relationship of performance with nanofiller content in the biomimetic layered nanocomposites. Nanoscale 2013;5:6356–62.
[44] Luzinov I, Minko S, Tsukruk VV. Responsive brush layers: from tailored gradients to reversibly assembled nanoparticles. Soft Matter 2008;4:714–25.
[45] Kharlampieva E, Zimnitsky D, Gupta MK, Bergman KN, Kaplan DL, Naik RR, Tsukruk VV. Redox-active ultrathin template of silk fibroin: effect of secondary structure on gold nanoparticle reduction. Chem Mater 2009;21:2696–704.
[46] Corbierre MK, Cameron NS, Sutton M, Mochrie SGJ, Lurio LB, Rühm A, Lennox RB. Polymer-stabilized gold nanoparticles and their incorporation into polymer matrices. J Am Chem Soc 2001;123:10411–2.
[47] Hussain I, Brust M, Papworth AJ, Cooper AI. Preparation of acrylate-stabilized gold and silver hydrosols and gold–polymer composite films. Langmuir 2003;19:4831–5.
[48] Hou Y, Cheng Y, Hobson T, Liu J. Design and synthesis of hierarchical MnO_2 nanospheres/carbon nanotubes/conducting polymer ternary composite for high performance electrochemical electrodes. Nano Lett 2010;10:2727–33.
[49] Beek WJE, Wienk MM, Janssen RAJ. Efficient hybrid solar cells from zinc oxide nanoparticles and a conjugated polymer. Adv Mater 2004;16:1009–13.
[50] Kabra D, Song MH, Wenger B, Friend RH, Snaith HJ. High efficiency composite metal oxide-polymer electroluminescent devices: a morphological and material based investigation. Adv Mater 2008;20:3447–52.
[51] Sirisinha C, Prayoonchatphan N. Study of carbon black distribution in BR/NBR blends based on damping properties: influences of carbon black particle size, filler, and rubber polarity. J Appl Polym Sci 2001;81:3198–203.
[52] Shamir D, Siegmann A, Narkis M. Vibration damping and electrical conductivity of styrene–butyl acrylate random copolymers filled with carbon black. J Appl Polym Sci 2010;115:1922–8.
[53] Hu K, Chung DDL. Flexible graphite modified by carbon black paste for use as a thermal interface material. Carbon 2011;49:1075–86.
[54] Friddle RW, LeMieux MC, Cicero G, Artyukhin AB, Tsukruk VV, Grossman JC, Galli G, Noy A. Single functional group interactions with individual carbon nanotubes. Nat Nanotechnol 2007;2:692–7.
[55] Grady BP. Carbon nanotube-polymer composites: manufacture, properties, and applications. Hoboken: John Wiley & Sons Inc.; 2011, 368 p.

[56] Koning C, Grossiord N, Hermant MC. Polymer carbon nanotube composites: the polymer latex concept. Singapore: Pan Stanford; 2012, 256 p.
[57] Coleman JN, Khan U, Blau WJ, Gun'ko YK. Small but strong: a review of the mechanical properties of carbon nanotube–polymer composites. Carbon 2006;44:1624–52.
[58] Bauhofer W, Kovacs JZ. A review and analysis of electrical percolation in carbon nanotube polymer composites. Compos Sci Technol 2009;69:1486–98.
[59] Pandey G, Thostenson ET. Carbon nanotube-based multifunctional polymer nanocomposites. Polym Rev 2012;52:355–416.
[60] Britnell L, Ribeiro RM, Eckmann A, Jalil R, Belle BD, Mishchenko A, Kim YJ, Gorbachhev RV, Georgiou T, Morozov SV, Grigorenko AN, Geim AK, Casiraghi C, Castro Meto AH, Novoselov KS. Strong light-matter interactions in heterostructures of atomically thin films. Science 2013;340:1311–4.
[61] El-Kady MF, Kaner RB. Scalable fabrication of high-power graphene micro-supercapacitors for flexible and on-chip energy storage. Nat Commun 2013;4:1475/1–1475.
[62] Kim KS, Zhao Y, Jang H, Lee SY, Kim JM, Kim KS, Ahn JH, Kim P, Choi JY, Hong BH. Large-scale pattern growth of graphene films for stretchable transparent electrodes. Nature 2009;457:706–10.
[63] Tetsuka H, Asahi R, Nagoya A, Okamoto K, Tajima I, Ohta R, Okamoto A. Optically tunable amino-functionalized graphene quantum dots. Adv Mater 2012;24:5333–8.
[64] Hu K, Gupta MK, Kulkarni DD, Tsukruk VV. Ultra-robust graphene oxide-silk fibroin nanocomposite membranes. Adv Mater 2013;25:2301–7.
[65] Mannoor MS, Tao H, Clayton JD, Sengupta A, Kaplan DL, Naik RR, Verma N, Omenetto FG, McAlpine MC. Graphene-based wireless bacteria detection on tooth enamel. Nat Commun 2012;3:763/1–763.
[66] Guo W, Cheng C, Wu Y, Jiang Y, Gao J, Li D, Jiang L. Bio-inspired two-dimensional nanofluidic generators based on a layered graphene hydrogel membrane. Adv Mater 2013;25:6064–8.
[67] Shahil KMF, Balandin AA. Thermal properties of graphene and multilayer graphene: applications in thermal interface materials. Solid State Commun 2012;152:1331–40.
[68] Geim AK, Grigorieva IV. Van der Waals heterostructures. Nature 2013;499:419–25.
[69] Kim H, Abdala AA, Macosko CW. Graphene/polymer nanocomposites. Macromolecules 2010;43:6515–30.
[70] Kuilla T, Bhadra S, Yao D, Kim NH, Bose S, Lee JH. Recent advances in graphene based polymer composites. Prog Polym Sci 2010;35:1350–75.
[71] Compton OC, Nguyen ST. Graphene oxide, highly reduced graphene oxide, and graphene: versatile building blocks for carbon-based materials. Small 2010;6:711–23.
[72] Huang X, Yin Z, Wu S, Qi X, He Q, Zhang Q, Yan Q, Boey F, Zhang H. Graphene-based materials: synthesis, characterization, properties, and applications. Small 2011;7:1876–902.
[73] Young RJ, Kinloch IA, Gong L, Novoselov KS. The mechanics of graphene nanocomposites: a review. Compos Sci Technol 2012;72:1459–76.
[74] Wu D, Zhang F, Liang H, Feng X. Nanocomposites and macroscopic materials: assembly of chemically modified graphene sheets. Chem Soc Rev 2012;41:6160–77.
[75] Yang M, Hou Y, Kotov NA. Graphene-based multilayers: critical evaluation of materials assembly techniques. Nano Today 2012;7:430–47.
[76] Lee C, Wei X, Kysar JW, Hone J. Measurement of the elastic properties and intrinsic strength of monolayer graphene. Science 2008;321:385–8.
[77] Balandin AA, Ghosh S, Bao W, Calizo I, Teweldebrhan D, Miao F, Lau CN. Superior thermal conductivity of single-layer graphene. Nano Lett 2008;8:902–7.
[78] Du X, Skachko I, Barker A, Andrei EY. Approaching ballistic transport in suspended graphene. Nat Nanotechnol 2008;3:491–5.
[79] Allen MJ, Tung VC, Kaner RB. Honeycomb carbon: a review of graphene. Chem Rev 2009;110:132–45.
[80] Liu Y, Yu D, Zeng C, Miao Z, Dai L. Biocompatible graphene oxide-based glucose biosensors. Langmuir 2010;26:6158–60.
[81] Wang K, Ruan J, Song H, Zhang J, Wo Y, Guo S, Cui D. Biocompatibility of graphene oxide. Nanoscale Res Lett 2011;6:8.
[82] Zhang X, Yin J, Peng C, Hu W, Zhu Z, Li W, Fan C, Huang Q. Distribution and biocompatibility studies of graphene oxide in mice after intravenous administration. Carbon 2011;49:986–95.
[83] Compton OC, An Z, Putz KW, Hong BJ, Hauser BG, Catherine Brinson LC, Nguyen ST. Additive-free hydrogelation of graphene oxide by ultrasonication. Carbon 2012;50:3399–406.
[84] Li D, Muller MB, Gilje S, Kaner RB, Wallace GG. Processable aqueous dispersions of graphene nanosheets. Nat Nanotechnol 2008;3:101–5.
[85] Hummers WS, Offeman RE. Preparation of graphitic oxide. J Am Chem Soc 1958;80:1339.
[86] Dreyer DR, Park S, Bielawski CW, Ruoff RS. The chemistry of graphene oxide. Chem Soc Rev 2010;39:228–40.
[87] Bachtold A, Fuhrer MS, Plyasunov S, Forero M, Anderson EH, Zettl A, McEuen PL. Scanned probe microscopy of electronic transport in carbon nanotubes. Phys Rev Lett 2000;84:6082–5.
[88] Gómez-Navarro C, Moreno-Herrero F, de Pablo PJ, Colchero J, Gómez-Herrero J, Baró AM. Contactless experiments on individual DNA molecules show no evidence for molecular wire behavior. Proc Natl Acad Sci U S A 2002;99:8484–7.
[89] Jespersen TS, Nygård J. Charge trapping in carbon nanotube loops demonstrated by electrostatic force microscopy. Nano Lett 2005;5:1838–41.
[90] Kulkarni DD, Kim S, Chyasnavichyus M, Hu K, Fedorov AG, Tsukruk VV. Chemical reduction of individual graphene oxide sheets as revealed by electrostatic force microscopy. J Am Chem Soc 2014, http://dx.doi.org/10.1021/ja5005416.
[91] Lv C, Xue Q, Xia D, Ma M, Xie J, Chen H. Effect of chemisorption on the interfacial bonding characteristics of graphene–polymer composites. J Phys Chem C 2010;114:6588–94.
[92] Loh KP, Bao Q, Eda G, Chhowalla M. Graphene oxide as a chemically tunable platform for optical applications. Nat Chem 2010;2:1015–24.
[93] Gómez-Navarro C, Burghard M, Kern K. Elastic properties of chemically derived single graphene sheets. Nano Lett 2008;8:2045–9.
[94] Suk JW, Piner RD, An J, Ruoff RS. Mechanical properties of monolayer graphene oxide. ACS Nano 2010;4:6557–64.
[95] An Z, Compton OC, Putz KW, Brinson LC, Nguyen ST. Bio-inspired borate cross-linking in ultra-stiff graphene oxide thin films. Adv Mater 2011;23:3842–6.
[96] Chen C, Yang QH, Yang Y, Lv W, Wen Y, Hou PX, Wang M, Cheng HM. Self-assembled free-standing graphite oxide membrane. Adv Mater 2009;21:3007–11.
[97] Park S, Dikin DA, Nguyen ST, Ruoff RS. Graphene oxide sheets chemically cross-linked by polyallylamine. J Phys Chem C 2009;113:15801–4.
[98] Pei S, Cheng HM. The reduction of graphene oxide. Carbon 2012;50:3210–28.
[99] Mao S, Pu H, Chen J. Graphene oxide and its reduction: modeling and experimental progress. RSC Adv 2012;2:2643–62.
[100] Kuila T, Mishra AK, Khanra P, Kim NH, Lee JH. Recent advances in the efficient reduction of graphene oxide and its application as energy storage electrode materials. Nanoscale 2013;5:52–71.
[101] Feng H, Cheng R, Zhao X, Duan X, Li J. A low-temperature method to produce highly reduced graphene oxide. Nat Commun 2013;4:1539/1–1539.
[102] Fan Z, Wang K, Wei T, Yan J, Song L, Shao B. An environmentally friendly and efficient route for the reduction of graphene oxide by aluminum powder. Carbon 2010;48:1686–9.
[103] El-Kady MF, Strong V, Dubin S, Kaner RB. Laser scribing of high-performance and flexible graphene-based electrochemical capacitors. Science 2012;335:1326–30.
[104] Moon IK, Lee J, Ruoff RS, Lee H. Reduced graphene oxide by chemical graphitization. Nat Commun 2010;1:73/1–73.
[105] Hu K, Tolentino LS, Kulkarni DD, Tsukruk VV. Written-in conductive patterns on robust graphene oxide biopaper by localized electrochemical reduction. Angew Chem Int Ed 2013;52:13784–8.
[106] Kulkarni DD, Kim S, Fedorov AG, Tsukruk VV. Light-induced plasmon-assisted phase transformation of carbon on metal nanoparticles. Adv Funct Mater 2012;22:2129–39.
[107] Israelachvili JN. Intermolecular and surface forces. San Diego: Academic Press; 2010, 710 p.
[108] Adamson AW. Physical chemistry of surfaces. New York: John Wiley & Sons Inc.; 1990, 777 p.
[109] Jiang LY, Huang Y, Jiang H, Ravichandran G, Gao H, Hwang KC, Liu B. A cohesive law for carbon nanotube/polymer interfaces based on the van der Waals force. J Mech Phys Solids 2006;54:2436–52.
[110] Shen B, Zhai W, Chen C, Lu D, Wang J, Zheng W. Melt blending in situ enhances the interaction between polystyrene and graphene through p-p stacking. ACS Appl Mater Interfaces 2011;3:3103–9.

[111] Zhang HL, Wei XL, Zang Y, Cao JY, Liu S, He XP, Chen Q, Long YT, Li J, Chen GR, Chen K. Fluorogenic probing of specific recognitions between sugar ligands and glycoprotein receptors on cancer cells by an economic graphene nanocomposite. Adv Mater 2013;25:4097–101.
[112] Cheng Q, Wu M, Li M, Jiang L, Tang Z. Ultratough artificial nacre based on conjugated cross-linked graphene oxide. Angew Chem Int Ed 2013;52:3750–5.
[113] Liu J, Fu S, Yuan B, Li Y, Deng Z. Toward a universal "adhesive nanosheet" for the assembly of multiple nanoparticles based on a protein-induced reduction/decoration of graphene oxide. J Am Chem Soc 2010;132:7279–81.
[114] Kim J, Cote LJ, Kim F, Yuan W, Shull KR, Huang J. Graphene oxide sheets at interfaces. J Am Chem Soc 2010;132:8180–6.
[115] Berg JM, Deis FH, Tymoczko JL, Stryer L, Gerber NC, Gumport R, Koeppe RE. Biochemistry student companion. New York: W. H. Freeman; 2011, 608 p.
[116] Israelachvili J, Pashley R. The hydrophobic interaction is long range, decaying exponentially with distance. Nature 1982;300:341–2.
[117] Sinnokrot MO, Valeev EF, Sherrill CD. Estimates of the Ab initio limit for π–π interactions: the benzene dimer. J Am Chem Soc 2002;124:10887–93.
[118] Bondi A. Van der Waals volumes and radii. J Phys Chem 1964;68:441–51.
[119] Kerner EH. The elastic and thermo-elastic properties of composite media. Proc Phys Soc Sect B 1956;69:808–13.
[120] Smallwood HM. Limiting law of the reinforcement of rubber. J Appl Phys 1944;15:758–66.
[121] Agarwal BD, Broutman LJ, Chandrashekhara K. Analysis and performance of fiber composites. New York: John Wiley & Sons Inc.; 2006, 562 p.
[122] Wan C, Chen B. Reinforcement and interphase of polymer/graphene oxide nanocomposites. J Mater Chem 2012;22:3637–46.
[123] Affdl JCH, Kardos JL. The Halpin–Tsai equations: a review. Polym Eng Sci 1976;16:344–52.
[124] Fornes TD, Paul DR. Modeling properties of nylon 6/clay nanocomposites using composite theories. Polymer 2003;44:4993–5013.
[125] Tandon GP, Weng GJ. The effect of aspect ratio of inclusions on the elastic properties of unidirectionally aligned composites. Polym Compos 1984;5:327–33.
[126] Gao H, Ji B, Jäger IL, Arzt E, Fratzl P. Materials become insensitive to flaws at nanoscale: lessons from nature. Proc Natl Acad Sci U S A 2003;100:5597–600.
[127] Lipatov YS. Interfaces in polymer–polymer composites. In: Ishida H, editor. Controlled interphases in composite materials. Amsterdam: Elsevier Science Publ Co. Inc.; 1990. p. 599–611.
[128] Terrones M, Martín O, González M, Pozuelo J, Serrano B, Cabanelas JC, Vega-Díaz SM, Baselga J. Interphases in graphene polymer-based nanocomposites: achievements and challenges. Adv Mater 2011;23:5302–10.
[129] Kovalev A, Shulha H, Lemieux M, Myshkin N, Tsukruk VV. Nanomechanical probing of layered nanoscale polymer films with atomic force microscopy. J Mater Res 2004;19:716–28.
[130] Stankovich S, Dikin DA, Dommett GHB, Kohlhaas KM, Zimney EJ, Stach EA, Piner RD, Nguyen ST, Ruoff RS. Graphene-based composite materials. Nature 2006;442:282–6.
[131] Dikin AK, Stankovich S, Zimney EJ, Piner RD, Dommett GHB, Evmenenko G, Nguyen ST, Ruoff RS. Preparation and characterization of graphene oxide paper. Nature 2007;448:457–60.
[132] Ramanathan T, Abdala AA, Stankovich S, Dikin DA, Alonso MH, Piner RD, Adamson DH, Schniepp HC, Chen X, Ruoff RS, Nguyen ST, Aksay IA, Prud'Homme RK, Brinson LC. Functionalized graphene sheets for polymer nanocomposites. Nat Nanotechnol 2008;3:327–31.
[133] Xu Y, Wang Y, Jiajie L, Huang Y, Ma Y, Wan X, Chen Y. A hybrid material of graphene and poly(3, 4-ethyldioxythiophene) with high conductivity, flexibility, and transparency. Nano Res 2009;2:343–8.
[134] Quan H, Zhang B, Zhao Q, Yuen RKK, Li RKY. Facile preparation and thermal degradation studies of graphite nanoplatelets (GNPs) filled thermoplastic polyurethane (TPU) nanocomposites. Composites A 2009;40:1506–13.
[135] Eda G, Chhowalla M. Graphene-based composite thin films for electronics. Nano Lett 2009;9:814–8.
[136] Liang J, Xu Y, Huang Y, Zhang L, Wang Y, Ma Y, Li F, Guo T, Chen Y. Infrared-triggered actuators from graphene-based nanocomposites. J Phys Chem 2009;113:9921–7.
[137] Kim H, Macosko CW. Processing–property relationships of polycarbonate/graphene nanocomposites. Polymer 2009;50:3797–809.
[138] Ramanathan T, Stankovich S, Dikin DA, Liu H, Shen H, Nguyen ST, et al. Graphitic nanofillers in PMMA nanocomposites-an investigation of particle size and dispersion and their influence on nanocomposite properties. J Polym Sci B Polym Phys 2007;45:2097–112.
[139] Kim S, Do I, Drzal LT. Multifunctional *x*GnP/LLDPE nanocomposites prepared by solution compounding using various screw rotating systems. Macromol Mater Eng 2009;294:196–205.
[140] Liang J, Huang Y, Zhang L, Wang Y, Ma Y, Guo T, Chen Y. Molecular-level dispersion of graphene into poly(vinyl alcohol) and effective reinforcement of their nanocomposites. Adv Funct Mater 2009;19:2297–302.
[141] Zhao X, Zhang Q, Chen D. Enhanced mechanical properties of graphene-based poly(vinyl alcohol) composites. Macromolecules 2010;43:2357–63.
[142] Kalaitzidou K, Fukushima H, Drzal LT. A new compounding method for exfoliated graphite-polypropylene nanocomposites with enhanced flexural properties and lower percolation threshold. Compos Sci Technol 2007;67:2045–51.
[143] Zheng W, Lu X, Wong SC. Electrical and mechanical properties of expanded graphite-reinforced high-density polyethylene. J Appl Polym Sci 2004;91:2781–8.
[144] Zhao YF, Xiao M, Wang SJ, Ge XC, Meng YZ. Preparation and properties of electrically conductive PPS/expanded graphite nanocomposites. Compos Sci Technol 2007;67:2528–34.
[145] Du XS, Xiao M, Meng YZ. Synthesis and characterization of polyaniline/graphite conducting nanocomposites. J Polym Sci B Polym Phys 2004;42:1972–8.
[146] Cho D, Lee S, Yang G, Fukushima H, Drzal LT. Dynamic mechanical and thermal properties of phenylethynyl-terminated polyimide composites reinforced with expanded graphite nanoplatelets. Macromol Mater Eng 2005;290:179–87.
[147] Kim H, Miura Y, Macosko CW. Graphene/polyurethane nanocomposites for improved gas barrier and electrical conductivity. Chem Mater 2010;22:3441–50.
[148] Li H, Pang S, Wu S, Feng X, Müllen K, Bubeck C. Layer-by-layer assembly and UV photoreduction of graphene-polyoxometalate composite films for electronics. J Am Chem Soc 2011;133:9423–9.
[149] Cassagneau T, Fendler JH. High density rechargeable lithium-ion batteries self-assembled from graphite oxide nanoplatelets and polyelectrolytes. Adv Mater 1998;10:877–81.
[150] Hu H, Wang X, Wanga J, Wana L, Liu F, Zheng H, Chen R, Xu C. Preparation and properties of graphene nanosheets-polystyrene nanocomposites via in situ emulsion polymerization. Chem Phys Lett 2010;484:247–53.
[151] Leroux F, Besse JP. Polymer intercalated layered double hydroxide: a new emerging class of nanocomposites. Chem Mater 2001;13:3507–15.
[152] Stankovich S, Piner RD, Chen X, Wu N, Nguyen ST, Ruoff RS. Stable aqueous dispersions of graphitic nanoplatelets via the reduction of exfoliated graphite oxide in the presence of poly(sodium 4-styrenesulfonate). J Mater Chem 2006;16:155–8.
[153] Kim H, Macosko CW. Morphology and properties of polyester/exfoliated graphite nanocomposites. Macromolecules 2008;41:3317–27.
[154] Xu YX, Hong WJ, Bai H, Li C, Shi G. Strong and ductile poly(vinyl alcohol)/graphene oxide composite films with a layered structure. Carbon 2009;47:3538–43.
[155] Wu Q, Xu YX, Yao ZY, Liu AR, Shi GQ. Supercapacitors based on flexible graphene/polyaniline nanofiber composite films. ACS Nano 2010;4:1963–70.
[156] Yang X, Shang S, Li L. Layer-structured poly(vinyl alcohol)/graphene oxide nanocomposites with improved thermal and mechanical properties. J Appl Polym Sci 2011;120:1355–60.
[157] Yasmin A, Luo JJ, Daniel IM. Processing of expanded graphite reinforced polymer nanocomposites. Compos Sci Technol 2006;66:1182–9.
[158] Li Y, Umer R, Samad YA, Zheng L, Liao K. The effect of the ultrasonication pre-treatment of graphene oxide (GO) on the mechanical properties of GO/polyvinyl alcohol composites. Carbon 2013;55:321–7.
[159] Wajid AS, Tanvir Ahmed HS, Das S, Irin F, Jankowski AF, Green MJ. High-performance pristine graphene/epoxy composites with enhanced mechanical and electrical properties. Macromol Mater Eng 2013;298:339–47.
[160] Sayyar S, Murray E, Thompson BC, Gambhir S, Officer DL, Wallace GG. Covalently linked biocompatible graphene/polycaprolactone composites for tissue engineering. Carbon 2013;52:296–304.

[161] Wang D, Zhang X, Zha JW, Zhao J, Dang JM, Hu GH. Dielectric properties of reduced graphene oxide/polypropylene composites with ultralow percolation threshold. Polymer 2013;54:1916–22.
[162] Lalwani G, Henslee AM, Farshid B, Lin L, Kasper FK, Qin YX, Mikos AG, Sitharaman B. Two-dimensional nanostructure-reinforced biodegradable polymeric nanocomposites for bone tissue engineering. Biomacromolecules 2013;14:900–9.
[163] Kim IH, Jeong YG. Polylactide/exfoliated graphite nanocomposites with enhanced thermal stability, mechanical modulus, and electrical conductivity. J Polym Sci B Polym Phys 2010;48:850–8.
[164] Zhang HB, Zheng WG, Yan Q, Yang Y, Wang JW, Lu ZH, Ji GY, Yu ZZ. Electrically conductive polyethylene terephthalate/graphene nanocomposites prepared by melt compounding. Polymer 2010;51:1191–6.
[165] Dasari A, Yu ZZ, Mai YW. Electrically conductive and super-tough polyamide-based nanocomposites. Polymer 2009;50:4112–21.
[166] Araby S, Zaman I, Menz Q, Kawashima N, Michelmore A, Kuan HC, Majewski P, Ma J, Zhang L. Melt compounding with graphene to develop functional, high-performance elastomers. Nanotechnology 2013;24:165601–14.
[167] Steurer P, Wissert R, Thomann R, Mülhaupt R. Functionalized graphenes and thermoplastic nanocomposites based upon expanded graphite oxide. Macromol Rapid Commun 2009;30:316–27.
[168] Han Y, Wu Y, Shen M, Huang X, Zhu J, Zhang X. Preparation and properties of polystyrene nanocomposites with graphite oxide and graphene as flame retardants. J Mater Sci 2013;48:4214–22.
[169] Song P, Liu L, Fu S, Yu Y, Jin C, Wu Q, Zhang Y, Li Q. Striking multiple synergies created by combining reduced graphene oxides and carbon nanotubes for polymer nanocomposites. Nanotechnology 2013;24:125704–11.
[170] Gao T, Ye Q, Pei X, Xia Y, Zhou F. Grafting polymer brushes on graphene oxide for controlling surface charge states and templated synthesis of metal nanoparticles. J Appl Polym Sci 2013;127:3074–83.
[171] Luzinov I, Minko S, Tsukruk VV. Adaptive and responsive surfaces through controlled reorganization of interfacial polymer layers. Prog Polym Sci 2004;29:635–98.
[172] Shen B, Zhai W, Tao M, Lu D, Zheng W. Chemical functionalization of graphene oxide toward the tailoring of the interface in polymer composites. Compos Sci Technol 2013;77:87–94.
[173] Li D, Huang JX, Kaner RB. Polyaniline nanofibers: a unique polymer nanostructure for versatile applications. Acc Chem Res 2009;42:135–45.
[174] Wei H, Zhua J, Wuc S, Wei S, Guo Z. Electrochromic polyaniline/graphite oxide nanocomposites with endured electrochemical energy storage. Polymer 2013;54:1820–31.
[175] Zhu J, Chen M, Qu H, Zhang X, Wei H, Luo Z, Colorado HA, Wei S, Guo Z. Interfacial polymerized polyaniline/graphite oxide nanocomposites toward electrochemical energy storage. Polymer 2012;53:5953–64.
[176] Ning G, Li T, Yan J, Xu C, Wei T, Fan Z. Three-dimensional hybrid materials of fish scale-like polyaniline nanosheet arrays on graphene oxide and carbon nanotube for high-performance ultracapacitors. Carbon 2013;54:241–8.
[177] Ye L, Meng XY, Ji X, Li ZM, Tang JH. Synthesis and characterization of expandable graphite-poly(methyl methacrylate) composite particles and their application to flame retardation of rigid polyurethane foams. Polym Degrad Stab 2009;94:971–9.
[178] Weng W, Wu C. Exfoliation of graphite flakes and its nanocomposites. Carbon 2003;41:619–21.
[179] Moujahid EM, Besse JP, Leroux F. Poly(styrene sulfonate) layered double hydroxide nanocomposites Stability and subsequent structural transformation with changes in temperature. J Mater Chem 2003;13:258–64.
[180] Shi H, Li Y, Guo T. In situ preparation of transparent polyimide nanocomposite with a small load of graphene oxide. J Appl Polym Sci 2013;128:3163–9.
[181] Decher G. Fuzzy nanoassemblies: toward layered polymeric multicomposites. Science 1997;277:1232–7.
[182] Decher G, Schlenoff JB, editors. Multilayer thin films: sequential assembly of nanocomposite materials. 2nd ed. Weinheim: Wiley-VCH; 2012, 1112 p.
[183] Lvov Y, Möhwald H. Protein architecture: interfacial molecular assembly and immobilization biotechnology. New York: Marcel Dekker; 2000, 416 p.
[184] Ariga K, editor. Layer-by-layer (LbL) assembly, in: organized organic ultrathin films, fundamentals and applications. Weinheim: Wiley-VCH; 2013, 226 p.
[185] Jiang C, Tsukruk VV. Freestanding nanostructures via layer-by-layer assembly. Adv Mater 2006;18:829–40.
[186] Jiang C, Markutsya S, Pikus Yu, Tsukruk VV. Freely suspended nanocomposite membranes as highly sensitive sensors. Nat Mater 2004;3:721–8.
[187] Kotov NA, Dekany I, Fendler JH. Ultrathin graphite oxide-polyelectrolyte composites prepared by self-assembly: transition between conductive and non-conductive states. Adv Mater 1996;8:637–41.
[188] Kovtyukhova NI, Ollivier PJ, Martin BR, Mallouk TE, Chizhik SA, Buzaneva EV, Gorchinskiy AD. Layer-by-layer assembly of ultrathin composite films from micron-sized graphite oxide sheets and polycations. Chem Mater 1999;11:771–8.
[189] Zhao X, Zhang QH, Hao YP, Li YZ, Fang Y, Chen DJ. Enhanced mechanical properties of graphene-based poly(vinyl alcohol) composites. Macromolecules 2010;43:9411–6.
[190] Zhu J, Zhang H, Kotov NA. Thermodynamic and structural insights into nanocomposites engineering by comparing two materials assembly techniques for graphene. ACS Nano 2013;7:4818–29.
[191] Fan W, Zhang C, Tjiu WW. Fabrication of electrically conductive graphene/polystyrene composites via a combination of latex and layer-by-layer assembly approaches. J Mater Res 2013;28:611–9.
[192] Choi I, Kulkarni DD, Xu W, Tsitsilianis C, Tsukruk VV. Star polymer unimicelles on graphene oxide flakes. Langmuir 2013;29:9761–9.
[193] Layek RK, Samanta S, Nandi AK. The physical properties of sulfonated graphene/poly(vinyl alcohol) composites. Carbon 2012;50:815–27.
[194] Wagner HD, Vaia RA. Nanocomposites: issues at the interface. Mater Today 2004;7:38–42.
[195] Velasco-Santos C, Martinez-Hernandez AL, Castano VM. Carbon nanotube-polymer nanocomposites: the role of interfaces. Compos Interfaces 2005;11:567–86.
[196] Giannelis EP. Polymer layered silicate nanocomposites. Adv Mater 1996;8:29–35.
[197] Vaia RA, Vasudevan S, Krawiec W, Scanlon LG, Giannelis EP. New polymer electrolyte nanocomposites: melt intercalation of poly(ethylene oxide) in mica-type silicates. Adv Mater 1995;7:154–6.
[198] Moniruzzaman M, Winey KI. Polymer nanocomposites containing carbon nanotubes. Macromolecules 2006;39:5194–205.
[199] Wang MC, Yan C, Ma L. Graphene nanocomposites. In: Ning H, editor. Composites and their properties. Shanghai: In Tech; 2012, 502 p.
[200] Sham AYW, Notley SM. A review of fundamental properties and applications of polymer-graphene hybrid materials. Soft Matter 2013;9:6645–53.
[201] Gong X, Liu J, Baskaran S, Voise RD, Young JS. Surfactant-assisted processing of carbon nanotube/polymer composites. Chem Mater 2000;12:1049–52.
[202] Spitalsky Z, Tasis D, Papagelis K, Galiotis C. Carbon nanotube–polymer composites: chemistry, processing, mechanical and electrical properties. Prog Polym Sci 2010;35:357–401.
[203] Sahoo NG, Rana S, Cho JW, Li L, Chan SH. Polymer nanocomposites based on functionalized carbon nanotubes. Prog Polym Sci 2010;35:837–67.
[204] Haque A, Ramasetty A. Theoretical study of stress transfer in carbon nanotube reinforced polymer matrix composites. Compos Struct 2005;71:68–77.
[205] Fischer H. Polymer nanocomposites: from fundamental research to specific applications. Mater Sci Eng C 2003;23:763–72.
[206] Chen H, Müller MB, Gilmore KJ, Wallace GG, Li D. Mechanically strong, electrically conductive, and biocompatible graphene paper. Adv Mater 2008;20:3557–61.
[207] Gao Y, Liu LQ, Zu SZ, Peng K, Zhou D, Han BH, Zhang Z. The effect of interlayer adhesion on the mechanical behaviors of macroscopic graphene oxide papers. ACS Nano 2011;5:2134–41.
[208] Tian Y, Cao Y, Wang Y, Yang W, Feng J. Realizing ultrahigh modulus and high strength of macroscopic graphene oxide papers through crosslinking of mussel-inspired polymers. Adv Mater 2013;25:2980–3.
[209] Putz KW, Compton OC, Palmeri MJ, Nguyen ST, Brinson LC. High-nanofiller-content graphene oxide-polymer nanocomposites via vacuum-assisted self-assembly. Adv Funct Mater 2010;20:3322–9.
[210] Li Z, Young RJ, Kinloch IA. Interfacial stress transfer in graphene oxide nanocomposites. ACS Appl Mater Interfaces 2013;5:456–63.
[211] Xu P, Loomis J, Bradshaw RD, Panchapakesan B. Load transfer and mechanical properties of chemically reduced graphene

reinforcements in polymer composites. Nanotechnology 2012;23:505713/1–505713.
[212] Srivastava I, Mehta RJ, Yu ZZ, Schadler L, Koratkar N. Raman study of interfacial load transfer in graphene nanocomposites. Appl Phys Lett 2011;98:063102–63103.
[213] Chen Y, Qi Y, Tai Z, Yan X, Zhu F, Xue Q. Preparation, mechanical properties and biocompatibility of graphene oxide/ultrahigh molecular weight polyethylene composites. Eur Polym J 2012;48:1026–33.
[214] Laaksonen P, Walther A, Malho JM, Kainlauri M, Ikkala O, Linder MB. Genetic engineering of biomimetic nanocomposites: diblock proteins, graphene, and nanofibrillated cellulose. Angew Chem Int Ed 2011;50:8688–91.
[215] Li YQ, Yu T, Yang TY, Zheng LX, Liao K. Bio-inspired nacre-like composite films based on graphene with superior mechanical, electrical, and biocompatible properties. Adv Mater 2012;24:3426–31.
[216] Hoare TR, Kohane DS. Hydrogels in drug delivery: progress and challenges. Polymer 2008;49:1993–2007.
[217] Van Vlierberghe S, Dubruel P, Schacht E. Biopolymer-based hydrogels as scaffolds for tissue engineering applications: a review. Biomacromolecules 2011;12:1387–408.
[218] Zhang L, Shi G. Preparation of highly conductive graphene hydrogels for fabricating supercapacitors with high rate capability. J Phys Chem C 2011;115:17206–12.
[219] Gao H, Xiao F, Ching CB, Duan H. High-performance asymmetric supercapacitor based on graphene hydrogel and nanostructured MnO_2. ACS Appl Mater Interfaces 2012;4:2801–10.
[220] Stuart MC, Huck W, Genzer J, Müller M, Ober C, Stamm M, Sukhorukov GB, Szleifer I, Tsukruk VV, Urban M, Winnik F, Zauscher S, Luzinov I, Minko S. Emerging applications of stimuli-responsive polymer materials. Nat Mater 2010;9:101–13.
[221] Xu Y, Sheng K, Li C, Shi G. Self-assembled graphene hydrogel via a one-step hydrothermal process. ACS Nano 2010;4:4324–30.
[222] Kozlovskaya V, Kharlampieva E, Khanal BP, Manna P, Zubarev ER, Tsukruk VV. Ultrathin layer-by-layer hydrogels with incorporated gold nanorods as pH-sensitive optical materials. Chem Mater 2008;20:7474–85.
[223] Shen J, Yan B, Li T, Long Y, Li N, Ye M. Mechanical, thermal and swelling properties of poly(acrylic acid)-graphene oxide composite hydrogels. Soft Matter 2012;8:1831–6.
[224] Lutz JF, Akdemir Ö, Hoth A. Point by point comparison of two thermosensitive polymers exhibiting a similar LCST: is the age of poly(NIPAM) over? J Am Chem Soc 2006;128:13046–7.
[225] Zhang Y, Furyk S, Bergbreiter DE, Cremer PS. Specific ion effects on the water solubility of macromolecules: PNIPAM and the Hofmeister series. J Am Chem Soc 2005;127:14505–10.
[226] Ruel-Gariépy E, Leroux JC. In situ-forming hydrogels—review of temperature-sensitive systems. Eur J Pharm Biopharm 2004;58:409–26.
[227] Zhang XZ, Wu DQ, Chu CC. Synthesis, characterization and controlled drug release of thermosensitive IPN–PNIPAAm hydrogels. Biomaterials 2004;25:3793–805.
[228] Alzari V, Nuvoli D, Scognamillo S, Piccinini M, Gioffredi E, Malucelli G, Marceddu S, Sechi M, Sanna V, Mariani A. Graphene-containing thermoresponsive nanocomposite hydrogels of poly(N-isopropylacrylamide) prepared by frontal polymerization. J Mater Chem 2011;21:8727–33.
[229] Sun S, Wu P. A one-step strategy for thermal- and pH-responsive graphene oxide interpenetrating polymer hydrogel networks. J Mater Chem 2011;21:4095–7.
[230] Bai H, Sheng K, Zhang P, Li C, Shi G. Graphene oxide/conducting polymer composite hydrogels. J Mater Chem 2011;21:18653–8.
[231] Rafiee MA, Rafiee J, Wang Z, Song H, Yu ZZ, Koratkar N. Enhanced mechanical properties of nanocomposites at low graphene content. ACS Nano 2009;3:3884–90.
[232] Zhang K, Zhang LL, Zhao XS, Wu J. Graphene/polyaniline nanofiber composites as supercapacitor electrodes. Chem Mater 2010;22:1392–401.
[233] Jung JH, Jeon JH, Sridhar V, Oh IK. Electro-active graphene-Nafion actuators. Carbon 2011;49:1279–89.
[234] Brownson DAC, Kampouris DK, Banks CE. An overview of graphene in energy production and storage applications. J Power Sources 2011;196:4873–85.
[235] Huang X, Qi X, Boey F, Zhang H. Graphene-based composites. Chem Soc Rev 2012;41:666–86.
[236] Li J, Guo S, Zhai Y, Wang E. Nafion-graphene nanocomposite film as enhanced sensing platform for ultrasensitive determination of cadmium. Electrochem Commun 2009;11:1085–8.
[237] Fang M, Wang K, Lu H, Yang Y, Nutt S. Covalent polymer functionalization of graphene nanosheets and mechanical properties of composites. J Mater Chem 2009;19:7098–105.
[238] Li J, Guo S, Zhai Y, Wang E. High-sensitivity determination of lead and cadmium based on the Nafion-graphene composite film. Anal Chim Acta 2009;649:196–201.
[239] Al-Mashat L, Shin K, Kalantar-zadeh K, Plessis JD, Han SH, Kojima RW, Kaner RB, Li D, Guo X, Ippolito SJ, Wlodarski W. Graphene/polyaniline nanocomposite for hydrogen sensing. J Phys Chem C 2010;114:16168–73.
[240] Zeng Y, Zhou Y, Kong L, Zhou T, Shi G. A novel composite of SiO_2-coated graphene oxide and molecularly imprinted polymers for electrochemical sensing dopamine. Biosens Bioelectron 2013;45:25–33.
[241] Kim S, Oh WK, Jeong YS, Jang J. Dual-functional poly(3,4-ethylenedioxythiophene)/MnO_2 nanoellipsoids for enhancement of neurite outgrowth and exocytosed biomolecule sensing in PC12 cells. Adv Funct Mater 2013;23:1947–56.
[242] Wang L, Pu KY, Li J, Qi X, Li H, Zhang H, Fan C, Liu B. A graphene-conjugated oligomer hybrid probe for light-up sensing of lectin and *Escherichia coli*. Adv Mater 2011;23:4386–91.
[243] He Q, Wu S, Gao S, Cao X, Yin Z, Li H, Chen P, Zhang H. Transparent, flexible, all-reduced graphene oxide thin film transistors. ACS Nano 2011;5:5038–44.
[244] Llobet E. Gas sensors using carbon nanomaterials: a review. Sensors Actuat B 2013;179:32–45.
[245] Kumar SK, Castro M, Saiter A, Delbreilh L, Feller JF, Thomas S, Grohens Y. Development of poly(isobutylene-co-isoprene)/reduced graphene oxide nanocomposites for barrier, dielectric and sensingapplications. Mater Lett 2013;96:109–12.
[246] Zheng Z, Du Y, Feng Q, Wang Z, Wang C. Facile method to prepare Pd/graphene–polyaniline nanocomposite and used as new electrode material for electrochemical sensing. J Mol Catal A 2012;(353–354):80–6.
[247] Konwer S, Guha A, Dolui S. Graphene oxide-filled conducting polyaniline composites as methanol-sensing materials. J Mater Sci 2013;48:1729–39.
[248] Xing XJ, Liu XG, He Y, Lin Y, Zhang CL, Tang HW, Pang DW. Amplified fluorescent sensing of DNA using graphene oxide and a conjugated cationic polymer. Biomacromolecules 2012;14:117–23.
[249] Wang Y, Wu Z, Liu Z. Upconversion fluorescence resonance energy transfer biosensor with aromatic polymer nanospheres as the lable-free energy acceptor. Anal Chem 2012;85:258–64.
[250] Tung TT, Castro M, Kim TY, Suh KS, Feller JF. Graphene quantum resistive sensing skin for the detection of alteration biomarkers. J Mater Chem 2012;22:21754–66.
[251] Qiu JD, Shi L, Liang RP, Wang GC, Xia XH. Controllable deposition of a platinum nanoparticle ensemble on a polyaniline/graphene hybrid as a novel electrode material for electrochemical sensing. Chem Eur J 2012;18:7950–9.
[252] Worsley MA, Pauzauskie PJ, Olson TY, Biener J, Satcher JH, Baumann TF. Synthesis of graphene aerogel with high electrical conductivity. J Am Chem Soc 2010;132:14067–9.
[253] Yang YH, Bolling L, Priolo MA, Grunlan JC. Super gas barrier and selectivity of graphene oxide-polymer multilayer thin films. Adv Mater 2013;25:503–8.
[254] Choudalakis G, Gotsis AD. Permeability of polymer/clay nanocomposites: a review. Eur Polym J 2009;45:967–84.
[255] Lee D, Choi MC, Ha CS. Polynorbornene dicarboximide/amine functionalized graphene hybrids for potential oxygen barrier films. J Polym Sci A Polym Chem 2012;50:1611–21.
[256] Liu H, Kuila T, Kim NH, Ku BC, Lee JH. In situ synthesis of the reduced graphene oxide-polyethyleneimine composite and its gas barrier properties. J Mater Chem A 2013;1:3739–46.
[257] Tseng IH, Liao YF, Chiang JC, Tsai MH. Transparent polyimide/graphene oxide nanocomposite with improved moisture barrier property. Mater Chem Phys 2012;136:247–53.
[258] Song P, Yu Y, Zhang T, Fu S, Fang Z, Wu Q. Permeability, viscoelasticity, and flammability performances and their relationship to polymer nanocomposites. Ind Eng Chem Res 2012;51:7255–63.
[259] Yun JM, Yeo JS, Kim J, Jeong HG, Kim DY, Noh YJ, Kim SS, Ku BC, Na SI. Solution-processable reduced graphene oxide as a novel alternative to PEDOT:PSS hole transport layers for highly efficient and stable polymer solar cells. Adv Mater 2011;23:4923–8.
[260] Li SS, Tu KH, Lin CC, Chen CW, Chhowalla M. Solution-processable graphene oxide as an efficient hole transport layer in polymer solar cells. ACS Nano 2010;4:3169–74.

[261] Tung VC, Kim J, Huang J. Graphene oxide: single-walled carbon nanotube-based interfacial layer for all-solution-processed multi-junction solar cells in both regular and inverted geometries. Adv Energy Mater 2012;2:299–303.
[262] Angmo D, Krebs FC. Flexible ITO-free polymer solar cells. J Appl Polym Sci 2013;129:1–14.
[263] Zhang W, Zhao B, He Z, Zhao X, Wang H, Yang S, Wu H, Cao Y. High-efficiency ITO-free polymer solar cells using highly conductive PEDOT:PSS/surfactant bilayer transparent anodes. Energy Environ Sci 2013;6:1956–64.
[264] Sun Y, Shi G. Graphene/polymer composites for energy applications. J Polym Sci B Polym Phys 2013;51:231–53.
[265] Dai L. Functionalization of graphene for efficient energy conversion and storage. Acc Chem Res 2012;46:31–42.
[266] Iwan A, Chuchmała A. Perspectives of applied graphene: polymer solar cells. Prog Polym Sci 2012;37:1805–28.
[267] Akhtar MS, Kwon S, Stadler FJ, Yang OB. High efficiency solid state dye sensitized solar cells with graphene-polyethylene oxide composite electrolytes. Nanoscale 2013;5:5403–11.
[268] Qiao Z, Guojia F, Fei C, Hongwei L, Pingli Q, Caimao Z. Low-temperature solution-processed graphene oxide derivative hole transport layer for organic solar cells. J Phys D Appl Phys 2013;46:135101.
[269] Ran C, Wang M, Gao W, Ding J, Shi Y, Song X, Chen H, Ren Z. Study on photoluminescence quenching and photostability enhancement of MEH-PPV by reduced graphene oxide. J Phys Chem C 2012;116:23053–60.
[270] Qu S, Li M, Xie L, Huang X, Yang J, Wang N, Yang S. Noncovalent functionalization of graphene attaching [6,6]-phenyl-phenyl-C61-butyric acid methyl ester (PCBM) and application as electron extraction layer of polymer solar cells. ACS Nano 2013;7:4070–81.
[271] Chuchmała A, Palewicz M, Sikora A, Iwan A. Influence of graphene oxide interlayer on PCE value of polymer solar cells. Synth Met 2013;169:33–40.
[272] Liu X, Kim H, Guo LJ. Optimization of thermally reduced graphene oxide for an efficient hole transport layer in polymer solar cells. Org Electron 2013;14:591–8.
[273] Lee RH, Huang JL, Chi CH. Conjugated polymer-functionalized graphite oxide sheets thin films for enhanced photovoltaic properties of polymer solar cells. J Polym Sci B Polym Phys 2013;51:137–48.
[274] Wang DH, Kim JK, Seo JH, Park I, Hong BH, Park JH, Heeger AJ. Transferable graphene oxide by stamping nanotechnology: electron-transport layer for efficient bulk-heterojunction solar cells. Angew Chem Int Ed 2013;52:2874–80.
[275] Huxtable ST, Cahill DG, Shenogin S, Xue L, Ozisik R, Barone P, Usrey M, Strano MS, Siddons G, Shim M, Keblinski P. Interfacial heat flow in carbon nanotube suspensions. Nat Mater 2003;2:731–4.
[276] Yu A, Ramesh P, Sun X, Bekyarova E, Itkis ME, Haddon RC. Enhanced thermal conductivity in a hybrid graphite nanoplatelet – carbon nanotube filler for epoxy composites. Adv Mater 2008;20:4740–4.
[277] Veca LM, Meziani MJ, Wang W, Wang X, Lu F, Zhang P, Lin Y, Fee R, Connell JW, Sun YP. Carbon nanosheets for polymeric nanocomposites with high thermal conductivity. Adv Mater 2009;21:2088–92.
[278] Ma WS, Li J, Zhao XS. Improving the thermal and mechanical properties of silicone polymer by incorporating functionalized graphene oxide. J Mater Sci 2013;48:5287–94.
[279] Cheng HKF, Basu T, Sahoo NG, Li L, Chan SH. Current advances in the carbon nanotube/thermotropic main-chain liquid crystalline polymer nanocomposites and their blends. Polymers 2012;4:889–912.
[280] Hsiao MC, Ma CCM, Chiang JC, Ho KK, Chou TY, Xie X, Tsai CH, Chang LH, Hsieh CK. Thermally conductive and electrically insulating epoxy nanocomposites with thermally reduced graphene oxide-silica hybrid nanosheets. Nanoscale 2013;5:5863–71.
[281] Wu C, Huang X, Wu X, Xie L, Yang K, Jiang P. Graphene oxide-encapsulated carbon nanotube hybrids for high dielectric performance nanocomposites with enhanced energy storage density. Nanoscale 2013;5:3847–55.
[282] Ha HW, Choudhury A, Kamal T, Kim DH, Park SY. Effect of chemical modification of graphene on mechanical, electrical, and thermal properties of polyimide/graphene nanocomposites. ACS Appl Mater Interfaces 2012;4:4623–30.
[283] Huang X, Iizuka T, Jiang P, Ohki Y, Tanaka T. Role of interface on the thermal conductivity of highly filled dielectric epoxy/AlN composites. J Phys Chem C 2012;116:13629–39.
[284] Bae S, Kim SJ, Shin D, Ahn JH, Hong BH. Towards industrial applications of graphene electrodes. Phys Scr 2012;T146:014024/1–14024.
[285] Wang J, Liang M, Fang Y, Qiu T, Zhang J, Zhi L. Rod-coating: towards large-area fabrication of uniform reduced graphene oxide films for flexible touch screens. Adv Mater 2012;24:2874–8.
[286] Wang Z, Nelson JK, Hillborg H, Zhao S, Schadler LS. Graphene oxide filled nanocomposite with novel electrical and dielectric properties. Adv Mater 2012;24:3134–7.
[287] Qi XY, Yan D, Jiang Z, Cao YK, Yu ZZ, Yavari F, Koratkar N. Enhanced electrical conductivity in polystyrene nanocomposites at ultra-low graphene content. ACS Appl Mater Interfaces 2011;3:3130–3.
[288] Huang Y, Qin Y, Zhou Y, Niu H, Yu ZZ, Dong JY. Polypropylene/graphene oxide nanocomposites prepared by in situ Ziegler–Natta polymerization. Chem Mater 2010;22:4096–102.
[289] Liu A, Li C, Bai H, Shi G. Electrochemical deposition of polypyrrole/sulfonated graphene composite films. J Phys Chem C 2010;114:22783–9.
[290] Wang H, Hao Q, Yang X, Lu L, Wang X. Graphene oxide doped polyaniline for supercapacitors. Electrochem Commun 2009;11:1158–61.
[291] Zhou X, Wu T, Hu B, Yang G, Han B. Synthesis of graphene/polyaniline composite nanosheets mediated by polymerized ionic liquid. Chem Commun 2010;46:3663–5.
[292] Yu D, Dai L. Self-assembled graphene/carbon nanotube hybrid films for supercapacitors. J Phys Chem Lett 2009;1:467–70.
[293] Ouyang W, Sun J, Memon J, Wang C, Geng J, Huang Y. Scalable preparation of three-dimensional porous structures of reduced graphene oxide/cellulose composites and their application in supercapacitors. Carbon 2013;62:501–9.
[294] Secor EB, Prabhumirashi PL, Puntambekar K, Geier ML, Hersam MC. Inkjet printing of high conductivity, flexible graphene patterns. J Phys Chem Lett 2013;4:1347–51.
[295] Huang P, Chen W, Yan L. An inorganic–organic double network hydrogel of graphene and polymer. Nanoscale 2013;5:6034–9.
[296] Liu HH, Peng WW, Hou LC, Wang XC, Zhang XX. The production of a melt-spun functionalized graphene/poly(ε-caprolactam) nanocomposite fiber. Compos Sci Technol 2013;81:61–8.
[297] Cong HP, Ren XC, Wang P, Yu SH. Flexible graphene-polyaniline composite paper for high-performance supercapacitor. Energy Environ Sci 2013;6:1185–91.
[298] Okhay O, Krishna R, Salimian M, Titus E, Gracio J, Guerra LM, Ventura J. Conductivity enhancement and resistance changes in polymer films filled with reduced graphene oxide. J Appl Phys 2013;113:064307.
[299] Shi Z, Phillips GO, Yang G. Nanocellulose electroconductive composites. Nanoscale 2013;5:3194–201.
[300] Tang L, Li X, Du D, He C. Fabrication of multilayer films from regenerated cellulose and graphene oxide through layer-by-layer assembly. Prog Nat Sci Mater Int 2012;22:341–6.
[301] Zhuang H, Xu X, Liu Y, Zhou Q, Xu X, Li H, Xu Q, Li N, Lu J, Wang L. Dual-mechanism-controlled ternary memory devices fabricated by random copolymers with pendent carbazole and nitro-azobenzene. J Phys Chem C 2012;116:25546–51.
[302] Yan D, Zhang HB, Jia Y, Hu J, Qi XY, Zhang Z, Yu ZZ. Improved electrical conductivity of polyamide 12/graphene nanocomposites with maleated polyethylene-octene rubber prepared by melt compounding. ACS Appl Mater Interfaces 2012;4:4740–5.
[303] Su Q, Pang S, Alijani V, Li C, Feng X, Müllen K. Composites of graphene with large aromatic molecules. Adv Mater 2009;21:3191–5.
[304] Ambrosi A, Chua CK, Bonanni A, Pumera M. Lithium aluminum hydride as reducing agent for chemically reduced graphene oxides. Chem Mater 2012;24:2292–8.
[305] Yuan J, Ma LP, Pei S, Du J, Su Y, Ren W, Cheng HM. Tuning the electrical and optical properties of graphene by ozone treatment for patterning monolithic transparent electrodes. ACS Nano 2013;7:4233–41.
[306] Edwards RS, Coleman KS. Graphene synthesis: relationship to applications. Nanoscale 2013;5:38–51.